T.R.
BOLU ABANT İZZET BAYSAL UNIVERSITY
INSTITUTE OF GRADUATE STUDIES
Department of Biology

SITE-DIRECTED MUTAGENESIS OF BILE SALT HYDROLASE (BSH) FROM *LACTOBACILLUS PLANTARUM* B14 AND SUBSTRATE SPECIFICITY ANALYSIS OF MUTANT BSH ENZYMES

DOCTOR OF PHILOSOPHY

ZEKİYE KILIÇSAYMAZ

ACADEMIC SUPERVISOR
Prof. Dr. Mehmet ÖZTÜRK

BOLU, JULY - 2024

APPROVAL OF THE THESIS

SITE-DIRECTED MUTAGENESIS OF BILE SALT HYDROLASE (BSH) FROM *LACTOBACILLUS PLANTARUM* B14 AND SUBSTRATE SPECIFICITY ANALYSIS OF MUTANT BSH ENZYMES submitted by **ZEKİYE KILIÇSAYMAZ** and defended before the Examining Committe Members listed below in partial fulfillment of the requirements for the degree of **Doctor of Philosophy** in **Department of Biology, Institute of Graduate Studies of Bolu Abant Izzet Baysal University in 25.06.2024** by

Examining Committee Members	**Signature**
Supervisor **Prof. Dr. Mehmet ÖZTÜRK** Bolu Abant İzzet Baysal University	.....
Member **Prof. Dr. Emel USLU** Bolu Abant İzzet Baysal University	.....
Member **Assoc. Prof. Dr. Özlem AKKAYA** Gebze Technical University	.....
Member **Assit. Prof. Dr. Yakup ERMURAT** Bolu Abant İzzet Baysal University	.....
Member **Assit. Prof. Dr. Cemalettin BEKPEN** Bahçeşehir University	.....

Prof. Dr. İbrahim KÜRTÜL

Director of Institute of Graduate Studies

ETHICAL DECLARATION

In this thesis dissertation that was properly prepared according to the Thesis Writing Rules of Bolu Abant İzzet Baysal University of the Institute of Graduates Studies, I hereby declare that;

- All data, information, and documents presented in the thesis were obtained in accordance with the academic and ethical rules,
- All data, documents, assessments, and results were presented in accordance with the scientific ethical and moral rules,
- All works that were benefitted in the thesis were appropriately cited,
- No alteration was made in the data used,
- Study presented in this thesis is original,

Otherwise, I declare that I accept the loss of all my rights in case any contradiction that may arise against me.

The similarity rate obtained by using the Turnitin program, a plagiarism detection software, is within the limits approved by the University Senate.

_____

Zekiye KILIÇSAYMAZ

ABSTRACT

SITE-DIRECTED MUTAGENESIS OF BILE SALT HYDROLASE (BSH) FROM *LACTOBACILLUS PLANTARUM* B14 AND SUBSTRATE SPECIFICITY ANALYSIS OF MUTANT BSH ENZYMES
PHD THESIS
ZEKİYE KILIÇSAYMAZ
BOLU ABANT IZZET BAYSAL UNIVERSITY
INSTITUTE OF GRADUATE STUDIES
DEPARTMENT OF BIOLOGY
(SUPERVISOR: PROF. DR. MEHMET ÖZTÜRK)

BOLU, JULY 2024
xiii + 82

Bile acid (BA) deconjugation is catalysed by the bile salt hydrolase (BSH) enzyme, which is a member of the cholylglycine hydrolase (CGH) family and produced by intestinal bacteria. The clinically significant BSH alters BA-mediated signalling pathways related to lipid absorption, energy homeostasis and glucose metabolism. Nevertheless, BSHs exhibit varied substrate preference to different bile salts across sources. Despite the considerable research on BSH, the investigations of its molecular mechanisms concerning BSH substrate recognition remain limited. This research aims to analyze the correlation between the substrate specificity of *Lactobacillus plantarum* B14's BSH enzyme (LpBSH) and two residues, V58 and Y65, in its loop II. These residues possess aliphatic-hydrophobic and aromatic-hydrophobic properties, respectively. PCR-based site-directed mutagenesis was utilised to substitute M58, F58, N58, F65, L65 and C65 amino acids for V58 and Y65, respectively. The mutant recombinant LpBSHs (mrLpBSHs) were expressed using the BLR (DE3) strain of *E. coli* and the activity of mrLpBSHs against six different BAs were detected. The study showed that the V58 and predominantly Y65 residues in loop II could play a vital role in the structural site that is responsible for substrate specificity and catalysis. The results suggest that the Y65 and V58 residues of LpBSH can be involved in substrate specificity. It was also observed that collate group, rather than amino acid moieties, may determine the substrate specificity of BSH. However, further mutagenesis-based research on other CGH family members is necessary to comprehend the structure and substrate specificity relationships of BSHs. Obtained results indicated that BSHs have developed the ability to identify BAs at the steroid nucleus of cholate as well as at the amino acid groups. As a result, it seems likely that the only requirements for binding might be that the cholate moieties and amino acids match and complement the substrate-binding pockets appropriately.

KEYWORDS: Substrate specificity, PCR-based site-directed mutagenesis, Bile salt hydrolase, *Lactobacillus plantarum* B14.

ÖZET

LACTOBACİLLUS PLANTARUM B14'TEN SAFRA TUZU HİDROLAZIN (STH) YÖNLENDİRİLMİŞ MUTAGENEZİ VE MUTANT BSH ENZİMLERİNİN SUBSTRAT ÖZGÜLLÜĞÜ ANALİZİ
DOKTORA TEZİ
ZEKİYE KILIÇSAYMAZ
BOLU ABANT İZZET BAYSAL ÜNİVERSİTESİ
LİSANSÜSTÜ EĞİTİM ENSTİTÜSÜ
BİYOLOJİ ANABİLİM DALI

(TEZ DANIŞMANI: PROF. DR. MEHMET ÖZTÜRK)

BOLU, TEMMUZ - 2024
xiii + 82

Safra asidi (SA) dekonjugasyonu, kolilglisin hidrolaz (KGH) ailesinin bir üyesi olan ve bağırsak bakterileri tarafından üretilen safra tuzu hidrolaz (STH) enzimi tarafından katalize edilir. Klinik olarak önemli olan STH, glikoz metabolizması, enerji homeostazı ve lipid emilimi ile ilgili SA aracılı sinyal yollarını değiştirir. Bununla birlikte, STH'ler kaynaklar arasında farklı safra tuzlarına karşı çeşitli substrat tercihleri sergilemektedir. STH üzerine yapılan kayda değer araştırmalara rağmen, STH substrat tanıma ile ilgili moleküler mekanizmalarının araştırılması sınırlı kalmıştır. Bu araştırma, *Lactobacillus plantarum* B14'ün STH enziminin (LpSTH) substrat özgüllüğü ile onun lup II bölgesinde bulunan V58 ve Y65'teki iki kalıntının arasındaki ilişkiyi analiz etmeyi amaçlamaktadır. Bu kalıntılar sırasıyla alifatik-hidrofobik ve aromatik-hidrofobik özelliklere sahiptir. V58 ve Y65 yerine sırasıyla M58, F58, N58, F65, L65 ve C65 aminoasitlerini ikame etmek için PCR tabanlı bölgeye yönelik mutagenez kullanılmıştır. Mutant rekombinant LpSTH'ler (mrLpSTH'ler) *E. coli*'nin BLR (DE3) suş'unda ifade edilmiş ve mrLpSTH'lerin altı farklı SA'ya karşı aktivitesi, belirlenmiştir. Çalışma, lup II'deki V58 ve ağırlıklı olarak Y65 kalıntılarının, substrat özgüllüğü ve katalizden sorumlu yapısal bölgede hayati bir rol oynayabileceğini göstermiştir. Sonuçlar, LpSTH'nin V58 ve Y65 kalıntılarının substrat özgüllüğüne dahil olabileceğini düşündürmektedir. Ayrıca, STH'nin substrat özgüllüğünü aminoasitlerden ziyade kolat grubunun belirleyebileceği gözlenmiştir. Bununla birlikte, BSH'lerin yapısı ve substrat özgüllüğü ilişkilerini anlamak için diğer KGH ailesi üyeleri üzerinde mutagenez temelli daha fazla araştırma yapılması gerekmektedir. Elde edilen sonuçlar, STH'lerin, kolatın steroid çekirdeğinde ve amino asit gruplarında safra asitlerini tanımlama yeteneğini geliştirmiş olması ihtimalini desteklemektedir. Sonuç olarak, bağlanma için tek gerekliliğin, kolat kısımlarının ve amino asitlerin substrat bağlama ceplerini uygun şekilde eşleştirmesi ve tamamlaması olabileceği muhtemel görünmektedir.

ANAHTAR KELİMELER: Substrat özgüllüğü, PCR tabanlı bölgeye yönelik mutagenez, Safra tuzu hidrolaz, *Lactobacillus plantarum* B14.

TABLE OF CONTENTS

LIST OF FIGURES

Page

LIST OF TABLES

Page

ACKNOWLEDGEMENTS

The author wishes to express her deepest gratitude to her supervisor Prof. Dr. Mehmet Öztürk for his guidance, advice, criticism, encouragements, and insight throughout the research.

The author would also like to thank Assist. Prof. Dr. Cansu Önal for her suggestions and comments.

1. INTRODUCTION

Liver-synthesized BAs have direct or indirect influence on the intestinal microbiota. Conjugated BAs bring about alterations in bacterial membrane architecture and DNA damage, which ultimately impede bacterial growth (1, 2). The effect of BAs on microbiota may also operate through nuclear receptors. Inagaki and colleagues demonstrated that the nuclear receptor farnesoid X receptor (FXR) activation by BAs can stimulate the expression of genes that impede microbial overgrowth and mucosal damage (3). These outcomes are coherent with the notion that BAs are essential in regulating intestinal microbiota, hence with profound implications for preserving balance between human host and intestinal microbiota.

BSH enzymes are widely distributed in the microbial communities of the human gastrointestinal tract and are essential for the physiology of both the host and microbes. The vital task of deconjugating primary BAs using BSH enzymes and their impact on host health is performed by the human gut microbiota (4, 5). One accepted selection criterion for identifying possible probiotics is the presence of active BSHs. Several studies have reported that most of the analyzed BSHs are encoded by lactic acid bacteria and are used as probiotics, mainly to prevent human metabolic diseases (6–8).

BSH enzymes, which have attracted a lot of research interest, can modify the host's cholesterol homeostasis, BA signaling processes and composition of the BA pool mediated the by the BA receptors, FXR and transmembrane G-protein coupled receptor (TGR5). It is unknown whether BSH agonism or inhibition would be advantageous to host metabolism given their intricate and dynamic involvement in metabolism. In order to better understand how BSHs control metabolism, more study is required. This could lead to new directions in drug development.

1.1 Bile Acids and Bile Salts

Conversion of cholesterol to primary BAs occurs in the human liver through two distinct enzymatic pathways - the classical and alternative pathways. Sterol 27 hydroxylase (CYP27A1, Cytochrome P450 family 27 subfamily A member 1) starts the alternative (acidic) BA synthesis pathway, while microsomal cholesterol 7α-hydroxylase (CYP7A1, Cytochrome P450 family 7 subfamily A

member 1) starts the classical (neutral) BA synthesis pathway (9, 10). The liver produces chenodeoxycholic acid (CDCA) and cholic acid (CA), primary BAs, from cholesterol through the action of the enzyme cholesterol 7 α-hydroxylase (CYP7A1). Primary bile salts are created in the liver's hepatocytes when taurine (T) or glycine (G) are conjugated to CA and CDCA. Additionally, pimary bile salts can undergo microbial conversion in the intestines, resulting in the formation of secondary bile salts. The hydrolysis of conjugated BAs' C24 N-acyl amide bond in the intestine is catalyzed by the enzyme BSH, which results in the deconjugation of G/T-CDCA and G/T-CA. The initial stage involves BSH catalyzing the deconjugation (splintering of taurine or glycine) to produce primary BAs. After the deconjugated BAs are produced, 7α-dehydroxylase dehydroxylates them. This process removes the 7α-hydroxyl group from the deconjugated BAs' 7α-position, resulting in the formation of secondary BAs, which are deoxycholic acid (DCA) and lithocholic acid (LCA), respectively. On the other hand, 7α-dehydrogenation via 7α-hydroxysteroid dehydrogenase (EC 1.1.1.159) can result in 7-oxo-lithocholic acids or 7-oxo-deoxycholic (11–13), one of which can, via epimerization, produce ursodeoxycholic acid (UDCA) (14). Eventually, in the liver's hepatocytes, they are conjugated to taurine or glycine and then stored in the gallbladder. Subsequently, the duodenum receives these substances for the purpose of breaking down and absorbing fat-soluble vitamins and fats that have been consumed (9, 10, 15, 16). BAs contribute to the mechanical processes of lipids and are then reabsorbed either in two ways active transport in the terminal ileum or passive diffusion in the superior section of the small intestine (9, 10). Through a recycling process called enterohepatic circulation, over 95% of them return to the liver for comparable subsequent activities (9, 10, 15, 16). The remaining 5% of BAs are excreted as fecal BAs (9, 10, 15). Enterohepatic circulation is the word for this process, which is depicted in Figure 1.1.

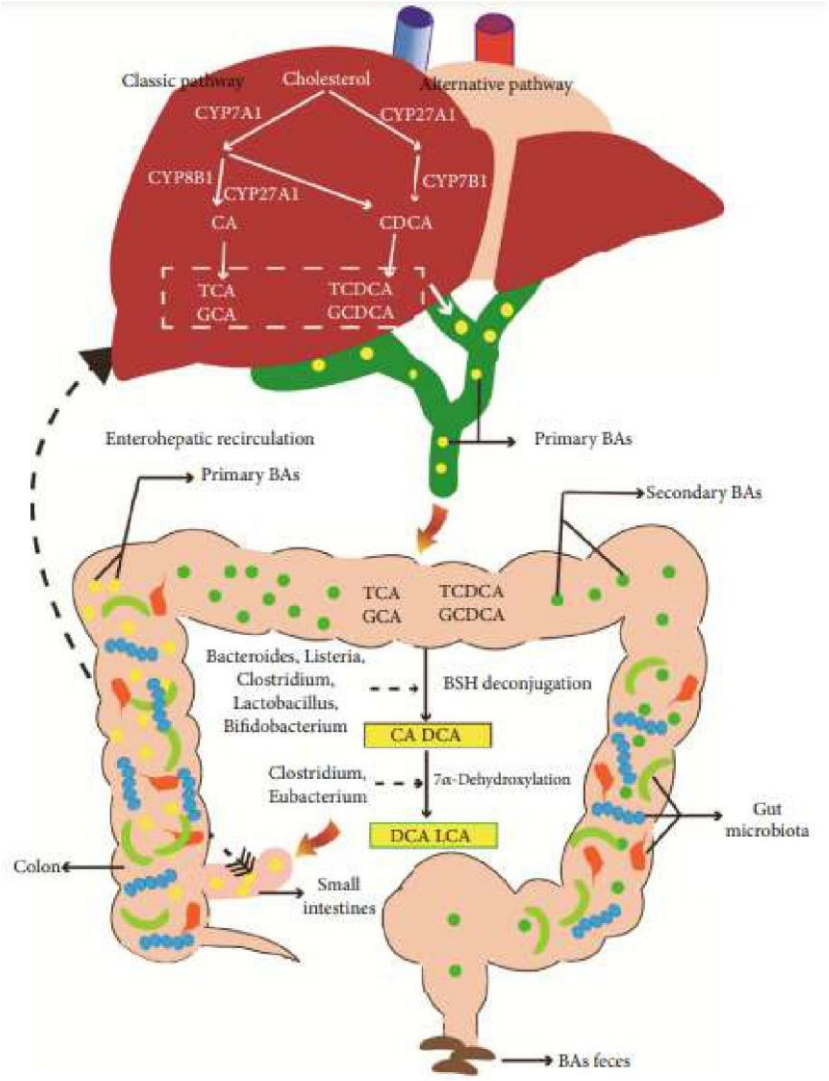

Figure 1. 1. Enterohepatic circulation of bile salts (adapted from https://www.researchgate.net/)

The bile acids' single bond, or -COOH group, is conjugated by the liver through a covalent bond with taurine or glycine.This happens during the hepatic phase of the enterohepatic circulation, following the synthesis of the primary bile acids. CA, taurocholic acid (TCA), glycocholic acid (GCA), and their corresponding free and conjugated forms, CDCA, LCA, DCA, and UDCA, are thus present in the bile. The primary and secondary bile acids' chemical structures are displayed in Figure 1.2.

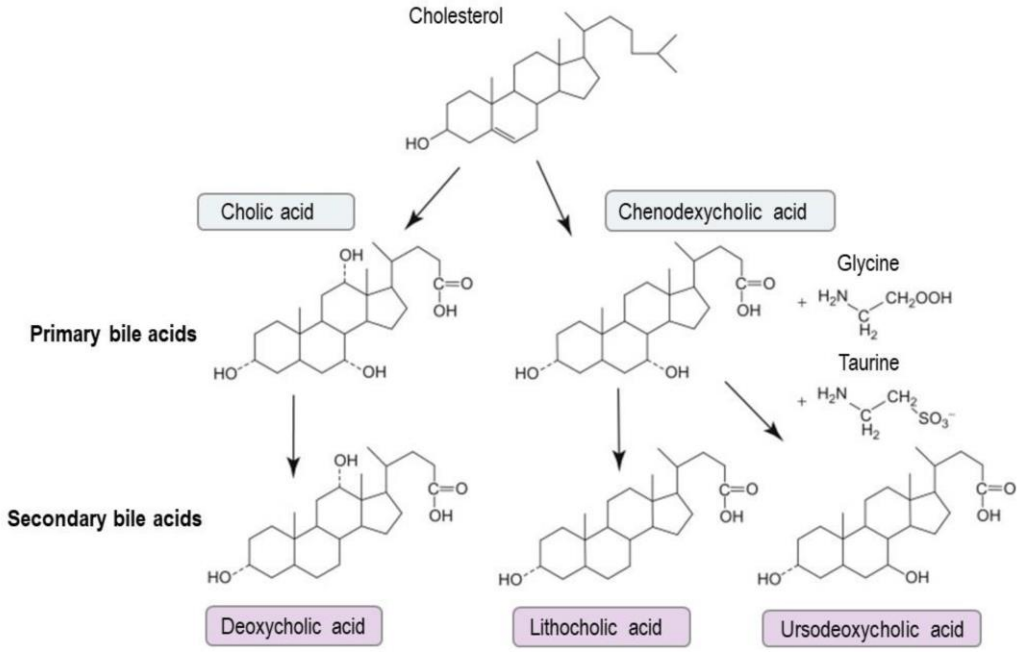

Figure 1. 2. Bile acid structures, both primary and secondary. The liver cells convert cholesterol into the primary bile acids, which are then expelled into the bile. Primary bile acids are transformed by intestinal bacteria into secondary bile acids, which are then reabsorbed in the terminal ileum together with the original, unaltered primary bile acids (186).

In addition to the primary BAs, intestinal microbiota can also generate approximately twenty different BA metabolites from CDCA and CA (17, 18). Approximately 40% of CA and CDCA and 20% of DCA make up the human BA pool, which is the total amount of BA found in the enterohepatic circulation (19). Conversely, CA is more hydrophilic than CDCA, implying that it leads to increased lipid absorption in the intestine (20). CDCA and CA exhibit varying hormone activity (21). Therefore, the CA and CDCA ratio has significant implications for fat absorption and homeostasis.

Humans contain the following proportions of different conjugated BAs: 26% glycocholic acid (GCA), 26% glycochenodeoxycholic acid (GCDCA), 22% glycodeoxycholic acid (GDCA), 9% taurodeoxycholic acid (TDCA), 9% taurocholic acid (TCA) and 8% taurochenodeoxycholic acid (TCDCA). Consequently, the ratio of taurine to glycine conjugates is roughly 1:3 (22).

By binding to BA nuclear and membrane receptors, BAs can function as signaling molecules. Two receptors are essential to the primary activities of BAs: TGR5 and FXR (23). These two receptors serve a wide range of physiological purposes and are dispersed differentially across tissues. As a result, BAs have

emerged as one of the most promising pharmaceutical targets for the management of primary sclerosing cholangitis (PSC), cholestatic illnesses, primary biliary cholangitis (PBC) and other metabolic diseases (24).

FXR exhibits vital functions in regulating BA synthesis, secretion, and transport in diverse tissues including the liver, intestine, kidney, and adrenal gland (25). Additionally, FXR modulates lipid and glucose metabolism, thereby demonstrating benefits against metabolic disorders such as type 2 diabetes, non-alcoholic fatty liver disease (NAFLD), dyslipidemia, and obesity (26). Furthermore, different types of BAs have varying effects on intestinal FXR. It is worth noting that some BAs are more potent than others, and their effects on FXR are varied. CDCA, TCA, DCA, and LCA are sorted according to the degree of activation from strong to weak, with CDCA being the strongest and LCA being the weakest. Conversely, UDCA and T-β-MCA inhibit intestinal FXR (27). Furthermore, apart from their influence on the aforementioned receptors, BAs exhibit strong agonistic properties towards the pregnane X receptors and vitamin D, which govern the regulation of bile and drug metabolism in the liver (1). While BAs are essential for human health, their accumulation in the liver and peripheral tissues can be highly toxic (28).

1.2. BSH

Penicillin V acylase (PVA) and BSH are members of the choloylglycine hydrolases (CGH) enzyme superfamily, which is related to the Ntn (N-terminal nucleophile) hydrolase enzyme superfamily (29). The Ntn-hydrolase fold allows for a wide range of substrate specificities amongst enzymes with only minor changes to the substrate binding pocket and active site (30). This enzyme superfamily is identified by the catalytic mechanism where the N-terminal residue launches a nucleophilic attack on the amide bond's substrate carbonyl carbon (31, 32). Four substrate binding loops encircling the active site are shared by CGHs; BSH loops are typically shorter to make room for the large steroid nucleus in the active site (1, 33). Loops 1 (20–26), 2 (59–68), and 3 (131–42) contain key residues for BSH activity, while loop 4 (263-275) contains no significant residues (22). The substrate selectivity and catalytic efficiency of PVA and BSH enzymes are significantly influenced by these loops (34). As a result of host pressure on PVA

enzymes, BSH developed as a beneficial adaptation that enhances BA tolerance for the microbe and modifies bile-mediated host-microbe signaling events for the host (35).

Encoded by 314-338 amino acid, BSHs are intracellular enzymes that have an optimal pH range of 3.8 to 7.0, with the exception of *L. johnsonii* PF01 BSHC, which has a temperature range of 70°C (36). Between 30 and 55°C is ideal for the majority of BSH enzymes to function at. The MWs of BSH subunits range from 34 to 42 kDa. The majority of BSHs, or bile salt hydrolases, are homotetramers. Nonetheless, homooctameric, homohexameric and homodimeric forms of *B. fragilis ssp. fragilis* ATCC 2528552, *B. longum* BB536, and BSH from *L. reuteri* CRL 1098 are known to exist, respectively (22).

Many isoforms of the enzyme have developed as a result of the prevalence of BSH, and a number of studies have suggested classification schemes to help with the characterization and identification of BSH enzymes in the future. The enzymes have previously been separated into sub-groups with nine (35), eight (38), five (37) and four (22) isoforms by phylogenetic analyses. Seven categories of classifications were produced by another study that used sequence similarity networks (39). It is interesting to note that a number of bacteria contain several BSH homologues, which can vary greatly in their substrate selectivity and catalytic capacity (29, 38). Compared to tauro-conjugates, this enzyme exhibits higher substrate selectivity for glyco-conjugated acids, according to multiple sources (40, 41). Additionally, during periods of stationary growth, its production is higher. The arrangement and presence of BSH-encoding genes vary substantially in bifidobacteria and lactobacilli.

There are only five three-dimensional BSH (Figure 1.3.) enzyme structures known, and they come from *Bifidobacterium longum* (33), *Bacteroides thetaiotaomicron* VPI-5482 (43), *Clostridium perfringens* (32), *Enterococcus faecalis* (34) and *Lactobacillus salivarius* (42).

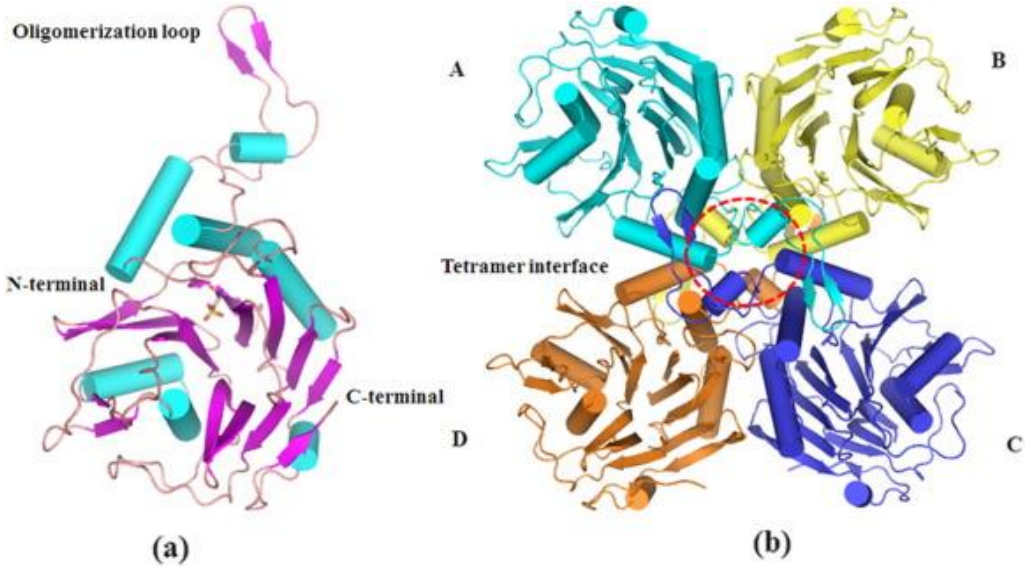

Figure 1. 3. (a) The composition of the *Bifidobacterium longum* BSH monomer subunit. (b) The bacterial BSH enzyme assembled into tetramers (1).

1.3. Substrate Specifty of BSH

Despite significant advancements in identifying and characterising new BSHs, the molecular mechanisms behind their discrimination and recognition of two substrate types remain unknown. The amino acid groups (glycine/taurine) and cholate steroid nucleus make up the substrates of BSH enzymes. When compared to taurine and glycine conjugates, Huijghebaert and Hofmann (44) showed that changing the amide bond or eliminating a negative charge from the terminal group of an amino acid residue in the BAs dramatically lowered the hydrolysis rate. According to Batta et al. (45), cholylglycine hydrolase was more effective at hydrolyzing conjugates of unconjugated BAs and taurine and glycine analogues with one or two methylene groups. However, the hydrolysis of conjugates which included analogues of taurine and glycine containing tertiary amide groups was fully inhibited. Most of the literature's kinetic data show that BSHs mainly identify substrates in amino acid moieties. Furthermore, because the sulphur atom in tauro-conjugated BAs causes steric hindrance, BSH enzymes are more attracted to glycine-conjugated bile salts than to their taurine-conjugated counterparts (22, 46). This substrate preference may have emerged because glyco-conjugated BAs exhibit greater toxicity to bacteria than tauro-conjugated BAs, particularly when pH is low (1, 22). Furthermore, the gut exhibits greater concentrations of glycine-conjugated BAs than taurine-conjugated BAs in certain host species (humans included), which may have provided selective pressure for this preference (47). Despite this, there is

some evidence indicating that the substrate preferences of BSH enzymes are affected by modifications in the side chains and the steroid ring system (48, 45, 49). It is plausible, consequently, BSHs have developed the ability to identify BAs at the steroid nucleus of cholate as well as at the amino acid groups. The affinities of BSH enzymes were not affected by the cholate's hydroxyl or epimerized hydroxyl substituents, according to Rossocha et al. (32) and Batta et al. (45). Moreover, cholate was bound by hydrophobic interactions rather than hydrogen bonds that made it challenging to identify recognition sites. As a result, it seems likely that the only requirements for binding might be that the cholate moieties and amino acids match and complement the substrate-binding pockets appropriately (33).

Enzymes that hydrolyze amide bonds, known as BSH enzymes, use their N-terminal nucleophile residue, Cys2, for this purpose. This residue is activated by a free α-amino group produced by an autocatalytic endoproteolytic process, which serves as a base in the catalytic reaction (31). Remaining residues in the catalytic reaction besides Cys2 which are strictly conserved in BSHs are Arg18, Asp21, Asn82, Asn173, and Arg226 (33, 50). Similar binding pocket residues may result in similar mechanisms of action for different enzymes (51). As a result, certain amino acids known as secondary structural elements and substrate-preference determining residues (SDRs) may be necessary for BSHs to prefer certain substrates (52). Recent methods such as binding site similarity-based scoring systems, crystal structures, comparative structural analyses, molecular docking and kinetic data have identified a number of important secondary structural elements and amino acid residues that may be involved in substrate binding in BSHs. The residues responsible for substrate binding are situated within three loops: Loop3 (131–142), Loop2 (59–68) and Loop1 (20–26). Nonetheless, no significant residues have been identified in Loop4 (261–269) (All residues in BlSBT2928_BSH's numbering system) (22). The four loops of BSHs demonstrate a high degree of hydrophobicity. However, the proportion of hydrophobic amino acids within these four loops is lowest in glyco-conjugating-specific BSHs compared to BSHs displaying substrate preference for TC/GC and TC. Rather, the four loops of these BSHs exhibit a greater proportion of charged and hydrophilic amino acids. According to research, BSH enzymes may use hydrophobic interactions with hydrophobic steroid moiety.

Furthermore, BSHs' catalytic framework and substrate preferences toward conjugated BAs are significantly influenced by polar complementarity (45, 54). All three of the GCA's hydroxyl groups showed polar complementarity and strong hydrogen bonding interactions when BlSBT2928_BSH and EfNCIM2403_BSH were analyzed. Compared to BlSBT2928_BSH, Cp13_CBAH1 exhibits reduced polar complementarity, which results in decreased enzyme activity (33, 54). Gaining more knowledge about the polar complementarity and structural alterations that occur during substrate binding would provide fresh perspectives on the various substrate preferences and roles that BSHs play.

1.4. Effects of Deconjugated Bile Acids

1.4.1 Cholesterol

Elevated blood cholesterol levels are deemed significant factors associated with cardiovascular disease in humans (55). Hypercholesterolaemia contributes mainly to atherosclerosis, the build-up of cholesterol in the coronary arteries resulting in atheroma, culminating in ischemic heart disease. Studies reveal that a decline in plasma cholesterol by 1% curbs the occurrence of coronary events by roughly 2-3% (56). The gut microbiota is linked with the metabolism of two cholesterol types: the first stems from the de novo synthesis of cholesterol from the liver or diet, while the second is cholesterol from tissues and BAs produced by cholesterol (57). Numerous studies (7, 58-69) have demonstrated the cholesterol-lowering effects of specific probiotics. The mechanisms of these probiotics involve absorbing cholesterol (62), integrating cholesterol into the cell membrane of probiotics (59, 62), transforming cholesterol into coprostanol (59), breaking down conjugated BAs via BSH activity (7, 60, 67, 70), attaching cholesterol to the cell membrane (62), and causing cholesterol precipitation with deconjugated BAs (67). The selection criteria for probiotic microbes that decrease cholesterol levels should include BSH activity. BSH-active probiotics have the capability to increase the deconjugation of bile salts in enterohepatic circulation resulting in heightened levels of deconjugated BAs in circulation. After deconjugation, the solubility of BAs decreases and they are absorbed in the intestinal tract, subsequently being excreted in faeces (71). Thereafter, cholesterol is utilised to synthesise de novo BAs in the body, eventually lowering serum cholesterol levels (29).

In their study, Oner et al. (72) researched the mechanism by which lactic acid bacteria and bifidobacteria reduce cholesterol. Their findings indicate that only probiotics containing the *bsh* gene are effective in reducing cholesterol levels. Additionally, enhanced activity of BSH results in a greater amount of bile being excreted in feces (73). In their study, Huang et al. (67) characterized and identified two BSH positive strains, namely *L. plantarum* Lp45and *L. plantarum* Lp09. Additionally, they looked into how *L. plantarum* Lp45 and *L. plantarum* Lp09 reduced cholesterol in male rats given a diet high in cholesterol. It is noteworthy that by giving immobilized BSH from *Lactobacillus buchneri* orally, Sridevi et al. (74) showed a significant decrease in serum cholesterol and triglycerides in a rodent model of hypercholesterolemia (60). It is noteworthy that, according to BSH, *L. reuteri* NCIMB30242 was the first probiotic strain to be sold for the purpose of lowering cholesterol (Cardioviva®). This implies that lipid metabolism may be impacted, and hypercholesterolemia may be decreased by microbial BSH activity. Additionally, it is worth mentioning that most *Lactobacillus* species that have been shown to have a hypocholesterolemic effect in human trials have been patented (75-78). The hypocholesterolemic effects are dependent on the deconjugation of primary intestinal BAs through BSH activity, leading to a reduction in cholesterol reabsorption (79).

1.4.2 Molecular Signals

Bacterial unconjugated BAs can enter cells freely and stimulate FXR, while conjugated BAs can only activate FXR in cells that express plasma membrane BA transporters (80). Furthermore, research conducted in vivo has demonstrated that conjugated bile salts are not as effective in activating FXR as unconjugated BAs (1). The activation of FXR enhances the liver's uptake of deconjugated BAs. Additionally, FXR in the liver helps to inhibit gluconeogenesis and lipogenesis. FXR was found to have an impact on the BA homeostasis, which led to a change in gut microbiota, ultimately causing weight reduction (81). Furthermore, FXR inhibits CYP7A1, thus preventing toxicity related to hydrophobic deconjugated BAs (82). Numerous established and theoretical concepts associate BA synthesis or metabolism with reducing weight gain. These include the increased rate of BSH activity and the activation of TGR5 and FXR by BAs serving as molecular signals (83).

Moreover, the activity of BSH can potentially impact the activation of TGR5 by altering BA pool composition. Various intracellular signalling pathways, which are related to energy expenditure and basal metabolism homeostasis, have been found to be activated by this G-protein coupled receptor (84). The secondary BAs, DCA and LCA, arising from unconjugated BAs, display the highest potential for the activation of TGR5, via LCA identified as the strongest natural ligand (85, 86). Stimulating glucagon-like peptide 1 (GLP-1) secretion via the activated enteroendocrine-bound TGR5 enhances pancreatic insulin release, ultimately elevating insulin sensitivity (87, 88). TGR5 activation has implications for energy metabolism in adipose tissue, as it can reduce weight gain and prevent insulin resistance in mice fed a high-fat diet (89).

1.4.3. Anti-Giardial Effect

One of the most prevalent waterborne parasite infections globally, giardiasis is a zoonotic disease caused by *Giardia duodenalis*, also referred to as *Giardia intestinalis* or *Giardia lamblia*. This flagellate protozoan infects a wide range of animals, including humans, mammals, reptiles, and birds (90, 91). It mainly affects children and people who are malnourished or immunocompromised in humans. Long-term infections must be treated with conventional antibiotic therapies, such as 5-nitroimidazole and benzimidazole medications, even though giardiasis may go away on its own (92). There are few alternative treatments available for *G. duodenalis* infections, which are common in cattle, small ruminants, and companion animals (93). Novel therapeutic approaches have been developed in response to the rise in clinical trial failures and the emergence of resilient *Giardia* strains in veterinary and medical applications (93, 94). In this context, it is established that the gut microbiota plays a central role in protecting against enteropathogens by producing antimicrobial compounds, competing for nutrients, and attaching to the mucosal surface (95, 96). Certain strains of lactobacilli, classified as probiotic bacteria, have demonstrated an ability to enhance host health by improving innate and adaptive immune responses (97, 98, 99). Furthermore, pre-clinical investigations indicate that the gut microbiota composition of the host plays a critical role in the colonisation of the small intestine by *G. duodenalis* trophozoites (100, 101, 102). In recent years, the use of probiotic-based therapies has been explored as a treatment for giardiasis (103). Despite the poor understanding of the

underlying mechanism (95, 104, 105), recent reports suggest a possible correlation between activity of BSH and protection against infection of *G. duodenalis* (106, 107). The conversion of primary BAs into deconjugated BAs through BSH activity may release secondary BAs, which, according to some suggestions, could be toxic and change the growth and survival of the parasite. Furthermore, the expression of BSH from *L. johnsonii* in engineered *E. coli* was found to inhibit the proliferation of *Giardia* in vitro and in vivo in a dose-dependent manner (107). Additionally, microbial BSH activity has several other effects on the host. Notably, Allain et al. (107) have recently reported that a BSH from *L. johnsonii* La1 is implicated in the anti-giardia effect of the strain both in vitro and in vivo. In a separate study, Allain and colleagues (108) looked into the anti-giardial properties of various lactobacilli strains derived from different origins.

1.4.4. Anti-Patojenic Effects

Clostridium difficile infection (CDI) is another gastrointestinal infectious disease. Patients receiving broad-spectrum antibiotic treatment may develop a colony of *C. difficile*, a pathogen that spores (109, 110). CDI encompasses a wide range of disorders, from diarrhoea to toxic and colitis megacolon (109). Upon germination, spores give rise to vegetative cells which produce toxins causing tissue damage, diarrhea and inflammation (111, 112). In the gastrointestinal tract, germination is initiated by a host-derived molecule which senses BAs using the germinant receptor (111, 113-115). DCA, CA and TCA were shown to activate germination, while CDCA was found to act as a competitive inhibitor (116). Recent reports have shown that patients with relapsing and severe CDI exhibit elevated TCA levels, along with reduced prevalence of species that produce BSH (117, 118). Additionally, supernatants derived from either genetically modified *E. coli* that expresses highly active BSH or organisms that naturally produce BSH (such as *Bacteroides vulgatus, Blautia obeum, Bacteroides ovatus* and *Collinsella aerofaciens*) have proven effective in reducing *C. difficile* germination mediated by TCA. These findings were confirmed in a recurring CDI mouse model using the BSH recombinant *E. coli* strain (117). These unique characteristics provide a potential avenue for the application of BSH active probiotics in the treatment of CDI.

An enzymatic mechanism has been found in *B. obeum* that breaks down the host-produced taurocholate (TC) molecule, which induces virulence. *B. obeum* uses this mechanism along with others to suppress the activation of the *Vibrio cholerae* virulence genes and colonisation (119). This mechanism is controlled by the enzyme BSH. This enzyme's activity reduced the colonization caused by *V. cholerae*, the major pathogen associated with diarrhoea in humans, by breaking down the bile salt TC that triggers the expression of virulence genes. The absence of these functions and species leads to an increase in personal, microbiome-specific infections. These findings offer new targets for personalised preventative strategies for *V. cholerae* infections by modifying the function and structure of the gut microbiome.

1.4.5. Other Positive Effects

A current investigation investigated the clinical responses to the effectiveness of the biotherapeutic agent UDCA in treating the intrahepatic cholestasis of pregnancy (ICP) (120). The authors explored the mechanism of reaction linked to the efficacy of UDCA in countering high levels of BAs (120). The study found that the gut microbiota plays a role in mediating the beneficial effects of UDCA through the enlargement of bacteria from the phylum Bacteroidetes that express BSH. Changes in the metabolism of BA have been associated with various liver diseases, such as primary sclerosing cholangitis (PSC). In a mice model, an analysis was performed on the BA composition and gut microbiota, which demonstrate that in germ-free mice, the severity of the illness increased (121). Tabibian et al. (121) also showed that the addition of UDCA reduces the effects of PSC, highlighting the potential of gut microbiota and BA for PSC protection.

In fact, primary BAs have been demonstrated to promote hepatic natural killer T cell (NKT cell) accumulation, leading to increased antitumor immunity and inhibition of tumorigenesis in a murine model (122). Additionally, BSHs are proposed to shield bacteria that are commensal in toxicity of BA and support gut colonization and bacterial survival (123-125). They are also thought to provide nutritional benefits as liberated amino acids can be utilized as origins of energy, carbon and nitrogen (29).

1.5. Negative Effects of BSH

BSH activity results in a rise in the formation of secondary BAs, which could negatively impact human health. The potential adverse effects of secondary bile salts on human health have been frequently discussed (17). Concentrations of these compounds in the intestine may enhance the development of carcinomas (126, 127, 128). Gallstones can form due to a modification in the proportion of bile salts to cholesterol resulting in the precipitation of cholesterol with bile pigments and calcium salts (129), or they may cause non-alcoholic fatty liver disease (130). Bile toxins may disturb the intestinal microflora, leading to diarrhoea, intestine mucosal inflammation and the initiation of carcinogenesis in the gut. Another disadvantage of deconjugated bile salts is their limited emulsifying capability in contrast to conjugated bile salts. This could lead to compromised lipid digestion and interfere with the absorption of monoglycerides and fatty acids (58). UCA is the sole therapeutic drug used for oral administration to dissolve gallstones (12). Furthermore, compared to the younger population, the elderly exhibit a higher level of fecal DCA (132,133). This demonstrates that excess BSH production in the small intestine causes an increase in the deconjugation of BAs (133). The subsequent exposure of the colon to high levels of deconjugated BAs elevates the risk of their conversion into cancer-causing compounds, ultimately leading to colon cancer development (131, 134). Modulating BSH activity to repress secondary BA metabolism might offer a novel form of treatment.

1.6. BSH Inhibitors

Since the 1950s, feed additives known as antibiotic growth promoters (AGPs), which are a class of antibiotics used in sub-therapeutic dosages, have been used to raise the feed conversion and average daily ratio of food animal weight gain (135, 136). Current epidemiological research clearly indicates that AGPs exert selection pressure on the formation, survival, and spread of bacteria resistant to antibiotics, which raises concerns about food safety and public health (136, 137) Due to concerns regarding AGP use in the feed industry, there is a worldwide trend to restrict their use (135, 136, 138). This necessitates the development of effective alternatives to AGPs to ensure the sustainability and productivity of food animals. It is widely acknowledged that AGPs enhance growth performance by modifying intestinal microbial diversity and causing shifts in bacterial populations (139).

Although the precise gut microbial community necessary for optimal growth promotion through AGP mediation remains largely unresolved, earlier animal studies (140-143) have suggested a strong, inverse correlation between the efficacy of AGPs in promoting growth in pigs and chickens, and diminished activity of BSH (EC 3.5.1.24), which is an enzyme created by several commensal bacteria found in the intestine (135, 29). Weight loss in the host may result from lipid malabsorption brought on by BSHs from gut bacteria deconjugating BAs (29, 144). Conversely, reducing the activity of intestinal BSHs improves energy harvesting and lipid metabolism, which boosts feed efficiency and growth performance in animals rose for food. Many BSH inhibitors have been developed recently to improve the productivity and growth performance of animals. It has been demonstrated that copper and zinc, which block BSH activity, enhance growth performance and feed efficiency in pigs (143, 145) and poultry (146, 147). Several BSH inhibitors, such as phenethyl caffeate and riboflavin, have been identified by an effective high-throughput screening system as potential substitutes for AGPs (139). The design of potent, safe and cost-effective BSH inhibitors, however, requires a detailed understanding of the molecular basis of BSH catalysis and substrate preference.

1.7. Distribution of BSH

Jones et al. (35) used functional metagenomic analysis to show that gut-related bacterial communities were generally home to active BSH proteins. All of the recognized gut microbiome's principal phyla, which include *Actinobacteria*, *Proteobacteria, Bacteroidetes* and *Firmicutes,* have been shown to contain the BSH enzyme (35, 148). The majority of them have been found in a number of genera of animal gut autochthonous microorganisms, such as *Streptococcus* (153), *Lactobacillus* (150, 151), *Bifidobacterium* (149) and *Enterococcus* (152). Most of the total amount of in vivo BSH activity is attributed to lactobacilli, which make up a significant portion of the animal intestinal microbiota (154). It has been demonstrated that certain human intestinal archaea species, including *Methanobrevibacter smithii* and *Methanosphaera stadtmanae*, produce BSHs (35). It has also been reported that some pathogens, such as *C. perfringens* (157), *Listeria monocytogenes* (156) and *Brucella abortus* (155), encode BSHs. The only Gram-negative bacteria known to display BSH activity are opportunistic pathogens from the *Bacteroides* (160, 161) and *Xanthomonas* (158, 159) genera, as well as *B.*

abortus (155). It's interesting to note that *Brevibacillus* species a free-living bacteria isolated from hot springs (162, 163).

L. gasseri (165, 166) showed a single gene. On the other hand, two genes have been verified in *L. acidophilus* NCFM (bshA and bshB) (48) and *L. johnsonii* (167) or three also in *L. johnsonii* PF01 (168). *L. salivarius* possesses two genes (169), but Jiang et al. (165) identified just one gene. The authors agreed that four distinct genes are present in *L. plantarum* that are involved in BSH activity (150, 151). Recent work has demonstrated that lactobacilli often harbor multiple distinct BSHs as a strategy to adapt to their host niche in the gut, making them a rich source of BSH diversity (170). Additionally, taxonomic profiling of BSHs demonstrated that lactobacilli encode for several prominent and highly active BSH phylotypes (38).

2. AIM AND SCOPE OF THE STUDY

The precise function of BSH remains unexplained to date. The initial assumption was that it aided in the detoxification of bile, thereby leading to improved survival under gastrointestinal conditions (123, 171). The notion that deconjugation products at low pH, such as those caused by lactic acid bacteria, can endure and leave the gastrointestinal tract likewise reinforces the detoxification theory (29). Nevertheless, deconjugated bile salts also exhibit strong antimicrobial properties. Free BAs, such as DCA and CA, might be more toxic compared to their conjugated counterparts. CA, in particular, is highly hydrophobic and can swiftly permeate cells (172). Consequently, some authors posit that deconjugation may represent a defensive strategy that bolsters indigenous gastrointestinal microbiota against pathogens (173).

Undoubtedly, BSH activity plays a crucial role in host physiological functions and BA balance. A variety of human illnesses, such as inflammatory bowel disease (IBD), irritable bowel syndrome (IBS) and susceptibility to *Clostridium difficile* infection (CDI), have been observed to be linked to decreased host BSH activity and abnormal BA pools (117, 174). If this hydrolysis is more extensive in the host's intestine, it could result in a condition known as steatosis. Furthermore, higher levels of secondary BAs have been linked to the promotion of colorectal carcinoma (175).

The relationship between residues in BSH substrate specificity and binding pockets is still unknown, despite the fact that important amino acids from these species and the crystal structures of BSHs are understood. Studies on mutagenesis involving these residues could aid scientists in gaining a deeper insight into the chemical interactions that transpire during the binding of substrates to these enzymes. The aim of this study was to investigate the correlation between substrate selectivity and the crucial loop II residues within the LpBSH substrate binding pocket. For tauro and glycol conjugated BAs, the LpBSH demonstrates catalytic activity (176, 177). The *L. plantarum* B14 strain is a good candidate to investigate the activity and specificity of BSH because of its affinity for bile salts conjugated with both taurine and glycine.

3. MATERIALS AND METHODS

3.1 Conditions of Culture, Plasmids and Bacterial Strains

Table 3.1 contains a list of the plasmid DNAs and bacterial strains that were used in this investigation. pCON1 was created in a previous study (176) to prepare the template DNA containing the *bsh* gene of *L. plantarum* B14. Cultures were incubated aerobically for two consecutive passages in LB Broth, also known as LB Medium, Lysogenia Broth, Luria Broth or Luria-Bertani medium (185). Transgenic *E. coli* XL1-Blue and BLR(DE3) strains that were harboring pBluescript (Stratagene, USA) and pET22b (Novagen, USA) plasmids were cultured in liquid or solid LB medium that was enhanced with ampicillin (100 µg/ml). The cultures were then cultivated for 16–18 hours at 37°C with 175 rpm shaking or in an incubator. Solid LB medium was prepared by adding 1.5% (w/v) agar to the medium.

Table 3.1. Plasmids and strains of bacteria

Strain	Genotype – Origin	Phenotype	Reference
Lb.plantarum B14	Human origin		(176)
Escherichia coli	**Genotype – Origin**	**Phenotype**	**Reference**
XL1-Blue	rec A end A 1 gyr A986 thi-1hsdr17supE44 rel A1 lac		Stratagene
BLR (DE3)	F-ompT gal dcm lon hsdSB (rB- mB-) λ(DE3)		Novagen
Plasmid	**Genotype**	**Phenotype**	**Reference**
pBluescript	SKII+	Amp^r	Fermentas
pCON1	pBluescript $SKII^+$ with 1.0 kb *bsh* gene insert	Amp^r	(176)
pET22b(+)	pelB, T7 lac, ApR, pBR322 ori (C-terminal His-tagged protein)	Amp^r	Novagen
pCON2	with 1.0 kb *bsh* gene insert and fragment from MCS site of $pET22b^{(+)}$	Amp^r	(176)
pCON1V58F	Substitution of valine for phenylalanine in pCON1	Amp^r	This work
pCON1V58M	Substitution of valine for methionine in pCON1	Amp^r	This work
pCON1V58N	Substitution of valine for asparagine in pCON1	Amp^r	This work
pCON1Y65C	Substitution of tyrosine for cysteine in pCON1	Amp^r	This work
pCON1Y65F	Substitution of tyrosine for phenylelanine in pCON1	Amp^r	This work
pCON1Y65L	Substitution of tyrosine for leucine in pCON1	Amp^r	This work
pCON1V58MY65F	Substitution of tyrosine-65 for phenylelanine in pCON1V58M	Amp^r	This work
pCON1V58MY65L	Substitution of tyrosine-65 for leucine in pCON1V58M	Amp^r	This work
pZEKV58F	Substitution of valine for phenylalanine in $pET22b^{(+)}$	Amp^r	This work
pZEKV58M	Substitution of valine for methionine in $pET22b^{(+)}$	Amp^r	This work
pZEKV58N	Substitution of valine for asparagine in $pET22b^{(+)}$	Amp^r	This work
pCON2Y65C	Substitution of tyrosine for cysteine in $pET22b^{(+)}$	Amp^r	This work
pCON2Y65F	Substitution of tyrosine for phenylelanine in $pET22b^{(+)}$	Amp^r	This work
pCON2Y65L	Substitution of tyrosine for leucine in $pET22b^{(+)}$	Amp^r	This work
pZEKV58MY65F	Substitution of valine for methionine-58 and tyrosine-65 for phenylelanine in $pET22b^{(+)}$	Amp^r	This work
pZEKV58MY65L	Substitution of valine for methionine-58 and tyrosine-65 for leucine in $pET22b^{(+)}$	Amp^r	This work

3.2 Mutant Constructions of pCON1

3.2.1 Analysis of Target Amino Acid Sequences

The BioEdit sequence alignment program was used to analyze and align the *L. plantarum* B14 *bsh* gene sequence, while the Clustal W program was used for alignment. The ExPASY program from http://web.expasy.org/compute_pi/ was used to calculate the theoretical molecular mass of BSH. The amino acid sequence of BSH was ascertained using Jalview 2.8 and contrasted with the *bsh* gene amino

acid sequences listed in GenBank (NCBI). The precise monomeric unit and target amino acid locations of the created BSH enzyme were ascertained using PyMOL (PyMOL Executable Build is Copyright (C) 2006 DeLano Scientific LLC, South San Francisco, California, USA).

3.2.2. Site-directed Mutagenesis on Wild-type BSH Enzyme

By using the appropriate primers in Table 3.2, PCR-based site-directed mutagenesis was used to replace the amino acids valine-58 (GTA) and tyrosine-65 (TAC), which are believed to be effective for the *L. plantarum* BSH enzyme's substrate selectivity, with different characteristic amino acids: phenylalanine-58 (TTT), methionine-58 (ATG), asparagine-58 (AAC), phenylalanine-65 (TTT), leucine-65 (CTG) and cysteine-65 (TGC). The target codons were replaced with the desired codons using the Quick Change Site-Directed Mutagenesis protocol (Stratagene) that target codons were designed on the basis of the *E. coli* codons used in the expression of a foreign gene in *E. coli* (Figure 3.1.) The reactions were conducted in a 50 µl volume with the following contents: plasmid DNA that used pCON1 DNA (pBluescript/bsh1) as a template, forward and reverse primers (25 µM each), dNTP mix (5 mM), MgCl2 (25 mM), reaction buffer (10X) and enzyme *Pfu* DNA polymerase (Fermentas, Europe) (Table 3.3). PCR amplicons were generated under the conditions outlined in Table 3.4 using a Techne 3000 PCR system (Barloworld Scientific). Following the PCR, methylated pCON1 template DNA was removed using *Dpn*I (Fermentas, Thermo Scientific) under the guidelines listed in Table 3.5.

	Codon	Amino acid[2]	%[3]	Ratio[4]	Codon	Amino acid	%	Ratio	Codon	Amino acid	%	Ratio	Codon	Amino acid	%	Ratio	
U	UUU	Phe (F)	1.9	0.51	UCU	Ser (S)	1.1	0.19	UAU	Tyr (Y)	1.6	0.53	UGU	Cys (C)	0.4	0.43	U
	UUC	Phe (F)	1.8	0.49	UCC	Ser (S)	1.0	0.17	UAC	Tyr (Y)	1.4	0.47	UGC	Cys (C)	0.6	0.57	C
	UUA	Leu (L)	1.0	0.11	UCA	Ser (S)	0.7	0.12	UAA	STOP	0.2	0.62	UGA	STOP	0.1	0.30	A
	UUG	Leu (L)	1.1	0.11	UCG	Ser (S)	0.8	0.13	UAG	STOP	0.03	0.09	UGG	Trp (W)	1.4	1.00	G
C	CUU	Leu (L)	1.0	0.10	CCU	Pro (P)	0.7	0.16	CAU	His (H)	1.2	0.52	CGU	Arg (R)	2.4	0.42	U
	CUC	Leu (L)	0.9	0.10	CCC	Pro (P)	0.4	0.10	CAC	His (H)	1.1	0.48	CGC	Arg (R)	2.2	0.37	C
	CUA	Leu (L)	0.3	0.03	CCA	Pro (P)	0.8	0.20	CAA	Gln (Q)	1.3	0.31	CGA	Arg (R)	0.3	0.05	A
	CUG	Leu (L)	5.2	0.55	CCG	Pro (P)	2.4	0.55	CAG	Gln (Q)	2.9	0.69	CGG	Arg (R)	0.5	0.08	G
A	AUU	Ile (I)	2.7	0.47	ACU	Thr (T)	1.2	0.21	AAU	Asn (N)	1.6	0.39	AGU	Ser (S)	0.7	0.13	U
	AUC	Ile (I)	2.7	0.46	ACC	Thr (T)	2.4	0.43	AAC	Asn (N)	2.6	0.61	AGC	Ser (S)	1.5	0.27	C
	AUA	Ile (I)	0.4	0.07	ACA	Thr (T)	0.1	0.30	AAA	Lys (K)	3.8	0.76	AGA	Arg (R)	0.2	0.04	A
	AUG	Met (M)	2.6	1.00	ACG	Thr (T)	1.3	0.23	AAG	Lys (K)	1.2	0.24	AGG	Arg (R)	0.2	0.03	G
G	GUU	Val (V)	2.0	0.29	GCU	Ala (A)	1.8	0.19	GAU	Asp (D)	3.3	0.59	GGU	Gly (G)	2.8	0.38	U
	GUC	Val (V)	1.4	0.20	GCC	Ala (A)	2.3	0.25	GAC	Asp (D)	2.3	0.41	GGC	Gly (G)	3.0	0.40	C
	GUA	Val (V)	1.2	0.17	GCA	Ala (A)	2.1	0.22	GAA	Glu (E)	4.4	0.70	GGA	Gly (G)	0.7	0.09	A
	GUG	Val (V)	2.4	0.34	GCG	Ala (A)	3.2	0.34	GAG	Glu (E)	1.9	0.30	GGG	Gly (G)	0.9	0.13	G
	U				C				A				G				

[1] The data shown in this table is from the Arabidopsis Research Companion on the World Wide Web (//weeds/mgh.harvard.edu). Codon frequencies for many other bacteria can be found at http://morgan.angis.su.oz.au/Angis/Tables.html.

[2] The letter in parenthesis represents the one-letter code for the amino acid.

[3] % represents the average frequency this codon is used per 100 codons.

[4] Ratio represents the abundance of that codon relative to all of the codons for that particular amino acid.

Figure 3. 1. Codon usage in *E. coli* Genes

Table 3.2. Primers for mutagenesis with site-directed

Primers name	Primer Sequences (5' to 3')	Tm
V58FF	5'- TGGAATTACTGCTGAT**TTT**GAAAGCTATCCAC -3'	63°C
V58FR	5'- GTGGATAGCTTTC**AAA**ATCAGCAGTAATTCCA -3'	63°C
V58MF	5'- TGGAATTACTGCTGAT**ATG**GAAAGCTATCCAC -3'	63°C
V58MR	5'- GTGGATAGCTTTC**CAT**ATCAGCAGTAATTCCA -3'	63°C
V58NF	5'- TGGAATTACTGCTGAT**AAC**GAAAGCTATCCAC -3'	63°C
V58NR	5'- GTGGATAGCTTTC**GTT**ATCAGCAGTAATTCCA -3'	63°C
Y65CF	5'- GCTATCCACTTTAC**TGC**GATGCGATGAATG -3'	66°C
Y65CR	5'- CATTCATCGCATC**GCA**GTAAAGTGGATAGC -3'	66°C
Y65FF	5'- GCTATCCACTTTAC**TTT**GATGCGATGAATG -3'	62°C
Y65FR	5'- CATTCATCGCATC**AAA**GTAAAGTGGATAGC -3'	62°C
Y65LF	5'- GCTATCCACTTTAC**CTG**GATGCGATGAATG -3'	65°C
Y65LR	5'- CATTCATCGCATC**CAG**GTAAAGTGGATAGC -3'	65°C

Table 3.3. PCR-Reactive materials for V58F, V58M, V58N, Y65C, Y65F and Y65L mutagenesis

Reactants	Concentrations	Quantities
UP (ultra pure) H_2O	-	33.25 µl
Template DNA (100 ng)	135 ng/µl	0.75µl
$MgCl_2$ (25 mM)	25 mM	4 µl
dNTP mix (5 mM)	5 mM	2 µl
Forward Primer (25 µM)	25 µM	2 µl
Reverse Primer (25 µM)	25 µM	2 µl
Pfu DNA Polymerase Buffer (10X)	10X	5 µl
Pfu DNA Polymerase Enzyme (2.5 U/µl)	2.5 u/µl	1 µl
TOTAL VOLUME	-	**50 µl**

Table 3.4. Conditions for PCR reactions

Cycles	Temperatures						Time
	V58F	V58M	V58N	Y65C	Y65F	Y65L	
Initial denaturation	95°C	95°C	95°C	95°C	95°C	95°C	30 sec
Denaturation	95°C	95°C	95°C	95°C	95°C	95°C	1 min
Annealing	59°C	59°C	59°C	62°C	58°C	61°C	1 min
Extension	72°C	72°C	72°C	72°C	72°C	72°C	9 min
Final extension	72°C	72°C	72°C	72°C	72°C	72°C	5 min
Number of cycles							**20**

Table 3.5. Conditions of reaction for *Dpn*I digestion of PCR products

Reactants	Quantities	
Up H_2O	4 µl	at 37 °C
PCR product (>500 ng)	40 µl	
Tango Buffer (10X)	5 µl	for 2 h.
*Dpn*I enzyme (10U/µl)	1 µl	
TOTAL VOLUME	**50 µl**	

3.2.3 Purifying Mutated PCR Products

Gel extraction kit Thermo Scientific GeneJET (Massachusetts, USA) was used to recover approximately 1 kb of PCR products from agarose gels after PCR products from pCON1*V58F, pCON1*V58M, pCON1*V58N, pCON1*Y65C, pCON1*Y65F, and pCON1*Y65L (* indicates desired mutations) were placed on gel with 1% agarose and electrophoresed for an hour at 75 volts.

3.2.4 Preparing XL1-Blue and BLR(DE3) Competent Cells

Plates of solid LB medium containing *E. coli* BLR(DE3) (Novagen, USA) or XL1-Blue (Stratagene, USA) strains were incubated at 37°C for an overnight. Three milliliters of LB broth were inoculated with a single colony of BLR(DE3) or XL1-Bluenand the mixture was shaken at a rate of 175 rpm for a period of 14 to 16 hours. After that, 1% of the medium was moved to 50 ml of LB, and it was once again incubated for 2 to 2.5 hours at 125 rpm until an 0,5 at OD_{600} was achieved. The culture medium was separated into two 20 ml sterile falcon tubes and the cells were centrifuged for 5 min at 4000 rpm and 4°C. Following that, the pellets were again suspended in 10 milliliters of calcium chloride, $CaCl_{2,}$ (pH: 7.0, 100mM,). This was followed by centrifugation at 4°C for 10 minutes at 4000 rpm. After resuspension of pellets in 1ml $CaCl_2$ solution with 10% glycerol, aliquots of 100 µl per culture tube were taken and stored in a freezer at -80°C.

3.2.5 Mutants of pCON1* Transforming into the *E. coli* XL1-Blue

For each transformation, 10 µl of PCR purified products from pCON1*V58F, pCON1*V58M, pCON1*V58N, pCON1*Y65C, pCON1*Y65F and pCON1*Y65L were added to 100 µl of competent cells and incubated for 45 minutes on ice and 5 minutes at 37°C, then re-incubated for 5 minutes on ice. After heat shock, the samples were incubated in 1 ml LB medium for 1 hour at 37 °C at 175 rpm. Pellets formed by centrifugation of the growing cells for 3 minutes at 6000 rpm were resuspended in 100 µl LB medium. The cell suspensions were plated on ampicillin-containing LB agar and cultivated at 37°C for 16-18 hour. The four randomly selected transformed colonies were grown overnight at 37°C in 5 ml LB medium containing amphicillin (100 µg/ml). Plasmid miniprep kit (Thermo Scientific GeneJET, Lithuania, EU) was used to isolate plasmid DNA from the cell pellets after the growing cell medium was centrifuged for 3 min at 6000 rpm.

3.2.6 Detection of Targeted Mutations by DNA Sequencing

Using M13/pUC forward and reverse universal primers, Macrogen Inc. (Seoul, Korea) carried out DNA sequencing of recombinant mutant DNAs. The BioEdit Sequence Alignment Programme confirmed the *bsh* gene with mutation, which is roughly 1 kb in size.

3.2.7 Preparation of Stock

The target-mutant clones pCON1V58F, pCON1V58M, pCON1V58N, pCON1Y65C, pCON1Y65F, and pCON1Y65L were cultured in 5 ml of LB containing ampicillin (100 µg/ml) at 37°C and 175 rpm of shaking for overnight. After that, cell medium was centrifuged for 4 minutes at 25°C and 4000 rpm. The pellets were resolved in 30% glycerol-containing 4 ml LB and stored in cryogenic tubes in a freezer maintained at -80°C for extended storage.

3.3 Making Mutant pZEK Constructs

3.3.1 Preparation of pET22b Expression Vector

A colony of *E. coli* BLR(DE3) carrying the pET22b expression vector was incubated overnight in 10 ml LB medium containing ampicillin (100 µg/ml) at 37°C with shaking at 175 rpm. The overnight cell culture was centrifuged at 4000 rpm for 4 minutes at 25°C and the pellet was obtained through centrifugation for 3 minutes at 6000 rpm after dissolution with 1 ml LB. Using the plasmid miniprep kit

(Thermo Scientific GeneJET, Lithuania, EU), plasmid DNAs were extracted from the pellet. The plasmid DNA of pET22b was digested by *Not*I and *EcoR*I restriction enzymes (Thermo Scientific) for 45 min at 37°C in order to clone the bsh gene carrying the target mutations into the pET22b expression vector, as shown in Table 3.6. after which the digested pET22b expression vector was extracted using the Gel DNA recovery kit (Vivantis, Selangor, Malasia) from 1% agarose gel.

Table 3.6. Conditions of pET22b DNA digestion by *Not*I and *EcoR*I.

Reactants	Quantities	
Up H_2O	20 µl	at 37 °C
pET22b (>500 ng)	30 µl	
Fast Digest Buffer (10X)	6 µl	for 45 min.
*EcoR*I enzyme (Fast Digest)	2 µl	
*Not*I enzyme (Fast Digest)	2 µl	
TOTAL VOLUME	**60 µl**	

3.3.2 Digestion of Mutant Recombinant DNAs by *Not*I and *EcoR*I Restriction Enzymes into pBluescript SKII $^+$ Vector

The V58M, V58F, V58N, Y65L, Y65F and Y65C, mutant *bsh* genes were obtained from pCON1V58M, pCON1V58F, pCON1V58N, pCON1Y65L, pCON1Y65F and pCON1Y65C clones using *Not*I and *EcoR*I restriction enzymes (Thermo Scientific, Lithuania, EU) (Table 3.7). The Vivantis GF-1 gel DNA recovery kit (Vivantis, Selangor, Malasia) was used to purify mutant V58F, V58M, V58N, Y65C, Y65F and Y65L *bsh* gene fragments from 1% agarose gel in accordance with the manufacturer's instructions.

Table 3.7. Conditions of mutant recombinant DNAs digestion by *EcoR*I and *Not*I.

Reactants	Quantities	
Up H_2O	18 µl	at 37 °C
Mutant Recombinant DNAs (>500 ng)	40 µl	
Fast Digest Buffer	7 µl	for 2 h.
*EcoR*I Enzyme (Fast Digest)	2.5 µl	
*Not*I Enzyme (Fast Digest)	2.5 µl	
TOTAL VOLUME	**70 µl**	

3.3.3 Mutant *bsh* genes Ligation into pET22b

The T4 DNA ligase enzyme (Thermo Scientific) was used to individually ligate the purified mutant V58M, V58F, V58N, Y65L, Y65F and Y65C, *bsh* genes into the pET22b expression vector. This process was carried out for one hour at

22°C (Table 3.8). The newly created constructs were given the names pCON2Y65C, pCON2Y65F, pCON2Y65L, pZEKV58F, pZEKV58M, and pZEKV58N. The following formula was used to calculate the proper amounts of insert and vector DNA for an efficient ligation:

$$\text{Insert Mass (ng)} = \text{Ration x} \left[\frac{\text{Insert Length (kb)}}{\text{Vector Length (kb)}} \right] \text{x Vector Mass (ng)}$$

Table 3.8. Insertion of mutant BSHs into pET22b

Reactants	Quantities	
Up H_2O	11 µl	at 22 °C
pET22b Vector (*EcoRI*/*Not*I digested) (>500 ng)	4 µl	
Mutant BSHs DNAs (*EcoRI*/*Not*I cut)	2 µl	for 1 h.
T4 10X Ligase Buffer	2 µl	
T4 DNA Ligase Enzyme (5 U/µl)	1 µl	
TOTAL VOLUME	**20 µl**	

3.3.4 Incorporation of pZEK Mutants into BLR (DE3) of *E. coli*

Samples containing 100 µl of BLR(DE3) competent cells and 10 µl of pZEKV58F, pZEKV58M, pZEKV58N, pCON2Y65C, pCON2Y65F or pCON2Y65L ligation products were incubated for 45 minutes on ice, followed by 5 min at 37°C and another 5 min on ice. Following an hour of growth in 1 ml LB broth medium at 175 rpm and 37°C in a shaking incubator, the ligation samples were centrifuged for 3 minutes at 6000 rpm, and the cell pellets were resuspended in 100 µl LB. For 37°C growth, the solved cells were plated on LB agar plates supplemented with ampicillin (100µg/ml).

3.3.5 Accuracy of Mutant *bsh* Genes in pZEK Constructs

Colonies randomly selected from ampicillin LB plates of transformants were grown in 10 ml LB medium supplemented with ampicillin (100 µg/ml) for 16-18 hours at 37°C at 175 rpm on a shaker and simultaneously plated onto ampicillin LB plates at 37°C overnight for later stocking. The growing transformant cells were pelleted by centrifugation for 3 minutes at 6000 rpm and using the Thermo Scientific GeneJET Plasmid Miniprep Kit (Lithuania, EU), DNA was extracted from *E. coli* BLR(DE3) clone pellets. To determine whether the mutant *bsh* genes were correctly inserted into the pZEKV58F, pZEKV58M, pZEKV58N,

pCON2Y65C, pCON2Y65F or pCON2Y65L constructs were digested with *Eco*RI and *Not*I resriction enzymes as specified in Table 3.9 and the digested pZEKV58F, pZEKV58M, pZEKV58N, pCON2Y65C, pCON2Y65F or pCON2Y65L DNA samples were loaded onto a 1% agarose gel and electrophoresed for 1 hour at 75 volts. The mutant gene-verified colonies from pZEKV58F, pZEKV58M, pZEKV58N, pCON2Y65C, pCON2Y65F or pCON2Y65L constructs were grown in 10 ml ampicillin (100 µg/ml) LB medium at 37°C for 16-18 hours at 175 rpm and then pelleted by centrifugation for 3 min at 6000 rpm. The pellets were again suspended in 30% glycerol in 4 ml of LB and stored at -80°C.

Table 3.9. Conditions of pZEK and pCON2 DNAs digestion by *Not*I and *Eco*RI

Reactants	Quantities	
Up H_2O	5.5 µl	at 37 °C
pZEK and pCON2 Mutant DNAs (>500 ng)	3 µl	
Fast Digest Buffer (10X)	1 µl	for 30 min.
*Eco*RI Enzyme (Fast digest)	0.25 µl	
*Not*I Enzyme (Fast digest)	0.25 µl	
TOTAL VOLUME	**10 µl**	

3.4 Assay of the BSH Activity in the pZEK Constructs

3.4.1 Direct Plate Assay

To ascertain the mutant BSH enzymes' BSH activity contained in the pZEK constructs, a direct plate assay developed by Christiaens et al. in 1992 (187) was used with a few modifications; these assay plates contained LB agar containing ampicillin (100 µg/ml) with 5 g/L TDCA or 2 mM GDCA 1 mM isopropyl-β-D-1-thiogalactopyranoside (IPTG), 0.35 g/L $CaCl_2$. Plates containing the negative control (pET22b), positive control (pCON2), and mutant transformants, pZEKV58F, pZEKV58M, pZEKV58N, pCON2Y65C, pCON2Y65F, or pCON2Y65L, were then incubated for 72 hours at 37°C and the plates were examined for opaque appearance. A positive reaction for BSH activity was seen when bile acid precipitation produced a bright, opaque halo (Figure 3.1).

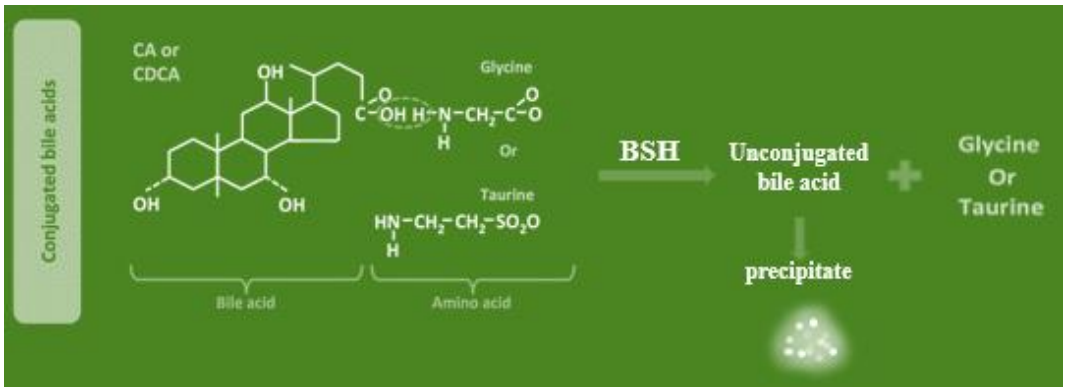

Figure 3.2. BSH Activity Assay

3.4.2 Overexpression of Mutant *bsh* Genes

The pZEKV58F, pZEKV58M, pZEKV58N, pCON2Y65C, pCON2Y65F or pCON2Y65L and pCON2 (*bsh*/pET22b) transformants were individually cultivated in ampicillin (100µg/ml) containing 10ml LB at 37°C and 175rpm on a shaker for 16-18 hours after successful transformation of pZEKV58F, pZEKV58M, pZEKV58N, pCON2Y65C, pCON2Y65F or pCON2Y65L into *E. coli* BLR(DE3) competent cells. From the overnight cultures, 5ml (2% of the total) was transferred to. 250 ml of LB broth supplemented with 4% glycerol and 100 µg/ml ampicillin. The cultures were then grown at 175 rpm and 37 °C until their optical density reached OD_{600}:0.45 - 0.6. 0.3 mM IPTG was used to induce the protein expression of mrBSH and rBSH. The cultures were then reincubated at 37°C and 175 rpm until they achieved OD_{600} values of 1.5-3.0. After the cultures reached an OD_{600} of 1.5–3.0, they were centrifuged at 8000g for 15 minutes and at 4˚C. Re-suspended pellets were placed in 2 ml of cold binding buffer (pH: 7.8) with 500 ml of sodium chloride and 20 ml of sodium phosphate. The cell suspension was then mixed with 1 mg/ml lysozyme and allowed to incubate for 10 minutes at 4°C on a rocking platform. After incubation, 1% Tween-20, 5µg/ml DNase and 5µg/ml RNase were added to the mixture and incubated for 10 minutes at 4°C on a rocking platform. The soluble fraction was centrifuged at 14000g for 20 minutes at 4°C to remove cell debris. The supernatant was filtered through a 0.45 µm filter and collected in clean polystyrene tubes. Ninhydrin assay and rBSH and mrBSH protein purification were performed on the prepared cell extracts. In the ninhydrin assay, the total protein concentration of the cell extract was measured using bovine serum albumin (BSA) as a standard protein according to the Lowry method (178).

3.4.3 Partially Purification of the Mutant BSH Enzymes

After overexpressing and extracting cells, the wild-type and mutant BSHs underwent partial purification using the nickel-chelated column on the GE Healthcare Bio-sciences ÄKTAprime plus™ chromatography system, in accordance with the manufacturer's guidelines. The His TrapTM HP column was loaded with the part of cell extracts that is soluble and contains wild-type and mutant BSHs. The protein-coupled column was eluted with elution buffer (at pH 6, 500 mM sodium chloride, 20 mM sodium phosphate buffer and 200mM imidazole).

3.4.4 Ninhydrine Assay

The ninhydrin assay, modified from Tanaka et al. (8), was used to determine the substrate specificity of the mutant BSH enzymes. The assay's foundation is the interaction of ninhydrin reagent with amino acids produced by the hydrolysis of conjugated bile salts, and the subsequent colorimetric shift that is observed. The Lowry test was used to determine the cell extracts' total protein concentration (178) and standardized to 10 µl of sample using the proper dilution before initiating the assay for ninhydrin. The substrate specificities of wild-type BSH (positive control) and mutant BSH enzymes against the six different human BAs, GCA, TCA, GDCA, TDCA, GCDCA and TCDCA, were determined by ninhydrin assay at 37ºC and pH 6. Initially, 10 µl sample was incorporated into the mixture that contained 50 µl of 40 mM bile salt, 50 µl of 40 mM dithiothreitol (DTT) and 100 µl of 0.1 M sodium phosphate buffer (pH: 6.0). The final mixture was incubated for 30 minutes at 37 °C. After adding 210 µl of trichloroacetic acid to the mixture in order to stop the enzymatic reaction, the mixture was centrifuged at 14000g for 15 min. 1.9 ml of ninhydrin reagent (0.5 ml of 1% ninhydrin in 0.5M sodium citrate buffer (pH 5.5), 1.2 ml of glycerol and 0.2 ml of 0.5M sodium citrate buffer (pH 5.5)) was mixed with 20 mL of supernatant and 80 ml of ultrapure water. Following a vortex and a 15-minute boil, the sample was treated. After cooling, the samples' absorbance at 570 nm was measured using a standard curve of glycine using the U-1900 spectrophotometer (HITACHI, Japan). All experiments were carried out in triplicate.

3.4.5 SDS PAGE Analysis

According to Laemmli's (184) instructions, sodium dodecyl sulfate-polyacrylamide gel electrophoresis (SDS-PAGE) was carried out on a 12% (w/v) polyacrylamide separating gel with 0.1% (w/v) SDS in order to observe the production of mutant and wild BSH enzymes. Coomassie Brilliant Blue R250 staining was used to detect protein bands. The Lowry method (178) using bovine serum albumin as a standard was used to determine protein concentration. The marker used was a Page Ruller Prestained Protein Ladder (Thermo Scientific).

3.5 Mutant Constructions of pCON1V58M-Y65F and pCON1V58M-Y65L

3.5.1. Site-directed Mutagenesis on pCON1V58M

In order to determine whether there is a relationship between the 58 and 65 regions of BSH, according to the ninhydrin results of the mutations, phenylalanin and leucine are effective on the activity in 65, cysteine was not selected because of almost completely effective, and 58 metionine that is more effective were selected and double mutations for V58M-Y65F and V58M-Y65L were determined. By using the appropriate primers in Table 3.10, PCR-based site-directed mutagenesis was used to replace the amino acids Tyrosine-65 (TAC) for double mutation with different characteristic amino acids: Phenylalanine-65 (TTT), leucine-65 (CTG) on mutant V58M *bsh* gene. The target codons were replaced with the desired codons using the Quick Change Site-Directed Mutagenesis protocol (Stratagene). The reactions were conducted in a 50 µl volume with the following contents: plasmid DNA that used pCON1V58M DNA as a template, forward and reverse primers (25 µM each), dNTP mix (5 mM), MgCl2 (25 mM), reaction buffer (10X) and enzyme *Pfu* DNA polymerase (Fermentas, Europe) (Table 3.11). PCR amplicons were generated under the conditions outlined in Table 3.12 using a Techne 3000 PCR system (Barloworld Scientific). Following the PCR, methylated pCON1V58M template DNA was removed using *Dpn*I (Fermentas, Thermo Scientific) under the guidelines listed in Table 3.13.

Table 3.10. Primers for mutagenesis with site-directed

Primers name	Primer Sequences (5' to 3')	Tm
Y65FF	5'- GCTATCCACTTTAC**TTT**GATGCGATGAATG -3'	62°C
Y65FR	5'- CATTCATCGCATC**AAA**GTAAAGTGGATAGC -3'	62°C
Y65LF	5'- GCTATCCACTTTAC**CTG**GATGCGATGAATG -3'	65°C
Y65LR	5'- CATTCATCGCATC**CAG**GTAAAGTGGATAGC -3'	65°C

Table 3.11. PCR-Reactive materials for pCON1V58M-Y65F and pCON1V58M-Y65L mutagenesis

Reactants	Concentrations	Quantities
UP (ultra pure) H_2O	-	33.25 µl
Template DNA pCON1V58M (100 ng)	135 ng/µl	0.75µl
$MgCl_2$ (25 mM)	25 mM	4 µl
dNTP mix (5 mM)	5 mM	2 µl
Forward Primer (25 µM)	25 µM	2 µl
Reverse Primer (25 µM)	25 µM	2 µl
Pfu DNA Polymerase Buffer (10X)	10X	5 µl
Pfu DNA Polymerase Enzyme (2.5 U/µl)	2.5 u/µl	1 µl
TOTAL VOLUME	-	**50 µl**

Table 3.12. Conditions for PCR reactions

Cycles			Time
	Y65F	**Y65L**	
Initial denaturation	95°C	95°C	30 sec
Denaturation	95°C	95°C	1 min
Annealing	58°C	61°C	1 min
Extension	72°C	72°C	9 min
Final extension	72°C	72°C	5 min
Number of cycles			**20**

Table 3.13. Conditions of reaction for *Dpn*I digestion of PCR products

Reactants	Quantities	
Up H_2O	4 µl	at 37 °C
PCR product (>500 ng)	40 µl	
Tango Buffer (10X)	5 µl	for 2 h.
*Dpn*I enzyme (10U/µl)	1 µl	
TOTAL VOLUME	**50 µl**	

3.5.2 Purifying Mutated PCR Products

Gel extraction kit Thermo Scientific GeneJET (Massachusetts, USA) was used to recover approximately 1 kb of PCR products from agarose gels after PCR products from pCON1V58M*-Y65F and pCON1V58M*-Y65L (* indicates desired mutations) were placed on gel with 1% agarose and electrophoresed for an hour at 75 volts.

3.5.3 Mutants of pCON1V58M*-Y65F and pCON1V58M*-Y65L Transforming into the *E. coli* XL1-Blue

For each transformation, 10 µl of PCR purified products from pCON1V58M*-Y65F and pCON1V58M*-Y65L were added to 100 µl of competent cells and incubated for 45 minutes on ice and 5 minutes at 37°C, then re-incubated for 5 minutes on ice. After heat shock, the samples were incubated in 1 ml LB medium for 1 hour at 37 °C at 175 rpm. Pellets formed by centrifugation of the growing cells for 3 minutes at 6000 rpm were resuspended in 100 µl LB medium. The cell suspensions were plated on ampicillin (100µg/ml) containing LB agar and cultivated at 37°C for 16-18 hour. The four randomly selected transformed colonies were grown overnight at 37°C in 5 ml LB medium containing amphicillin(100µg/ml). Plasmid miniprep kit (Thermo Scientific GeneJET, Lithuania, EU) was used to isolate plasmid DNA from the cell pellets after the growing cell medium was centrifuged for 3 min at 6000 rpm.

3.5.4 Detection of Double Mutations by DNA Sequencing

Using M13/pUC forward and reverse universal primers, Macrogen Inc. (Seoul, Korea) carried out DNA sequencing of recombinant mutant DNAs. The BioEdit Sequence Alignment Programme confirmed the bsh gene with double mutation, which is roughly 1 kb in size.

3.5.5 Preparation of Stock

The target-mutant clones pCON1V58M-Y65F and pCON1V58M-Y65L were cultured in 5 ml of LB containing ampicillin (100 µg/ml) at 37°C and 175 rpm of shaking for overnight. After that, cell mediums were centrifuged for 4 minutes at 25°C and 4000 rpm. The pellets were resolved in 30% glycerol-containing 4 ml LB and stored in cryogenic tubes in a freezer maintained at -80°C for extended storage.

3.6 Making Mutant pZEKV58M-Y65F and pZEKV58M-Y65L Constructs

3.6.1 Digestion of Mutant pCON1V58M-Y65F and pCON1V58M-Y65L DNAs by *Not*I and *Eco*RI Restriction Enzymes

The V58M-Y65F and V58M-Y65L, double mutant *bsh* genes were obtained from pCON1V58M-Y65F and pCON1V58M-Y65L clones using *Not*I and *EcoR*I

restriction enzymes (Thermo Scientific, Lithuania, EU) (Table 3.14). The vivantis GF-1 gel DNA recovery kit (Vivantis, Selangor, Malasia) was used to purify mutant V58M-Y65F and V58M-Y65L *bsh* gene fragments from 1% agarose gel in accordance with the manufacturer's instructions.

Table 3.14. Conditions of pCON1V58M-Y65F and pCON1V58M-Y65L DNAs digestion by *Not*I and *EcoR*I

Reactants	Quantities	
Up H_2O	18 µl	at 37 °C
pCON1V58MY65F and pCON1V58MY65L DNAs (>500 ng)	40 µl	
Fast Digest Buffer	7 µl	for 2 h.
*EcoR*I Enzyme (Fast Digest)	2.5 µl	
*Not*I Enzyme (Fast Digest)	2.5 µl	
TOTAL VOLUME	**70 µl**	

3.6.2 Double mutant *bsh* genes Ligation into pET22b

The T4 DNA ligase enzyme (Thermo Scientific) was used to individually ligate the purified mutant V58M-Y65F and V58M-Y65L *bsh* genes into the pET22b expression vector. This process was carried out for one hour at 22°C (Table 3.15). The newly created constructs were given the names pZEKV58M-Y65F and pZEKV58M-Y65L. The following formula was used to calculate the proper amounts of insert and vector DNA for an efficient ligation:

$$\text{Insert Mass (ng)} = \text{Ration x} \left[\frac{\text{Insert Length (kb)}}{\text{Vector Length (kb)}} \right] \text{x Vector Mass (ng)}$$

Table 3.15. Insertion of mutant V58M-Y65F and V58M-Y65L BSHs into the pET22b

Reactants	Quantities	
Up H_2O	11 µl	at 22 °C
pET22b Vector (*EcoR*I/*Not*I digested) (>500 ng)	4 µl	
Mutant V58MY65F and V58M65L BSH DNAs (*EcoR*I/*Not*I cut)	2 µl	for 1 h.
T4 10X Ligase Buffer	2 µl	
T4 DNA Ligase Enzyme (5 U/µl)	1 µl	
TOTAL VOLUME	**20 µl**	

3.6.3 Incorporation of pZEKV58M-Y65F and pZEKV58M-Y65L Mutants into BLR (DE3) of *E. coli*

Samples containing 100 µl of BLR(DE3) competent cells and 10 µl of pZEKV58M-Y65F or pZEKV58M-Y65L ligation products were incubated for 45

minutes on ice, followed by 5 min. at 37°C and another 5 min. on ice. Following an hour of growth in 1 ml LB broth medium at 175 rpm and 37°C in a shaking incubator, the ligation samples were centrifuged for 3 minutes at 6000 rpm, and the cell pellets were resuspended in 100 µl LB. For 37°C growth, the solved cells were plated on LB agar plates supplemented with ampicillin (100µg/ml).

3.6.4 Accuracy of Mutant *bsh* Genes in pZEKV58M-Y65F and pZEKV58M-Y65L Constructs

Colonies randomly selected from ampicillin LB plates of transformants were grown in 10 ml LB medium supplemented with ampicillin (100 µg/ml) for 16-18 hours at 37°C at 175 rpm on a shaker and simultaneously plated onto ampicillin (100 µg/ml) LB plates at 37°C overnight for later stocking. The growing transformant cells were pelleted by centrifugation for 3 minutes at 6000 rpm and using the Thermo Scientific GeneJET Plasmid Miniprep Kit (Lithuania, EU), DNA was extracted from *E. coli* BLR(DE3) clone pellets. To determine whether the mutant *bsh* genes were correctly inserted into the pZEKV58M-Y65F or pZEKV58M-Y65L constructs are digested with *EcoR*I and *Not*I resriction enzymes as specified in Table 3.16. and the digested pZEKV58M-Y65F or pZEKV58M-Y65L DNA samples were loaded onto a 1% agarose gel and electrophoresed for 1 hour at 75 volts. The mutant gene-verified colonies from pZEKV58M-Y65F or pZEKV58M-Y65L constructs were grown in 10 ml ampicillin (100 µg/ml) LB medium at 37°C for 16-18 hours at 175 rpm and then pelleted by centrifugation for 3 min. at 6000 rpm. The pellets were again suspended in 30% glycerol in 4 ml of LB and stored at -80°C.

Table 3.16. Conditions of pZEKV58M-Y65F and pZEKV58M-Y65L DNAs digestion by *Not*I and *EcoR*I

Reactants	Quantities	
Up H_2O	5.5 µl	at 37 °C
pZEKV58MY65F and pZEKV58MY65L DNAs (>500 ng)	3 µl	
Fast Digest Buffer (10X)	1 µl	for 30 min.
*EcoR*I Enzyme (Fast digest)	0.25 µl	
*Not*I Enzyme (Fast digest)	0.25 µl	
TOTAL VOLUME	**10 µl**	

3.7 Assay of the BSH Activity in the pZEKV58M-Y65F and pZEKV58M-Y65L Constructs

3.7.1 Overexpression of *bsh* Gene Mutants

The pZEKV58M-Y65F or pZEKV58M-Y65L transformants were individually cultivated in ampicillin (100µg/ml) containing 10ml LB at 37°C and 175 rpm on a shaker for 16-18 hours after successful transformation of pZEKV58M-Y65F or pZEKV58M-Y65L into *E. coli* BLR(DE3) competent cells. From the overnight cultures, 5ml (2% of the total) was transferred to 250 ml of LB broth supplemented with 4% glycerol and 100 µg/ml ampicillin. The cultures were then grown at 175 rpm and 37 °C until their optical density reached OD_{600}:0.45 - 0.6. 0.3 mM IPTG was used to induce the protein expression of pZEKV58M-Y65F or pZEKV58M-Y65L mrBSH. The cultures were then reincubated at 37°C and 175 rpm until they achieved OD_{600} values of 1.5-3.0. After the cultures reached an OD_{600} of 1.5–3.0, they were centrifuged at 8000g for 15 minutes and at 4˚C. Re-suspended pellets were placed in 2 ml of cold binding buffer (pH: 7.8) with 500 ml of sodium chloride and 20 ml of sodium phosphate. The cell suspension was then mixed with 1 mg/ml lysozyme and allowed to incubate for 10 minutes at 4°C on a rocking platform. After incubation, 1% Tween-20, 5µg/ml DNase and 5µg/ml RNase were added to the mixture and incubated for 10 minutes at 4°C on a rocking platform. The soluble fraction was centrifuged at 14000g for 20 minutes at 4°C to remove cell debris. The supernatant was filtered through a 0.45 µm filter and collected in clean polystyrene tubes. Ninhydrin assay and pCON2 rBSH and pZEKV58M-Y65F or pZEKV58M-Y65L mrBSH protein purification were performed on the prepared cell extracts. In the ninhydrin assay, the total protein concentration of the cell extract was measured using bovine serum albumin (BSA) as a standard protein according to the Lowry method (178).

3.7.2 Partially Purification of the Mutant BSH Enzymes

After overexpressing and extracting cells, the wild-type and pZEKV58M-Y65F or pZEKV58M-Y65L mutant BSHs underwent partial purification using the nickel-chelated column on the GE Healthcare Bio-sciences ÄKTAprime plus™ chromatography system, in accordance with the manufacturer's guidelines. The His TrapTM HP column was loaded with the part of cell extracts that is soluble and contains wild-type and pZEKV58M-Y65F or pZEKV58M-Y65L mutant BSHs.

The protein-coupled column was eluted with elution buffer (at pH 6, 500 mM sodium chloride, 20 mM sodium phosphate buffer and 200mM imidazole).

3.7.3 Ninhydrine Assay for V58M-Y65F and V58M-Y65L *bsh* genes

The ninhydrin assay, modified from Tanaka et al. (8), was used to determine the substrate specificity of the pZEKV58M-Y65F or pZEKV58M-Y65L double mutant BSH enzymes. The assay's foundation is the interaction of ninhydrin reagent with amino acids produced by the hydrolysis of conjugated bile salts, and the subsequent colorimetric shift that is observed. The Lowry test was used to determine the cell extracts' total protein concentration (178) and standardized to 10 µl of sample using the proper dilution before initiating the assay for ninhydrin. The substrate specificities of wild-type BSH (positive control) and pZEKV58M-Y65F or pZEKV58M-Y65L double mutant BSH enzymes against the six different human BAs, GCA, TCA, GDCA, TDCA, GCDCA and TCDCA, were determined by ninhydrin assay at 37ºC and pH 6. Initially, 10 µl sample was incorporated into the mixture that contained 50 µl of 40 mM bile salt, 50 µl of 40 mM DTT and 100 µl of 0.1 M sodium phosphate buffer (pH: 6.0). The final mixture was incubated for 30 minutes at 37 °C. After adding 210 µl of trichloroacetic acid to the mixture in order to stop the enzymatic reaction, the mixture was centrifuged at 14000g for 15 min. 1.9 ml of ninhydrin reagent (0.5 ml of 1% ninhydrin in 0.5M sodium citrate buffer (pH 5.5), 1.2 ml of glycerol and 0.2 ml of 0.5M sodium citrate buffer (pH 5.5)) was mixed with 20 ml of supernatant and 80 mL of ultrapure water. Following a vortex and a 15-minute boil, the sample was treated. After cooling, the samples' absorbance at 570 nm was measured using a standard curve of glycine using the U-1900 spectrophotometer (HITACHI, Japan). All experiments were carried out in triplicate.

4. RESULTS

4.1 Analysis of Target Amino Acid Sequences

The BioEdit sequence alignment program was used to analyze and align the *L. plantarum* B14 *bsh* gene sequence and visulated by the ExPASY program from http://web.expasy.org/compute_pi/. The codon of valine-58 was identified as GTA and the codon of tyrosine-65 was identified as TAC (Figure 4.1). A total of 30 BSH sequences, with different genetically and biochemically characterised amino acids sequences listed in GenBank (NCBI) and substrate preferences, were aligned with the *L. plantarum* B14 *bsh* gene using Jalview 2.8 (Figure 4.2a-d). Also, the phylogenetic tree of BSH isotypes was represented in a tree structure by Jalview 2.8 (Figure 4.3). The BLAST identity percentage of the amino acid sequences of BSH from *L. plantarum* B14 and various other sequences, including *Bifidobacterium*, *Clostridium*, *Enterococcus*, and *Lactobacillus* species, was examined using the Standard Protein BLAST software, which may be found at blast.ncbi.nlm.nih.gov (Figure 4.4). The BSHs of *L. plantarum* 80, *L. plantarum subsp. plantarum* ST-III BSH1, and *L. plantarum* WCSF1 were shown to have 99% identity with the BSH of *L. plantarum* B14. Conversely, the BSH of *L. plantarum* B14 exhibited 70% similarity to *E. faecalis* T2 and 54–45% similarity to *L. salivarius, L. acidophilus, L. reuteri, L. johnsoni*, and *L. gasseri* species; in contrast, there was 37–32% similarity to *Bifidobacterium* species and 29–26% similarity to *L. plantarum* CGMCC8198 BSH3, *L. fermentum* NCDO394 BSH, *L. plantarum* CGMCC8198 BSH4, and *L. rhamnosus* E9 BSH (Figure 4.3 and Figure 4.4). The substrate specificity of BSH isotypes with regard to sites 58 and 65 has been demonstrated, indicating that the Ntn-hydrolase superfamily members exhibited a partial conservation of residues implicated in substrate selectivity within the active site of BSH enzymes and in BSHs, the majority of the amino acids are hydrophobic at positions 65 and 58. In comparison to site Y65, site V58 has much more diversity, with types such as Met, Val, Phe, Ile, Thr, Asn, Glu, Ala, Leu and Pro (Figure 4.2 and Figure 4.4). Nonetheless, the amino acids at site 65 were identified as Phe, Ala, Tyr, Cys, Ser, Thr, and Val, and they were shown in the Figure 4.2 and Figure 4.4 to be more conserved than those at site 58. The monomeric unit and target amino acid positions of valine-58 (GTA) and tyrosine-65 (TAC), which are considered to be effective for the substrate specificity of the BSH enzyme of *L. plantarum* were

ascertained using PyMOL (PyMOL Executable Build is Copyright (C) 2006 DeLano Scientific LLC, South San Francisco, California, USA) (Figure 4.5).

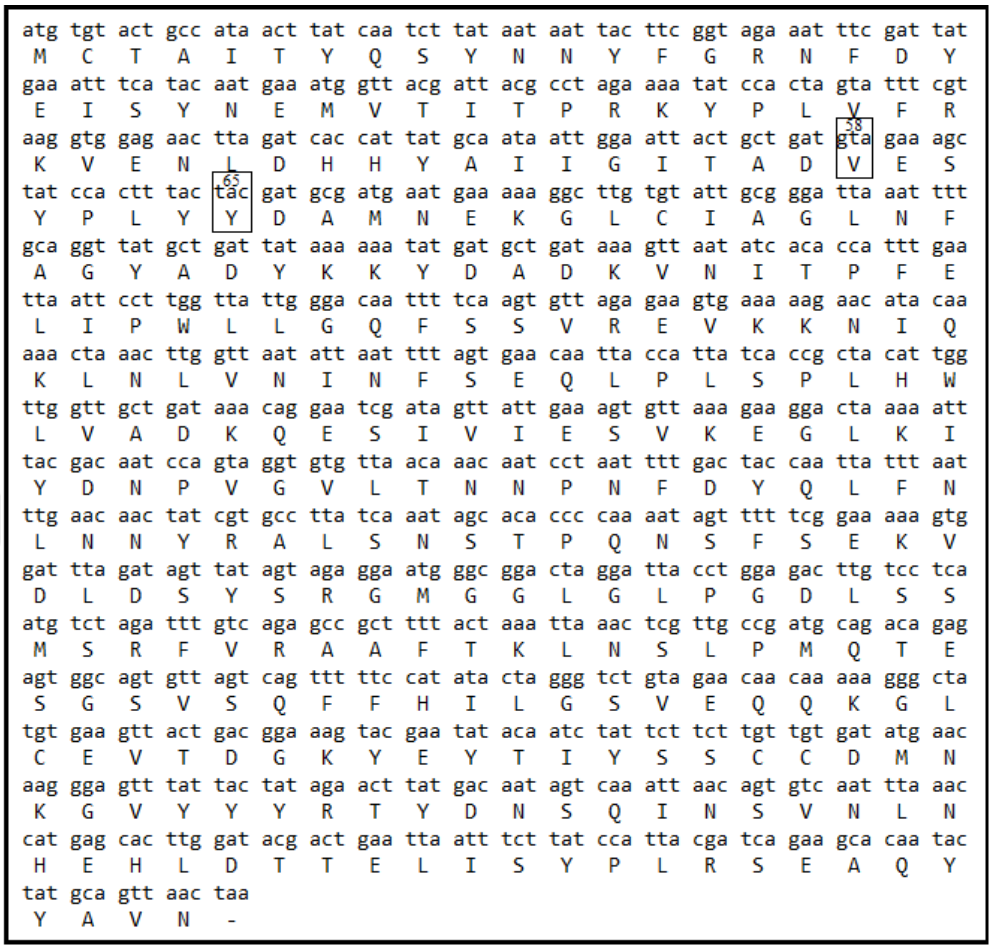

Figure 4.1. The amino acid residues of the wild type *bsh* gene. Frames represent target amino acids for site directed mutagenesis.

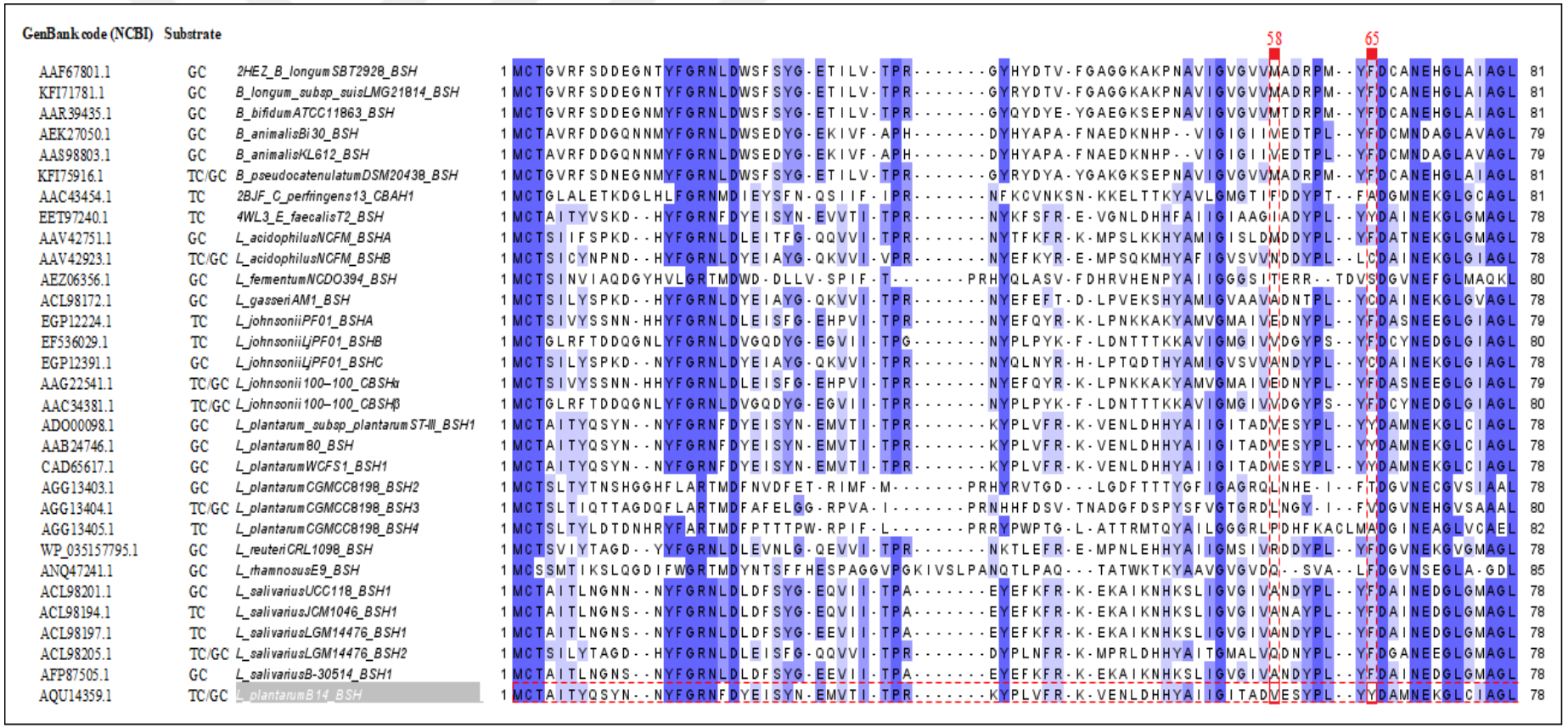

Figure 4.2. The multiple sequence alignment of BSH isotypes by Jalview 2.8.0b1. The first four sequences of BSH with available crystal structures are shown with the PDB code. GenBank access code are given for all BSH sequences. Substrate preference: to glycol-conjugated bile acids, GC or tauro-conjugated bile acids, TC is shown from Dong et al 2018. (a, 1- 78 aminoacid sequence, b, 79-160 aminoacid sequence, c, 161-250 aminoacid sequence, d, 251-3254 aminoacid sequence for *L. plantarum*).

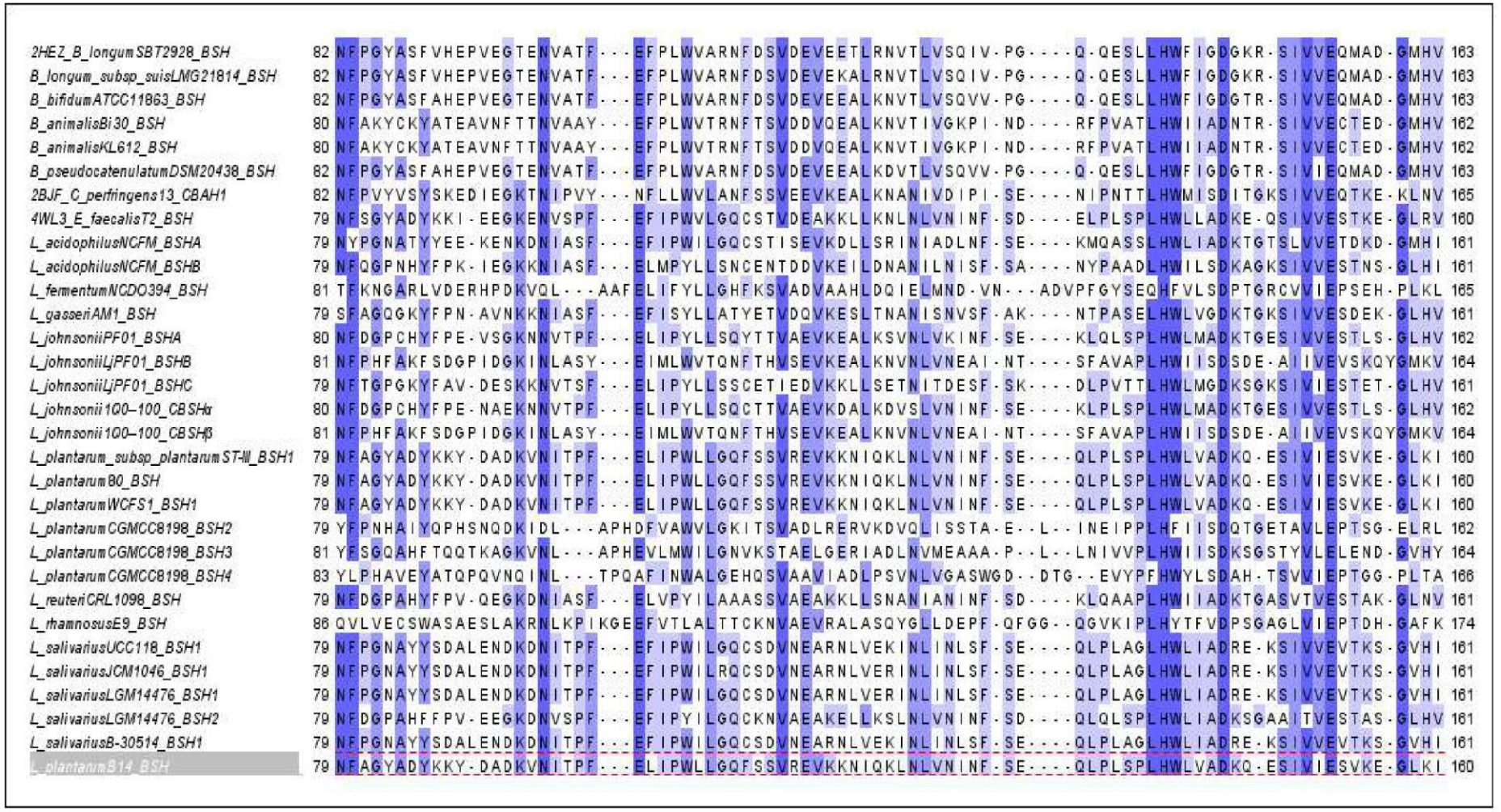

Figure 4.2.b (cont'd)

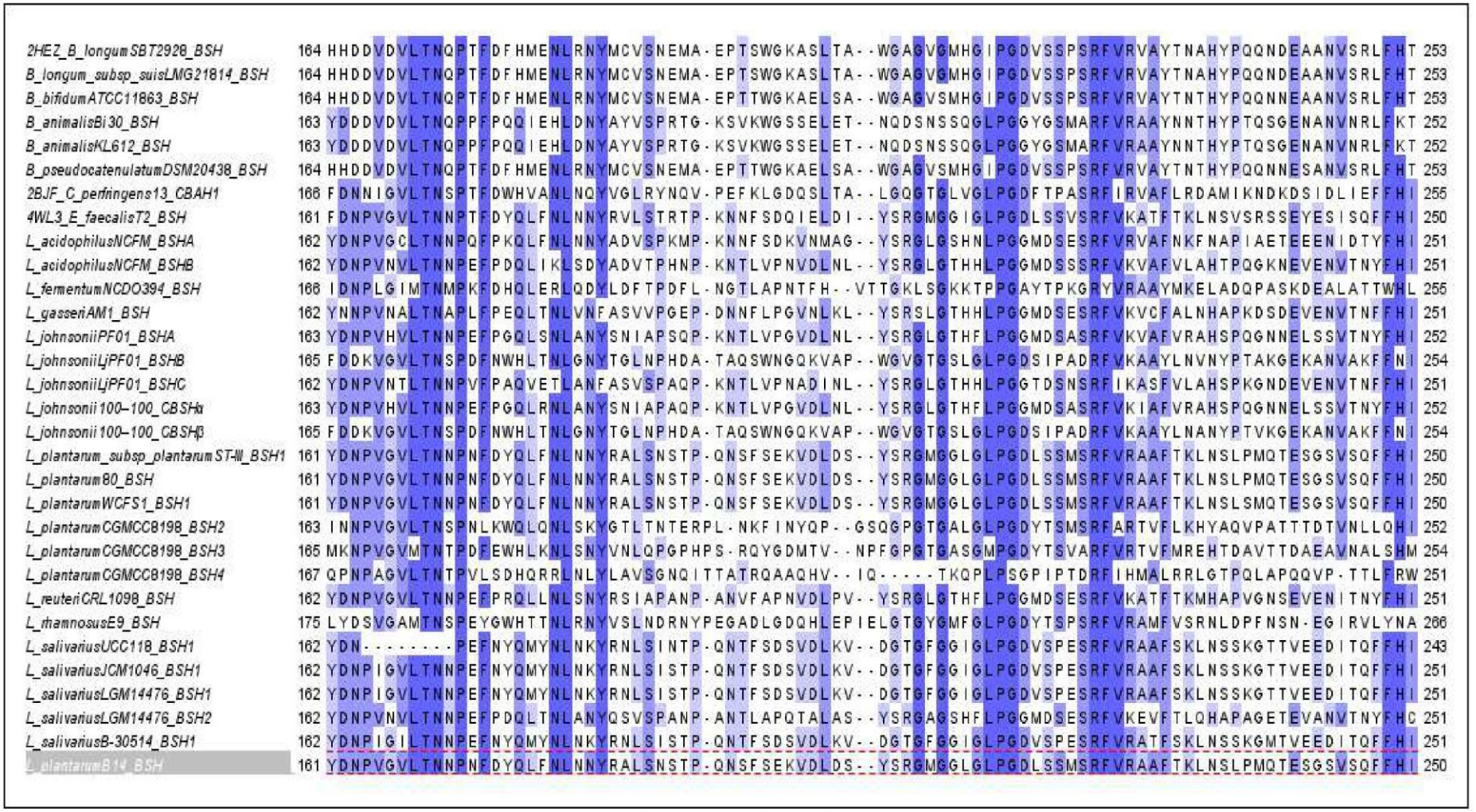

Figure 4.2.c (cont'd)

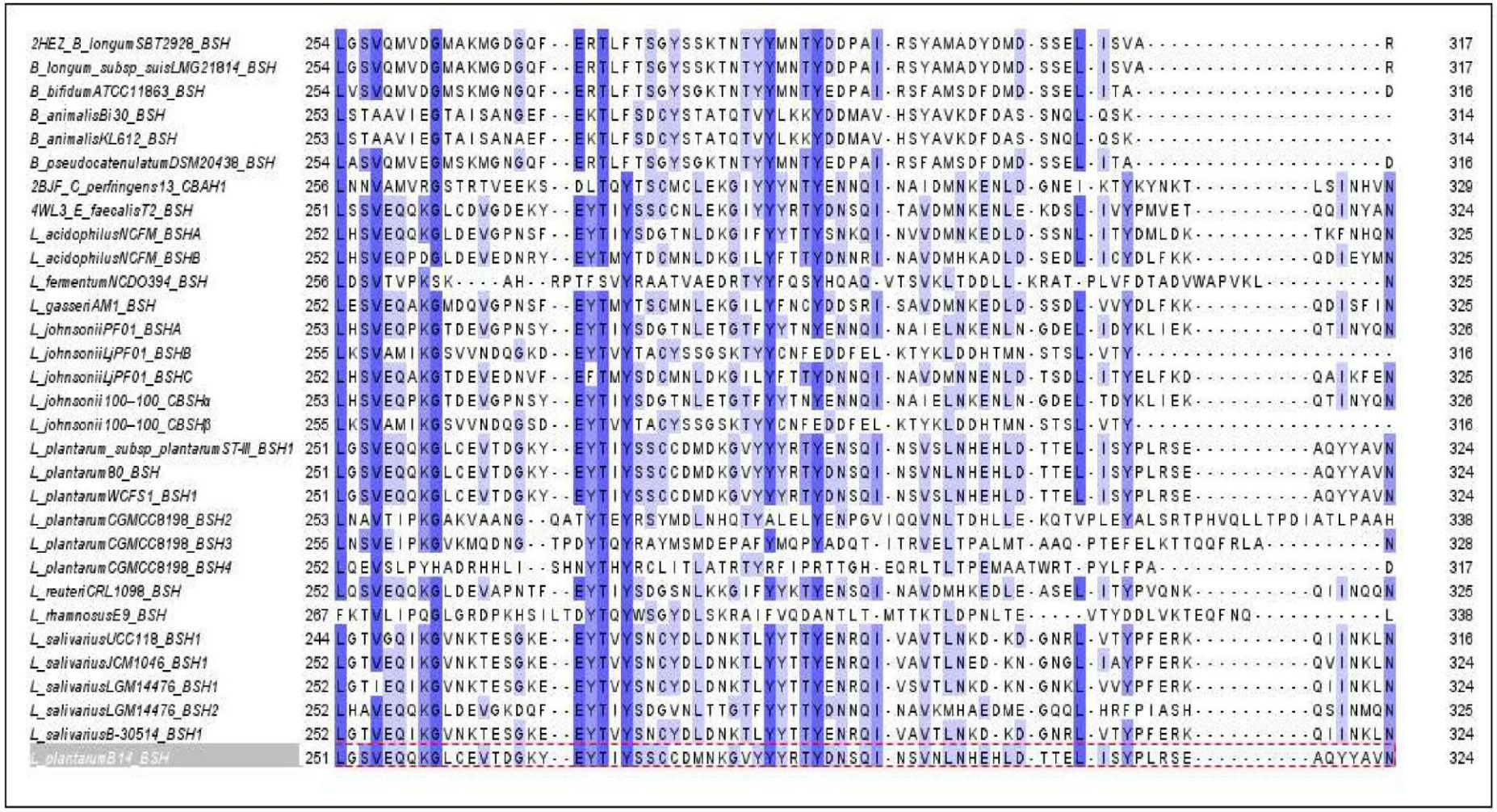

Figure 4.2.d (cont'd)

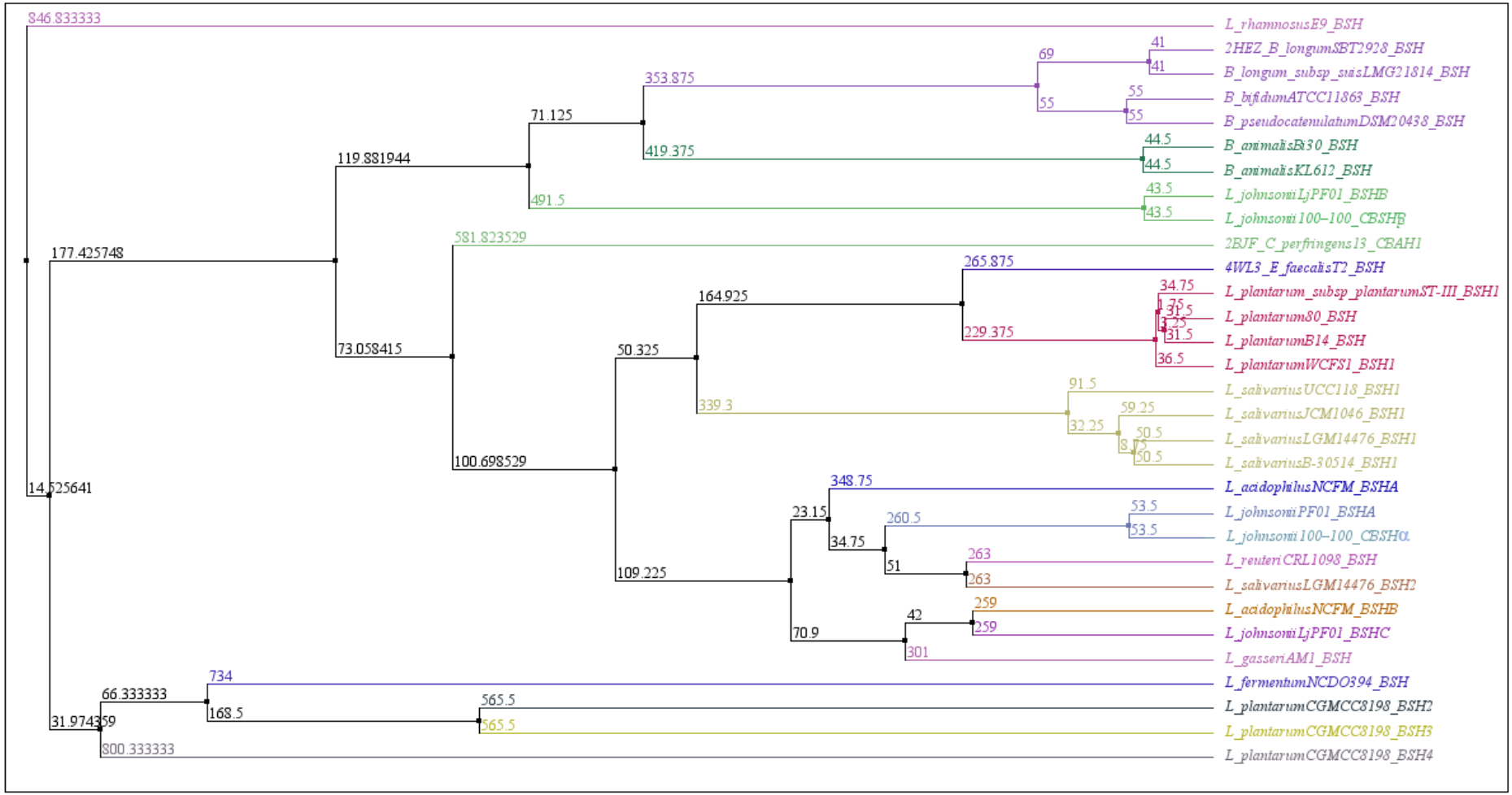

Figure 4.3. The phylogenetic tree of BSH isotypes. The tree structure containing *L. plantarum* B14 and other species; *Bifidobacterium, Clostridium, Enterococcus* and *Lactobacillus.*

Description	Percent Identidy	Accession Length	Substrate	58	65
L. plantarum B14 BSH	100	324	GC/TC	V	Y
L. plantarum 80 BSH	99.69	324	GC	V	Y
L. plantarum subsp. plantarum ST-III BSH1	99.07	324	GC	V	Y
L. plantarum WCFS1 BSH1	99.07	324	GC	V	Y
4WL3 *E. faecalis* T2 BSH	70.22	324	TC	I	Y
L. salivarius B-30514 BSH1	54.09	324	GC	A	F
L. salivarius LGM14476 BSH1	54.09	324	TC	A	F
L. salivarius JCM1046 BSH1	54.40	324	TC	A	F
L. johnsonii 100-100 CBSHα	53.16	326	GC/TC	E	F
L. johnsoni PF01 BSHA	53.16	326	TC	E	F
L. salivarius UCC118 BSH1	52.20	316	GC	A	F
L. acidophilus NCFM BSHA	51.71	325	GC	M	F
L. salivarius LGM14476 BSH2	51.10	325	GC/TC	Q	F
L. reuteri CRL1098 BSH	50.63	325	GC	R	F
L. johnsoni PF01 BSHC	49.52	325	GC	A	C
L. acidophilus NCFM BSHB	46.67	325	GC/TC	N	C
L. gasseri AM1 BSH	45.89	325	GC	A	C
2BJF *C. perfringens* 13 CBAH1	39.62	329	TC	F	A
L. johnsonii 100-100 BSH CBSHβ	38.05	316	GC/TC	V	F
L. johnsonii PF01 BSHB	38.05	316	TC	V	F
B. longum subsp. suis LMG21814 BSH	37.85	317	GC	M	F
2HEZ *B. longum* SBT2928 BSH	37.54	317	GC	M	F
B. pseudocatenulatum DSM20438 BSH	35.87	316	GC/TC	M	F
B. bifidum ATTCC 11863 BSH	35.56	316	GC	M	F
L. plantarum CGMCC8198 BSH2	33.55	338	GC	L	T
B. animalis Bi30 BSH	32.78	314	GC	V	F
B. animalis KL612 BSH	32.44	314	GC	V	F
L. plantarum CGMCC8198 BSH3	29.91	328	GC/TC	L	V
L. fermentum NCDO394 BSH	29.84	325	GC	T	S
L. plantarum CGMCC8198 BSH4	29.17	317	TC	P	A
L. rhamnosus E9 BSH	26.19	338	GC	Q	F

Figure 4.4. The BSH isotypes amino acid sequences' BLAST identity percentage analysiss and substrate specificity of BSH isotypes with sites 58 and 65. The Standard Protein BLAST program, accessible at blast.ncbi.nlm.nih.gov, was used to analyze the BLAST identity % of the amino acid sequences of BSH from *L. plantarum* B14 and several other sequences, *Bifidobacterium, Clostridium, Enterococcus* and *Lactobacillus.* In comparison to the amino acid residues localized at position 65, those at position 58 are more variable. A, M, Q, R, N, F, L, T, and P are the amino acids that are present at site 58. On the other hand, Y, F, C, A, V, S, and T are the amino acids that are primarily hydrophobic and found on site 65.

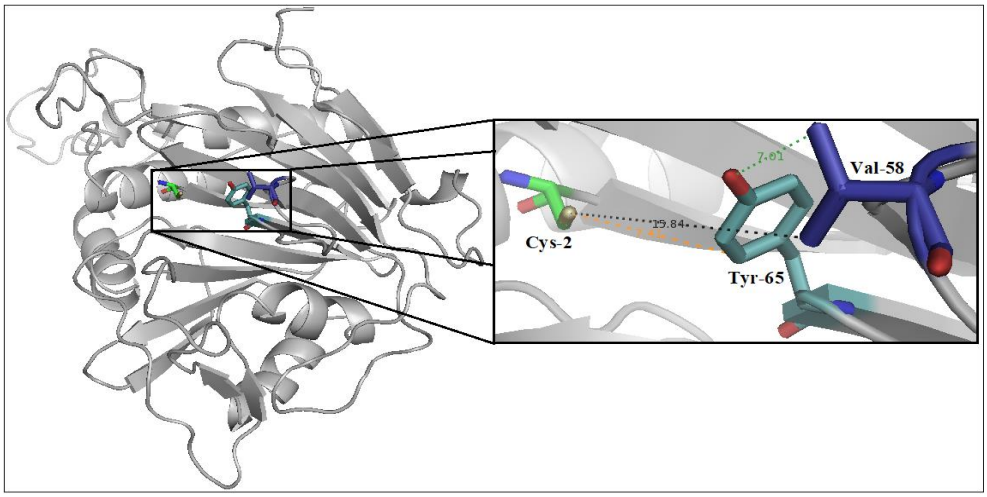

Figure 4.5. The 3D monomeric unit and target amino acid positions of *L. plantarum* B14 BSH protein with cysteine-2, valine-58 and tyrosine-65.

4.2 Mutant Constructions of pCON1

4.2.1 Target Amino Acid Site-Directed Mutagenesis

Primers containing the target amino acid codons (Figure 3.2) were used to convert the wild-type valine (GTA)-58 and tyrosine (TAC)-65 to phenylalanine (TTT)-58, methionine (ATG)-58, asparagine (ACC)-58, cysteine (TGC)-65, phenylalanine (TTT)-65 and leucine (CTG)-65 amino acid codons by PCR. Template DNA pCON1 (*bsh*/pBluescript; pBluescript (2961bp) and 975bp *bsh* gene of *L. planta*rum B14 (AN: KY080706)) was removed from the resulting PCR products using the restriction enzyme *Dpn*I (Figure 4.6).

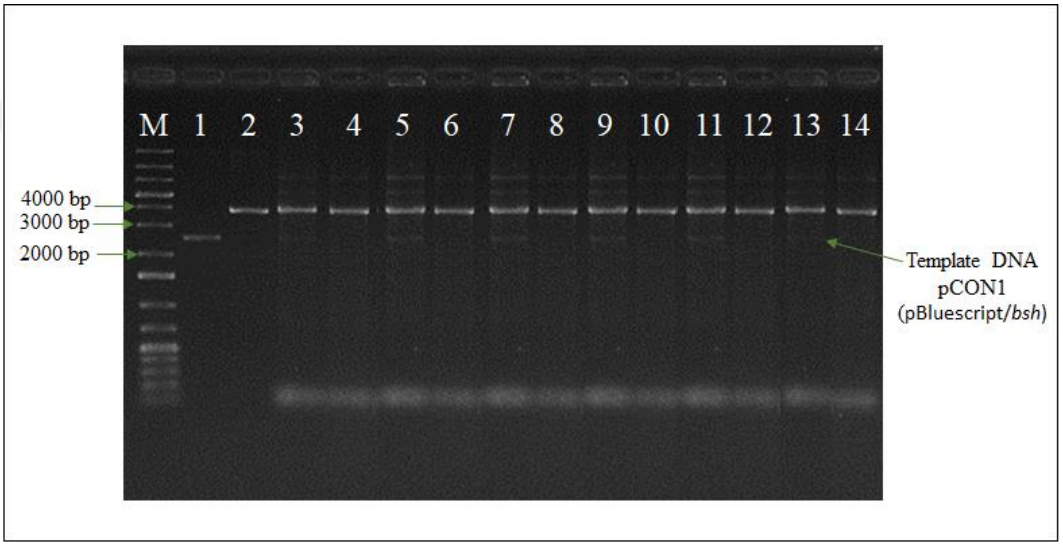

Figure 4.6. Mutation of pCON1* (* represents desired mutation) with site-directed. M, 1 kb plus DNA ladder; 1, uncut pCON1 template DNA (1/5 diluted); 2, *Xho*I cut pCON1 template DNA; 3, pCON1*V58F PCR product; 4, pCON1*V58F PCR product digested with *Dpn*I restriction enzyme; 5, pCON1*V58M PCR product; 6, pCON1*V58M PCR product digested with *Dpn*I restriction enzyme; 7, pCON1*V58N PCR product; 8, pCON1*V58N PCR product digested with *Dpn*I restriction enzyme; 9, pCON1*Y65C PCR product; 10, pCON1*Y65C PCR product digested with *Dpn*I restriction enzyme; 11, pCON1*Y65F PCR product; 12, pCON1*Y65F PCR product digested with *Dpn*I restriction enzyme; 13, pCON1*Y65L PCR product; 14, pCON1*Y65L PCR product digested with *Dpn*I restriction enzyme.

4.2.2 Purifying Mutated PCR Products

The pCON1*V58F, V58M, V58N, Y65C, Y65F and Y65L mutants digested with *Dpn*I restriction enzyme were individually purified from 1% agarose gels to eliminate non-specific PCR products and undigested methylated template DNA (Figure 4.7 and Figure 4.8).

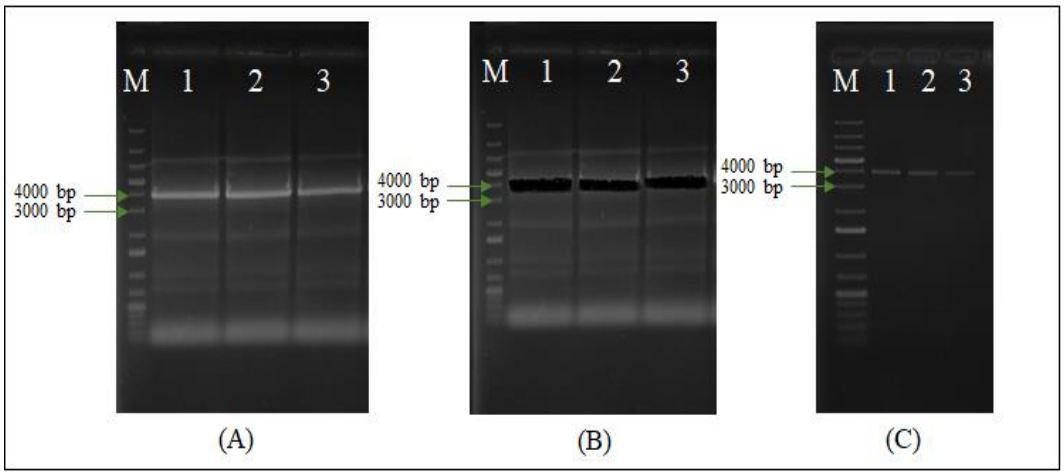

Figure 4. 7. Gel Purification of the pCON1*V58F, pCON1*V58M and pCON1*V58N PCR products from 1% agarose gel. M, 1 kb plus DNA ladder. (A) 1, pCON1*V58F PCR products; 2, pCON1*V58M PCR products; 3, pCON1*V58N PCR products; (B), 1, sliced pCON1*V58F PCR products; 2, sliced pCON1*V58M PCR products; 3, sliced pCON1*V58N PCR products; (C) 1, purified pCON1*V58F (4.0 kb); 2, purified pCON1*V58M (4.0 kb); 3, purified pCON1*V58N (4.0 kb)

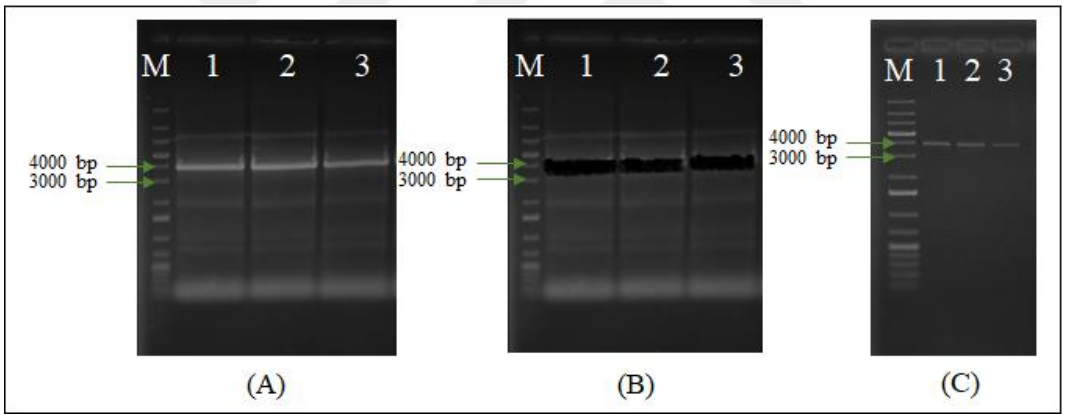

Figure 4. 8. Gel Purification of the pCON1*Y65C, pCON1*Y65F and pCON1*Y65L PCR products from 1% agarose gel. M, 1 kb plus DNA ladder. (A) 1, pCON1*Y65C PCR products; 2, pCON1*Y65F PCR products; 3, pCON1*Y65L PCR products; (B), 1, sliced pCON1*Y65C PCR products; 2, sliced pCON1*Y65F PCR products; 3, sliced pCON1*Y65L PCR products; (C) 1, purified pCON1*Y65C (4.0 kb); 2, purified pCON1*Y65F (4.0 kb); 3, purified pCON1*Y65L (4.0 kb)

4.2.3 Transformation of pCON1* Mutant Constructs

Gel- extracted pCON1* with V58M, V58F, V58N, Y65L, Y65F and Y65C DNAs were separately transferred into *E. coli* XL1-Blue competent cells and confirmed to be the same size (nearly 4.0 kb) as the pCON1 DNA by cutting pCON1*V58F, pCON1*V58M, pCON1*V58N, pCON1*Y65C, pCON1*Y65F and pCON1*Y65L DNAs with *Xho*I restriction enzyme (Figure 4.9 and 4.10).

Figure 4.9. Transformation of pCON1*V58F, pCON1*V58M and pCON1*V58N into *E. coli* XL1-Blue strains. M, 1 kb plus DNA ladder; 1, uncut pCON1 DNA; 2, *Xho*I cut pCON1 DNA; 3, pCON1*V58F DNA; 4, *Xho*I cut pCON1*V58F DNA; 5, pCON1*V58M DNA; 6, *Xho*I cut pCON1*V58M; 7, pCON1*V58N; 8, *Xho*I cut pCON1*V58N.

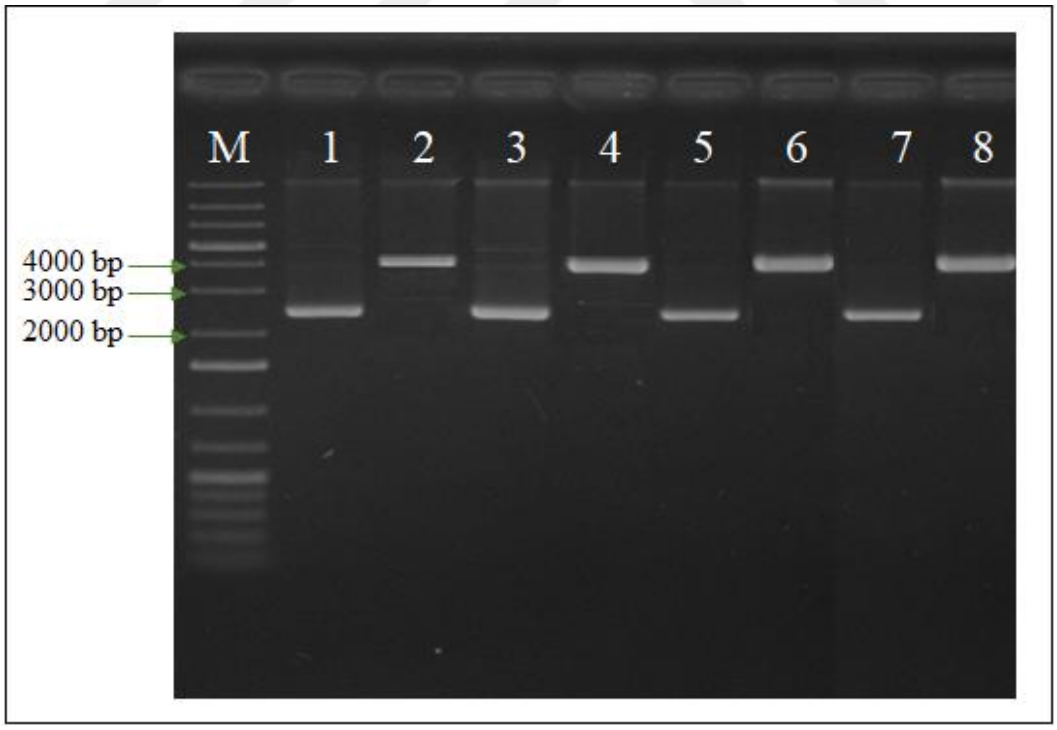

Figure 4.10. Transformation of pCON1*Y65C, pCON1*Y65F and pCON1*Y65L into *E. coli* XL1-Blue strains. M, 1 kb plus DNA ladder; 1, uncut pCON1 DNA; 2, *Xho*I cut pCON1 DNA; 3, pCON1*Y65C DNA; 4, *Xho*I cut pCON1*Y65C DNA; 5, pCON1*Y65F DNA; 6, *Xho*I cut pCON1*Y65F; 7, pCON1*Y65L; 8, *Xho*I cut pCON1*Y65L.

4.2.4 Detection of Targeted Mutations by DNA Sequencing

The DNAs of pCON1V58F, pCON1V58M, pCON1V58N, pCON1Y65C, pCON1Y65F and pCON1Y65L were sequenced by Macrogen (Seoul, Korea) using the universal primers, M13/pUC Reverse (5'-CAGGAAACAGCTATGAC-3') and M13/pUC Forward (5'-GTAAAACGACGGCCAGT-3') and reported using the BioEdit sequence alignment program. In the resulting DNA sequences, only target mutations were detected (Figure 4.11 – 4.16). Sequencing revealed that the GTA codon, which code for the amino acid valine 58, was converted to the TTT, ATG and AAC codons, which code for the amino acids phenylalanine 58, methionine 58 and asparagine 58 and also the TAC codon, which code for the amino acid tyrosine 65 was converted to the TGC, TTT and CTG codons, which code for the amino acids cysteine 65, phenylalanine 65 and leucine 65.

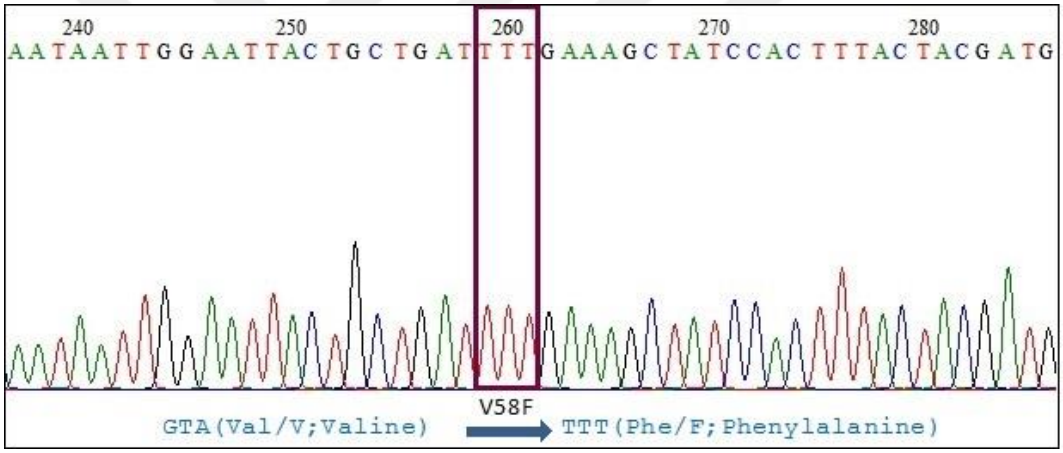

Figure 4.11. The target mutation of pCON1V58F. Valine (V) codon, GTA, was converted to Pheylalanine (F) codon, TTT, labelled with a frame.

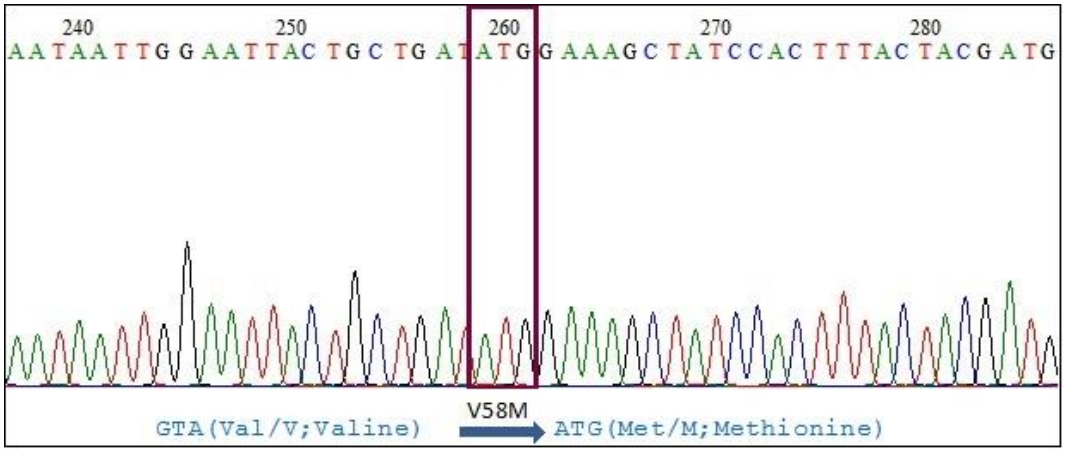

Figure 4.12. The target mutation of pCON1V58M. Valine (V) codon, GTA, was converted to Methionine (M) codon, ATG, labelled with a frame.

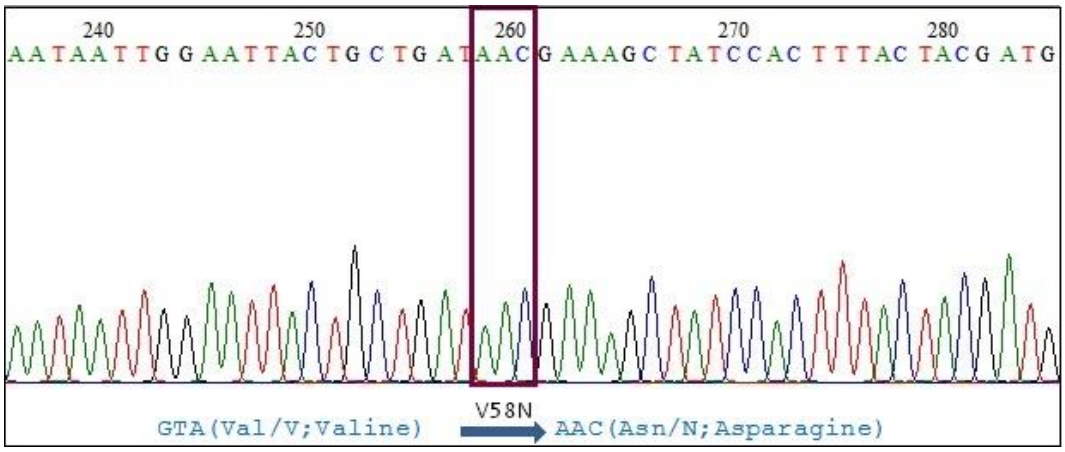

Figure 4.13. The target mutation of pCON1V58N. Valine (V) codon, GTA, was converted to Asparagine (N) codon, AAC, labelled with a frame.

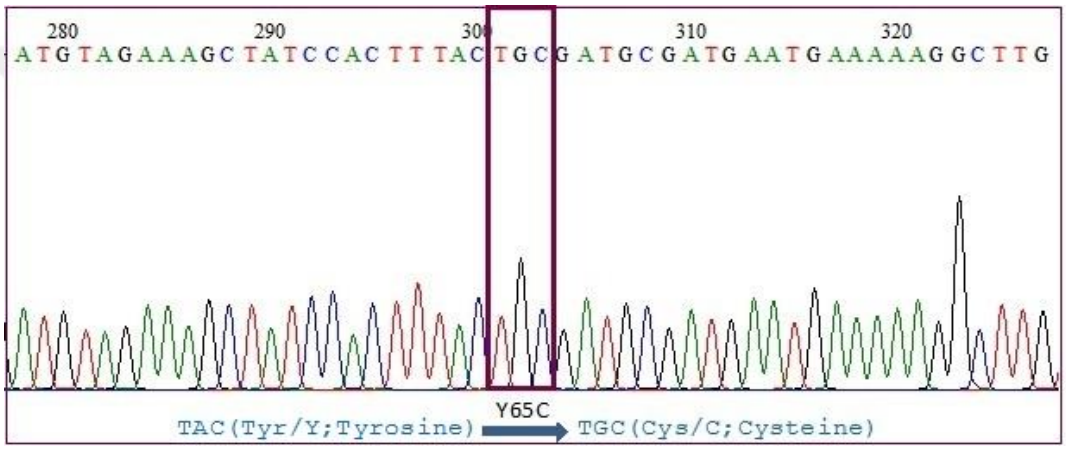

Figure 4.14. The target mutation of pCON1Y65C. Tyrosine (Y) codon, TAC, was converted to Cysteine (C) codon, TGC, labelled with a frame.

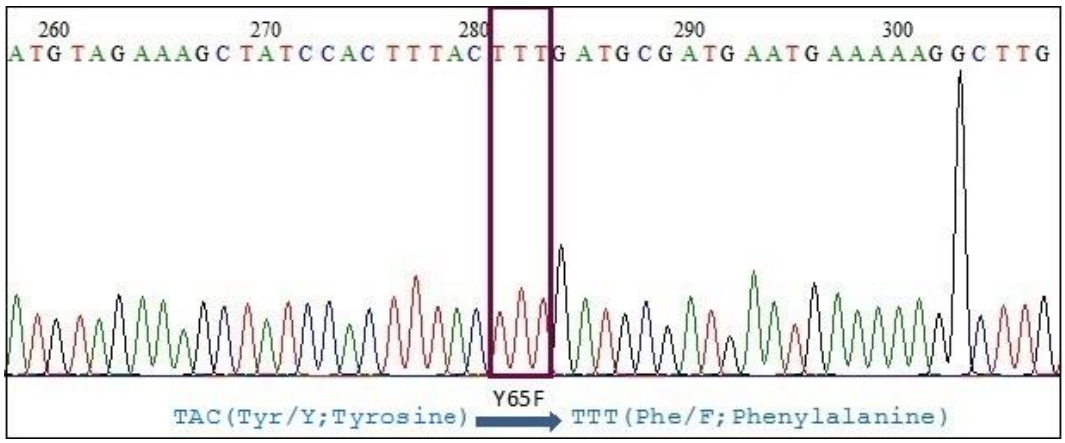

Figure 4.15. The target mutation of pCON1Y65F. Tyrosine (Y) codon, TAC, was converted to Phenylelanine (F) codon, TTT, labelled with a frame

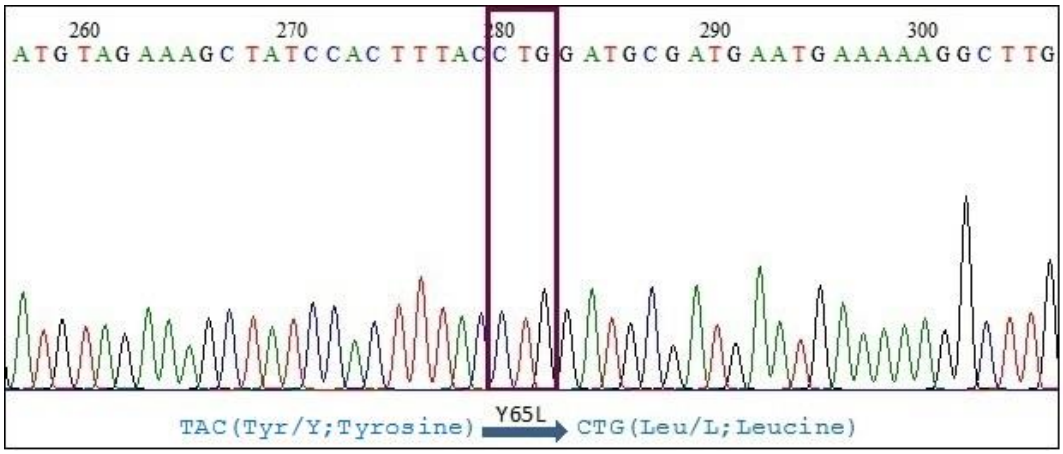

Figure 4.16. The target mutation of pCON1Y65L. Tyrosine (Y) codon, TAC, was converted to Leucine (L) codon, CTG, labelled with a frame.

4.3 Making Mutant pZEK Constructs

4.3.1 Making the Expression Vector for pET22b

A 5.5 kbp fragment of DNA was extracted from the expression vector pET22b, digested using *Not*I and *Eco*RI restriction enzymes, and purified using 1% agarose gels (Figure 4.17).

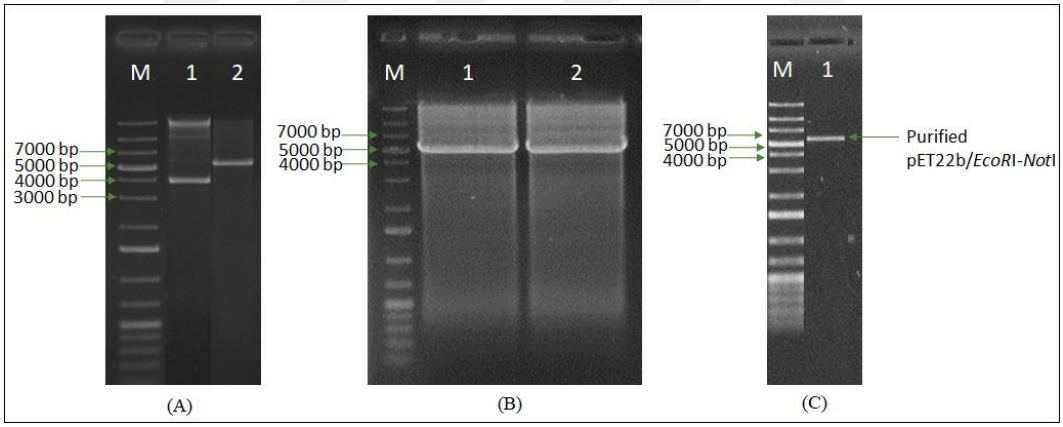

Figure 4. 17. Making the expression vector pET22b. M, 1 kb plus DNA ladder; A, 1: uncut pET22b DNA; 2: *Not*I and *Eco*RI digested pET22b DNA; B, *Not*I and *Eco*RI digested pET22b linear DNA before gel purification; C, gel purified linear pET22b DNA.

4.3.2 Digestion of Mutant Recombinant DNAs by *Eco*RI and *Not*I Restriction Enzymes into pBluescript SKII $^{+}$ Vector

Following the restriction enzyme cuts of the pCON1V58M, pCON1V58F, pCON1V58N, pCON1Y65L, pCON1Y65F and pCON1Y65C, plasmid DNAs with *Not*I and *Eco*RI, the resulting roughly 1 kbp mutant BSH fragments of DNA were extracted from gels with 1% agarose (Figure 4.18 and Figure 4.19).

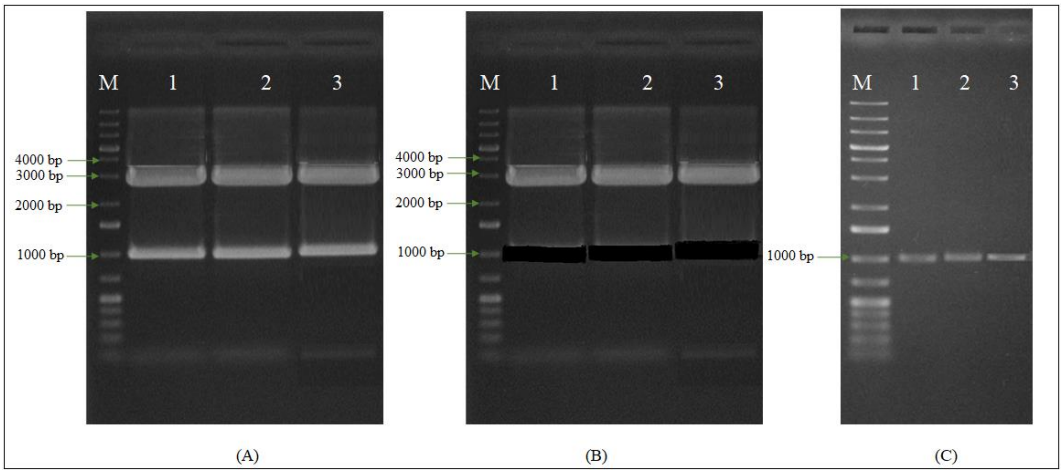

Figure 4.18. Digestion of pCON1V58F, pCON1V58M and pCON1V58N plasmid DNAs by *Not*I and *Eco*RI REs. M, 1 kb plus DNA ladder; A, 1: pCON1V58F DNA cut with *Eco*RI and *Not*I REs; 2, pCON1V58M DNA cut with *Eco*RI and *Not*I REs; 3, pCON1V58N DNA cut with *Eco*RI and *Not*I REs; B, 1, sliced V58F *bsh* DNA fragment from pCON1V58F DNA; 2, sliced V58M *bsh* DNA fragment from pCON1V58M DNA; 3, sliced V58N *bsh* DNA fragment from pCON1V58N DNA; C, 1, gel purified V58F *bsh* DNA fragment from pCON1V58F DNA; 2, gel purified V58M *bsh* DNA fragment from pCON1V58M DNA; 3, gel purified V58N *bsh* DNA fragment from pCON1V58N DNA.

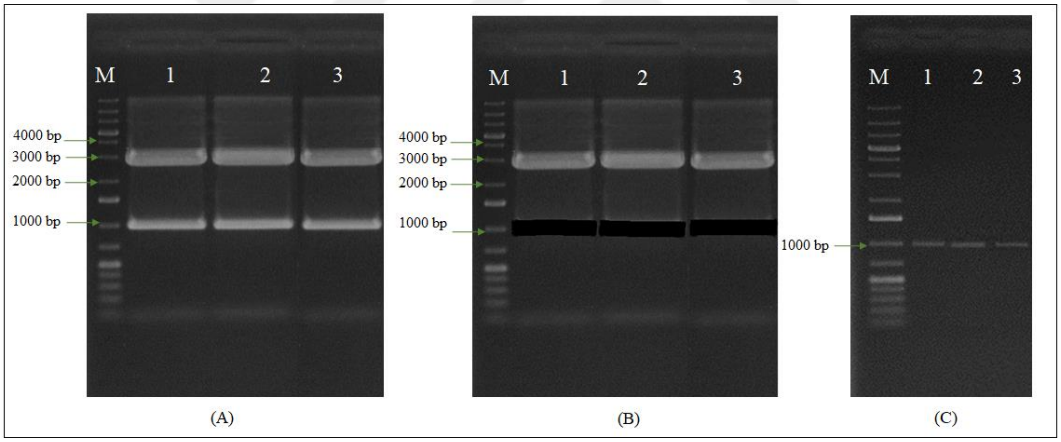

Figure 4.19. Digestion of pCON1Y65C, pCON1Y65F and pCON1Y65L plasmid DNAs by *Not*I and *Eco*RI REs. M, 1 kb plus DNA ladder; A, 1: pCON1Y65C DNA cut with *Eco*RI and *Not*I REs; 2, pCON1Y65F DNA cut with *Eco*RI and *Not*I REs; 3, pCON1Y65L DNA cut with *Eco*RI and *Not*I REs; B, 1, sliced Y65C *bsh* DNA fragment from pCON1Y65C DNA; 2, sliced Y65F *bsh* DNA fragment from pCON1Y65F DNA; 3, sliced Y65L *bsh* DNA fragment from pCON1Y65L DNA; C, 1, gel purified Y65C *bsh* DNA fragment from pCON1Y65C DNA; 2, gel purified Y65F *bsh* DNA fragment from pCON1Y65F DNA; 3, gel purified Y65L *bsh* DNA fragment from pCON1Y65L.

4.3.3 Accuracy of Mutant *bsh* Genes in pZEK and pCON2 Constructs

The correct insertion of the mutant bsh genes, approximately 1.0 kbp in size, into the pET22b, 5.5 kbp, vector was confirmed by the restriction enzymes *Not*I and

*Eco*RI (Figure 4.20). Correctly defined transformants were named pZEKV58F, pZEKV58M, pZEKV58N, pCON2Y65C, pCON2Y65F and pCON2Y65L.

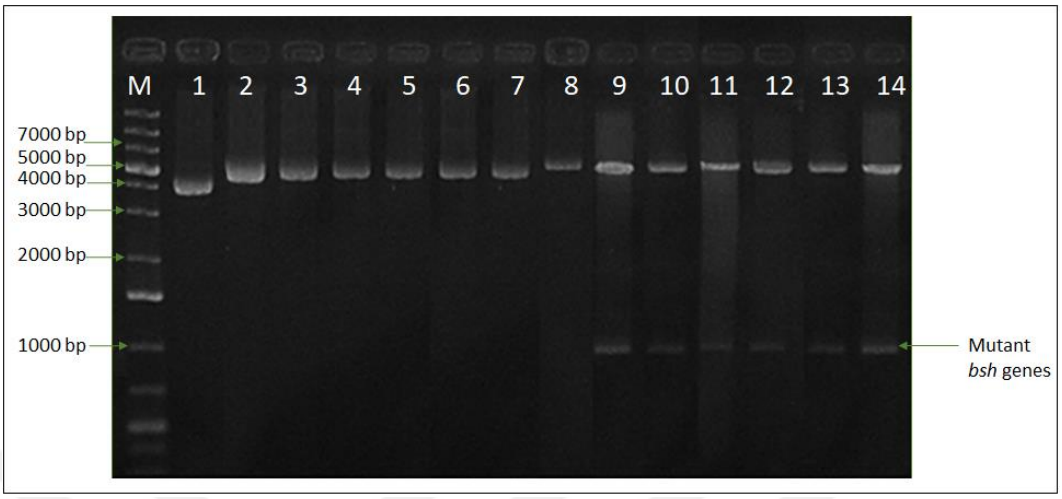

Figure 4.20. Accuracy of mutant *bsh* genes in pZEK and pCON2 constructs. M, 1 kb plus DNA ladder; 1, circular DNAs of pET22b; 2, circular DNAs of pZEKV58F; 3, circular DNAs of pZEKV58M; 4, circular DNAs of pZEK1V58N; 5, circular DNAs of pCON2Y65C; 6, circular DNAs of pCON2Y65F; 7, circular DNAs of pCON2Y65L; 8, *Not*I and *Eco*RI REs digested DNAs of pET22b; 9, *Not*I and *Eco*RI REs digested DNAs of pZEKV58F; 10, *Not*I and *Eco*RI REs digested DNAs of pZEKV58M; 11, *Not*I and *Eco*RI REs digested DNAs of pZEK1V58N; 12, *Not*I and *Eco*RI REs digested DNAs of pCON2Y65C; 13, *Not*I and *Eco*RI REs digested DNAs of pCON2Y65F; 14, *Not*I and *Eco*RI REs digested DNAs of pCON2Y65L.

4.4 Assay of the BSH Activity in the pZEK and pCON2 Constructs

4.4.1 Direct Plate Assay

The plate assay method was utilized to evaluate the BSH activity. Activity results of pCON2 (positive control), pET22b (negative control) and mutant strains pZEKV58F, pZEKV58M, pZEKV58N, pCON2Y65C, pCON2Y65F and pCON2Y65L, against TDCA and GDCA are presented in Figure 4.21-4.24. pCON2, pZEKV58F, pZEKV58M and pZEK1V58N, demonstrated BSH activity against TDCA and GDCA, with a precipitated cholic acid halo. Moreover, pCON2Y65F and pCON2Y65L demonstrated BSH activity towards GDCA but pCON2Y65C exhibited little activity towards GDCA. In contrast, only pCON2Y65F exhibited BSH activity against TDCA.

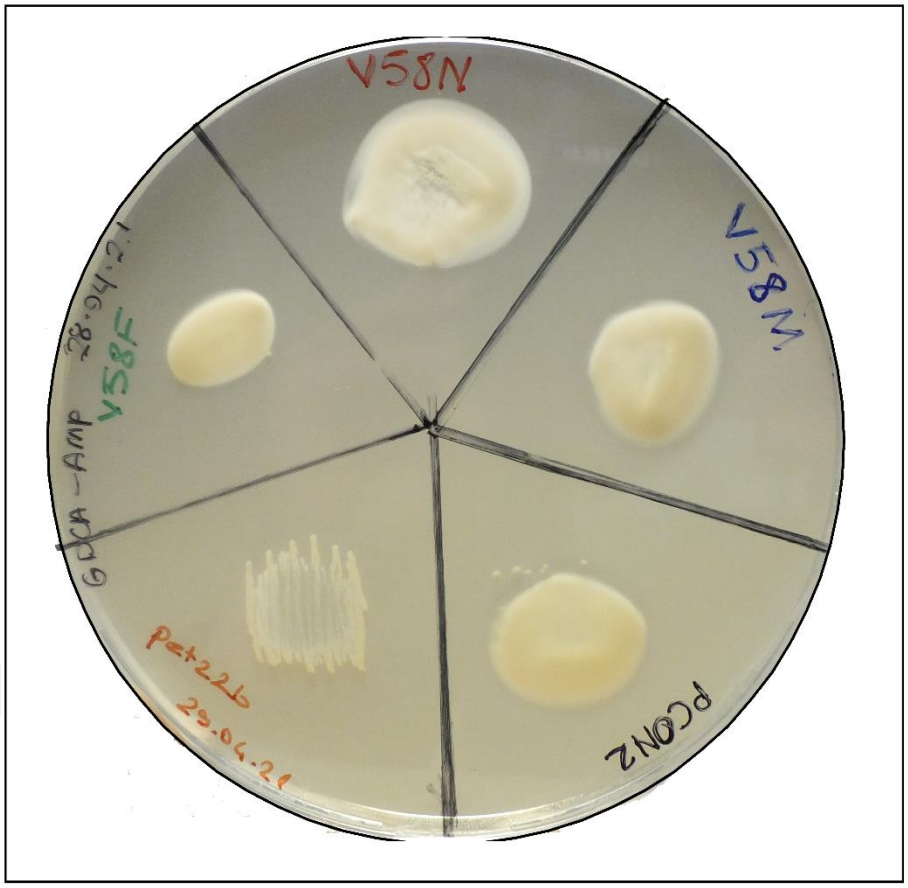

Figure 4.21. Detection of the pZEKV58F, pZEKV58M and pZEKV58N activity against GDCA by direct plate assay. Positive controls (pCON2/BLR(DE3), negative controls (pET22b/BLR(DE3) and BSH activity of pZEKV58F/BLR(DE3), pZEKV58M/BLR(DE3) and pZEKV58N/BLR(DE3) in LB-plate with GDCA.

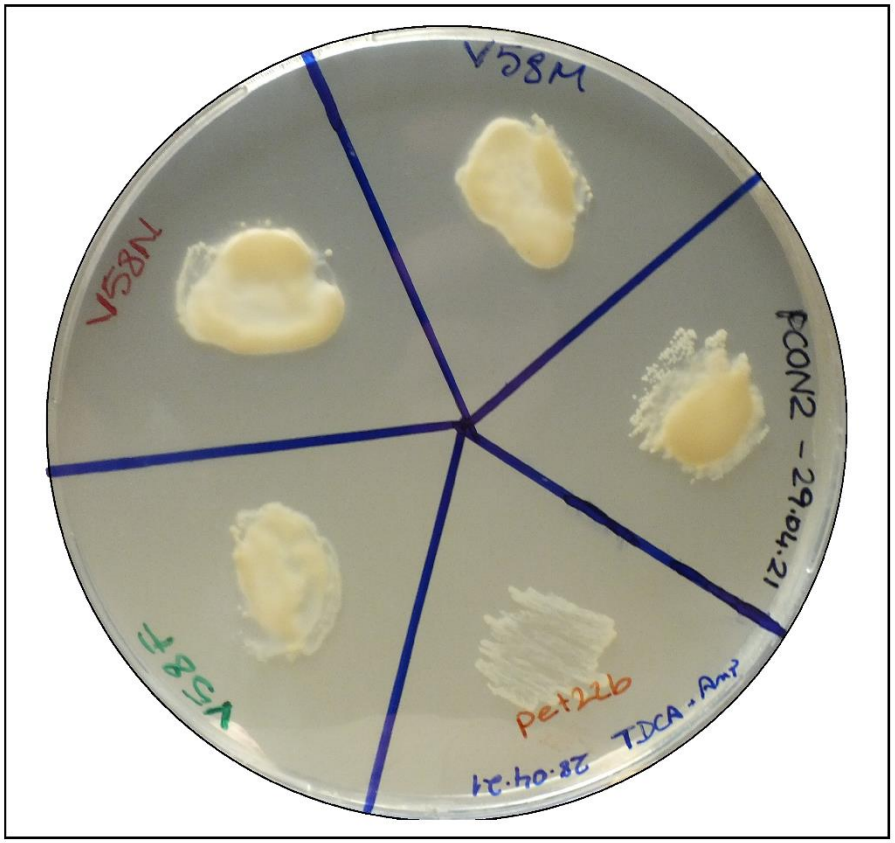

Figure 4.22. Detection of the pZEKV58F, pZEKV58M and pZEKV58N activity against TDCA by direct plate assay. Positive controls (pCON2/BLR(DE3), negative controls (pET22b/BLR(DE3) and BSH activity of pZEKV58F/BLR(DE3), pZEKV58M/BLR(DE3) and pZEKV58N/BLR(DE3) in LB-plate with TDCA.

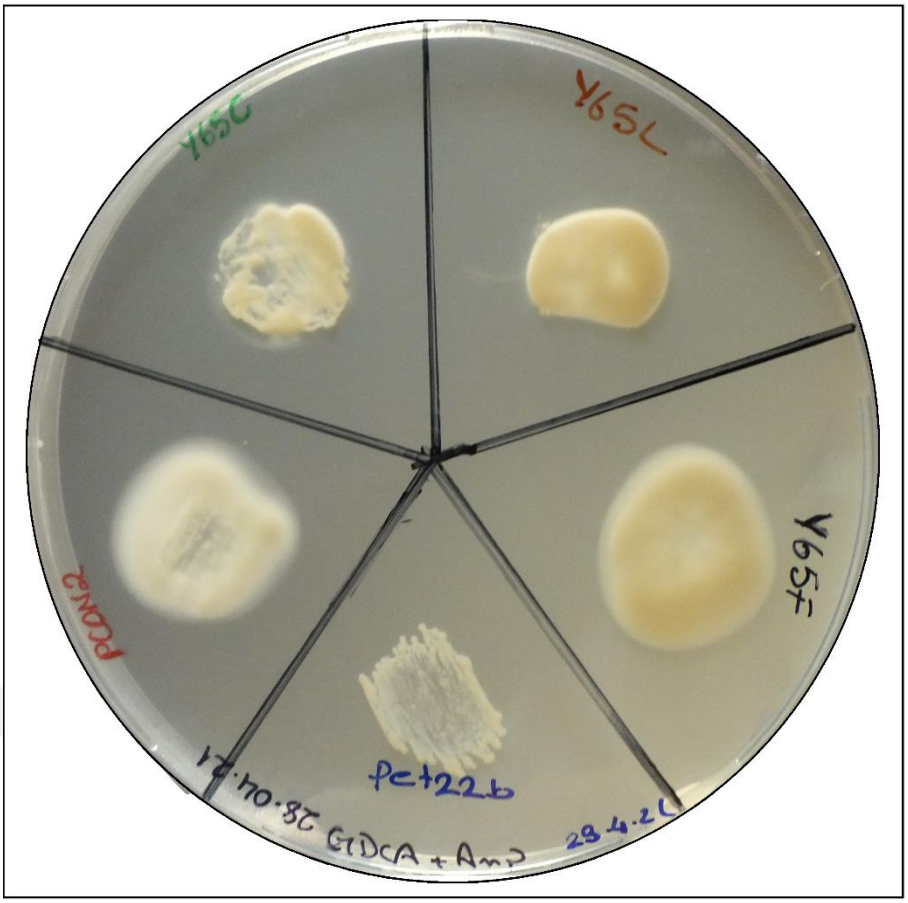

Figure 4.23. Detection of the pCON2Y65C, pCON2Y65F and pCON2Y65L activity against GDCA by direct plate assay. Positive controls (pCON2/BLR(DE3), negative controls (pET22b/BLR(DE3) and BSH activity of pCON2Y65C/BLR(DE3), pCON2Y65F/BLR(DE3) and pCON2Y65L/BLR(DE3) in LB-plate with GDCA.

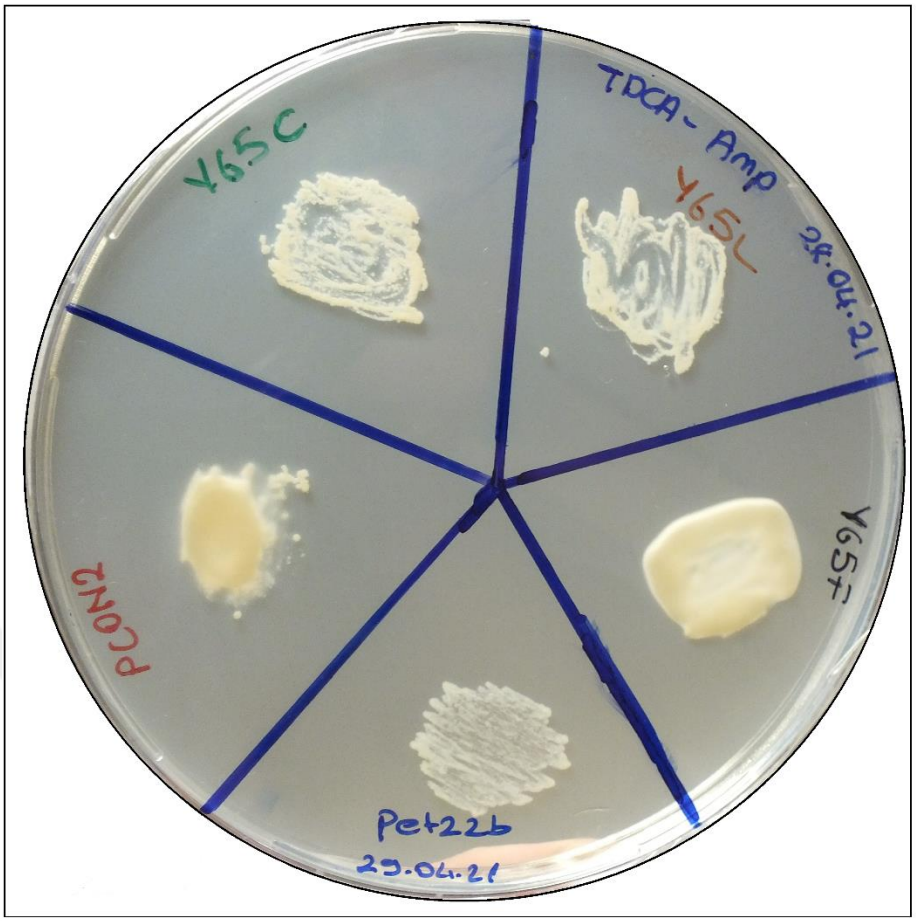

Figure 4.24. Detection of the pCON2Y65C, pCON2Y65F and pCON2Y65L activity against TDCA by direct plate assay. Positive controls (pCON2/BLR(DE3), negative controls (pET22b/BLR(DE3) and BSH activity of pCON2KY65C/BLR(DE3), pCON2Y65F/BLR(DE3) and pCON2Y65L/BLR(DE3) in LB-plate with TDCA.

4.4.2 Substrate Specificity of Mutant BSH Enzymes

pCON2 with wild type BSH enzyme exhibited varying levels of relative activity against six BAs (GCA, TCA, GDCA, TDCA, GCDCA, , and TCDCA) with values of 86.1 %, 100 %, 95.2 %, 11 %, 18 %, and 11.3%, as depicted in Figures 4.25 and 4.26. Mutant BSH enzymes exhibited varying levels of relative activity against six BAs with pZEKV58F values of 84.4 %, 98.8 %, 91.8 %, 6.2 %, 10.3 % and 1.7 %, pZEKV58N values of 88.7 %, 99.8 %, 89.2 %, 7 %, 11.5 % and 6.5 % and pZEKV58M values of 60.2 %, 73.9 %, 64 %, 4.6 %, 8 % and 2.9 % as depicted in Figures 4.25. Although the BSH enzyme's activity against glycine-conjugated BAs remained virtually unchanged after replacing valine-58 (V58) with asparagine (58N) and phenylalanine (58F) amino acids, the same mutations decreased

activities toward taurine-conjugated BAs by 40-85%. In contrast, the replacement of valine-58 (58V) with methioine (58M) was observed to significantly alter the effectiveness of BSH against conjugated BAs taurine and glycine by 30-75%. Mutant BSH enzymes exhibited varying levels of relative activity against six BAs with pCON2Y65L values of 21, 38.6 %, 23.3 %, 4.3 %, 6.5 % and 10.3 %, pCON2Y65F values of 64 %, 77 %, 50.4 %, 15.3 %, 13.4 % and 3.8 % and pCON2Y65C values of 12.5 %, 7% , 6.2 %, 2, 1 % and 3.6 % as depicted in Figures 4.26. Figure 4.26 illustrates that substituting the tyrosine-65 (65Y) amino acid with leucine (65L) or phenylalanine (65F) leads to reduced LpBSH enzyme activity against glycine and taurine conjugates. Additionally, it was found that the substitution of tyrosine-65 (Y65) amino acid with cysteine (C65) led to almost complete loss of activity against glycine and taurine conjugated BA (Figure 4.26).

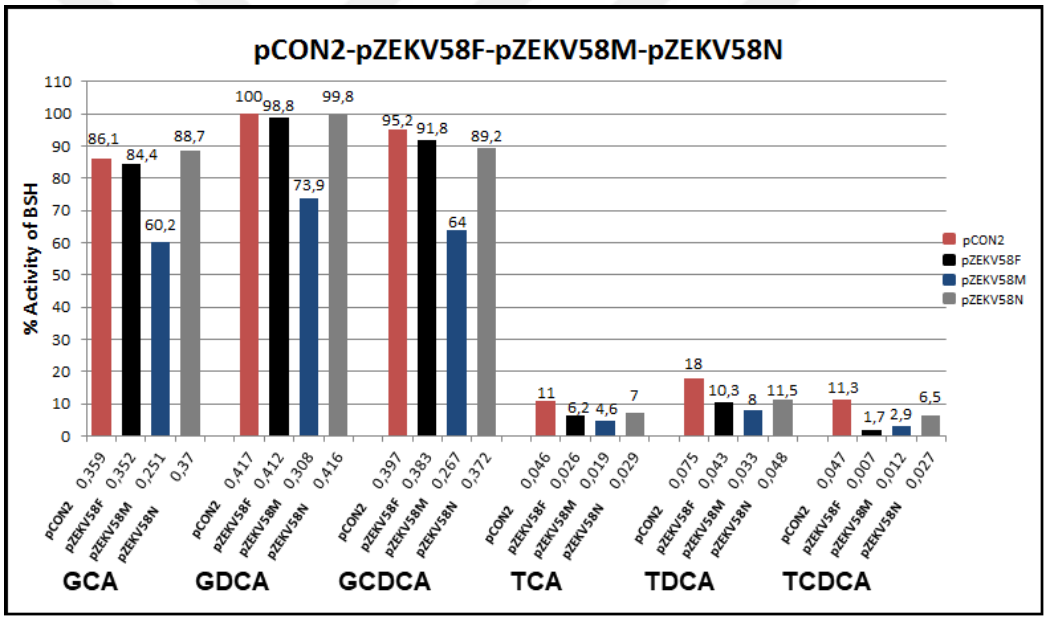

Figure 4.25. Comparison of substrate specificity between BSH enzymes of pZEKV58F, pZEKV58M, pZEKV58N and pCON2 using six bile salts. The deconjugation activity for each substrate was measured relative to the highest activity in the experiment, with 100% considered as GDCA.

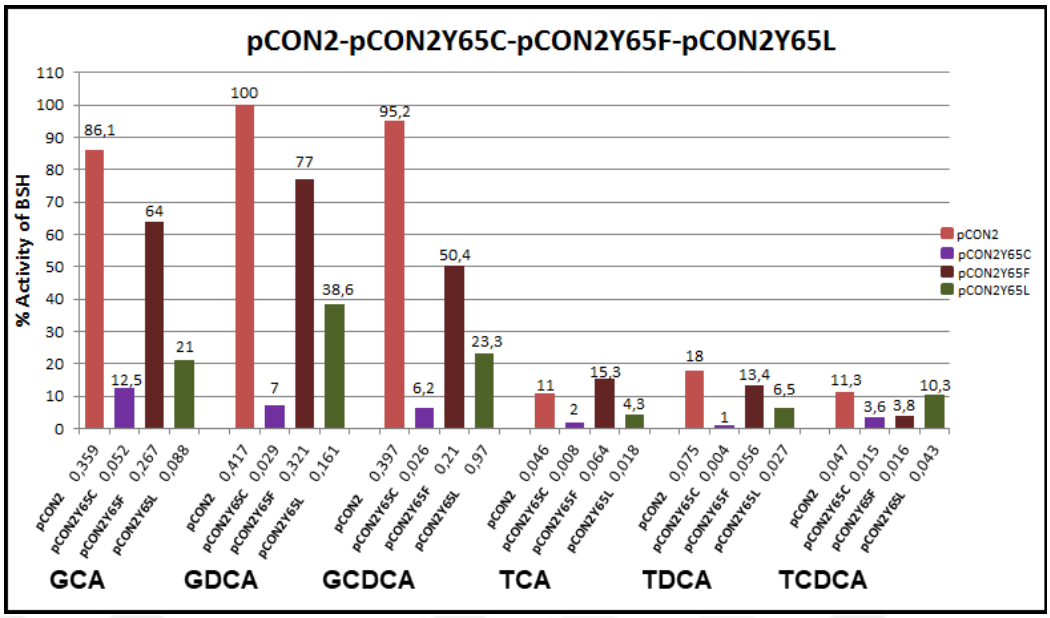

Figure 4.26. Comparison of substrate specificity between BSH enzymes of pCON2Y65C, pCON2Y65F, pCON2Y65L and pCON2 using six bile salts. The deconjugation activity for each substrate was measured relative to the highest activity in the experiment, with 100% considered as GDCA.

4.5 SDS PAGE Analysis of Mutant BSH Enzymes

A molecular weight of 37 kDa was detected in SDS-PAGE (Figure 4.28), which is in accordance with the predicted molecular weight of the BSH protein calculated using the ExPASy programme (http://web.expasy.org/protparam/) (Figure 4.27).

Number of amino acids: 324
Molecular weight: 37077.69
Theoretical pI: 5.21

Amino acid composition:

Ala (A)	14	4.3%	Lys (K)	17	5.2%
Arg (R)	10	3.1%	Met (M)	7	2.2%
Asn (N)	28	8.6%	Phe (F)	14	4.3%
Asp (D)	17	5.2%	Pro (P)	13	4.0%
Cys (C)	5	1.5%	Ser (S)	29	9.0%
Gln (Q)	13	4.0%	Thr (T)	15	4.6%
Glu (E)	19	5.9%	Trp (W)	2	0.6%
Gly (G)	18	5.6%	Tyr (Y)	27	8.3%
His (H)	6	1.9%	Val (V)	21	6.5%
Ile (I)	18	5.6%	Pyl (O)	0	0.0%
Leu (L)	31	9.6%	Sec (U)	0	0.0%

Total number of negatively charged residues (Asp + Glu): 36
Total number of positively charged residues (Arg + Lys): 27

Figure 4.27. Analysis of *L. plantarum* BSH 14's amino acid composition. Using the SIB (Swiss Institute of Bioinformatics) ExPASy ProtParam sequence analysis translate tool (http://web.expasy.org/protparam/).

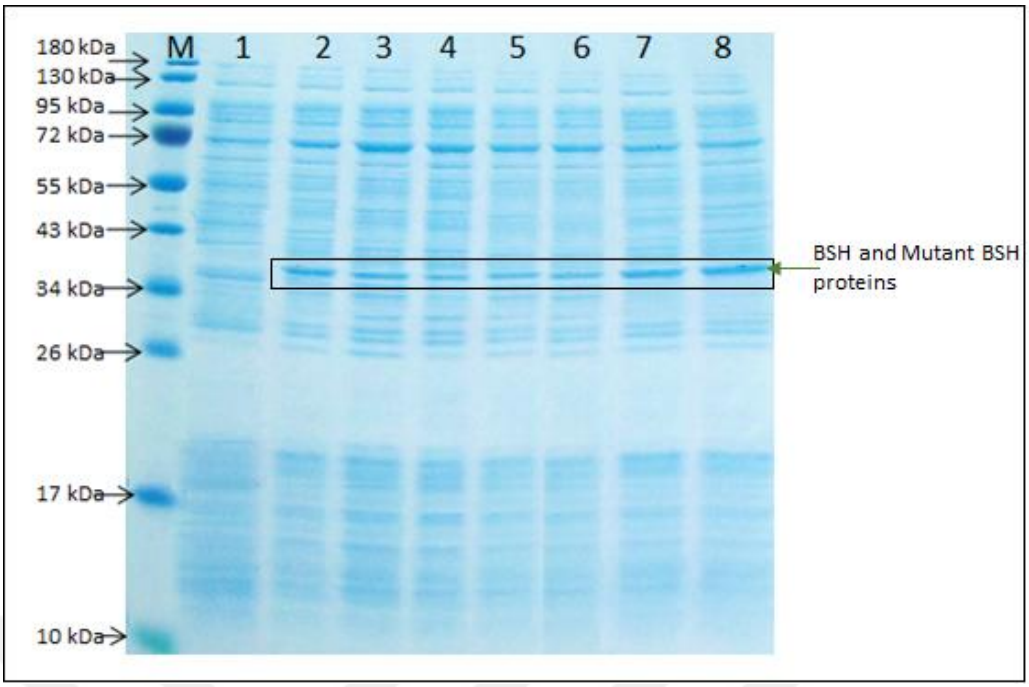

Figure 4.28. Analysis of partially purified mutant BSHs using SDS-PAGE. M, Protein ladder; lane 1, partially purified cell extracts of BLR(DE3) not carrying BSH in pET22b expression vector (negative control); lane 2, the partially purified BSH protein (positive control); lane 3, partially purified BSH/V58F protein; 4, partially purified V58M BSH protein; 5, partially purified V58N BSH protein; 6, partially purified Y65C

4.6 Mutant Constructions of pCON1V58M-Y65F and pCON1V58M-Y65L

4.6.1 Target Amino Acid Site-Directed Mutagenesis

In order to ascertain whether there is a correlation between the 58 and 65 regions of BSH, the results of the ninhydrin analysis of the mutations were considered. It was found that phenylalanine and leucine were effective in increasing the activity of the 65 region, while cysteine was not selected due to its almost complete effectiveness. Furthermore, it was determined that the methionine on the 58 region was more effective, and double mutations for V58M-Y65F and V58M-Y65L were identified. Primers containing the target amino acids (Figure 3.10) were used to convert the wild-type tyrosine (TAC)-65 to phenylalanine (TTT)-65 and leucine (CTG)-65 amino acids on pCON1V58M by PCR. Template DNA pCON1V58M was removed from the resulting PCR products using the restriction enzyme *Dpn*I (Figure 4.29).

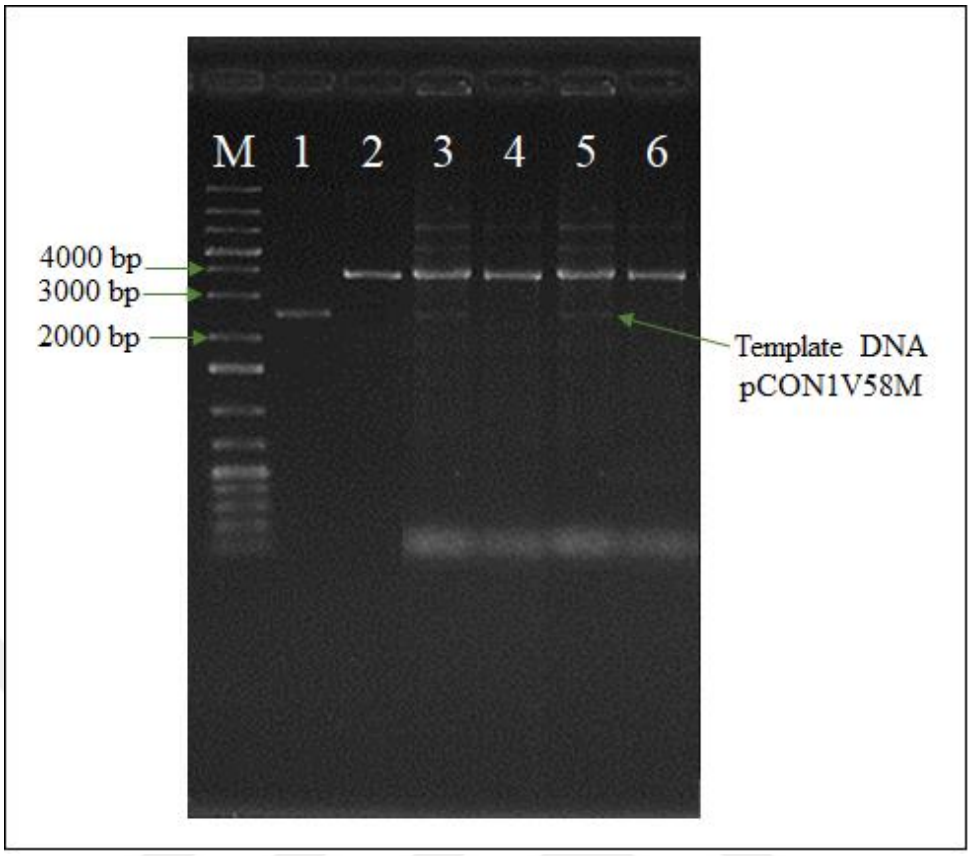

Figure 4.29. Mutation of pCON1V58M*-Y65L and pCON1V58M*-Y65L with site-directed (* represents desired mutation). M, 1 kb plus DNA ladder; 1, uncut pCON1V58M template DNA (1/5 diluted); 2, *Xho*I cut pCON1V58M template DNA; 3, pCON1V58M*-Y65F PCR product; 4, pCON1V58M*-Y65F PCR product digested with *Dpn*I restriction enzyme; 5, pCON1V58M*-Y65L PCR product; 6, pCON1V58M*-Y65L PCR product digested with *Dpn*I restriction enzyme.

4.6.2 Purifying Mutated PCR Products

The pCON1V58M*-Y65F and pCON1V58M*-Y65L mutants were individually purified from 1% agarose gels to eliminate non-specific PCR products and undigested methylated template DNA (Figure 4.30).

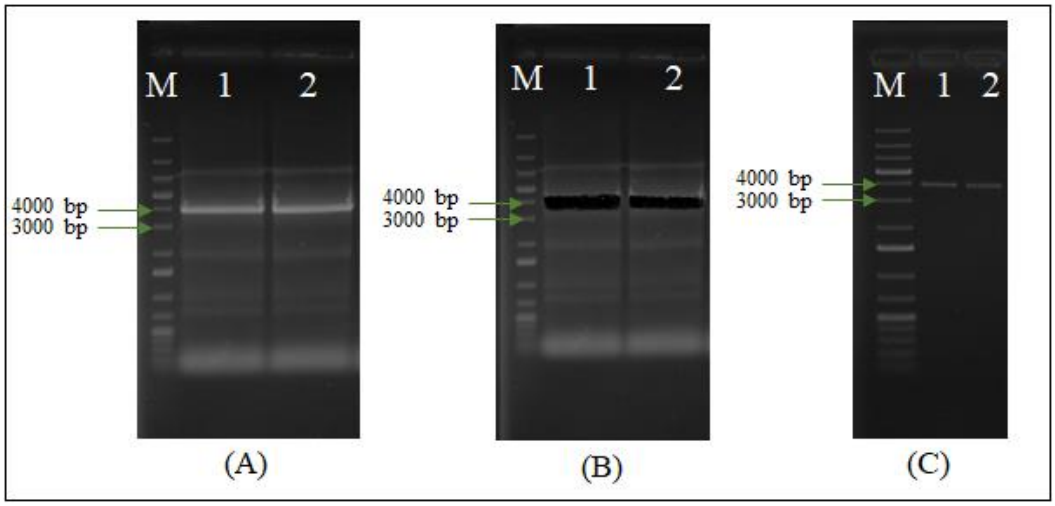

Figure 4. 30. Gel Purification for pCON1V58M*-Y65F and pCON1V58M*-Y65L. M, 1 kb plus DNA ladder. (A) 1, pCON1V58M*-Y65F PCR products; 2, pCON1V58M*-Y65L PCR products; (B), 1, sliced pCON1V58M*-Y65F PCR products; 2, sliced pCON1V58M*-Y65L PCR products; (C) 1, purified pCON1V58M*-Y65F (4.0 kb); 2, purified pCON1V58M*-Y65L (4.0 kb).

4.6.3 Transformation of pCON1V58M*-Y65F and pCON1V58M*-Y65L Mutant Constructs

Gel- extracted pCON1V58M*-Y65F and pCON1V58M*-Y65L DNAs were separately transferred into *E. coli* XL1-Blue competent cells and confirmed to be the same size (nearly 4.0 kb) as the pCON1V58M DNA by cutting pCON1V58M*-Y65F and pCON1V58M*-Y65L DNAs with *Xho*I restriction enzyme (Figure 4.31).

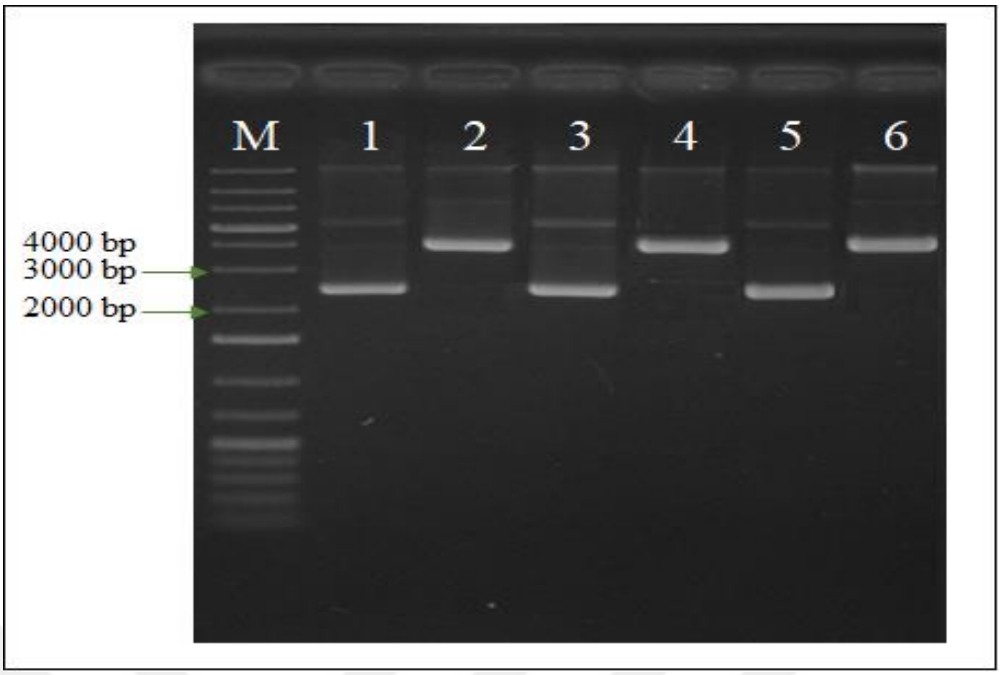

Figure 4.31. Transformation of pCON1V58M*-Y65F and pCON1V58M*-Y65L into *E. coli* XL1-Blue strains. M, 1 kb plus DNA ladder; 1, uncut pCON1V58M DNA; 2 *Xho*I cut pCON1V58M DNA; 3, pCON1V58M*-Y65F DNA; 4, *Xho*I cut pCON1V58M*-Y65F DNA; 5, pCON1V58M*-Y65L DNA; 6, *Xho*I cut pCON1V58M*-Y65L.

4.6.4 Detection of Targeted Mutations by DNA Sequencing

The DNAs of pCON1V58M-Y65F and pCON1V58M-Y65L were sequenced by Macrogen (Seoul, Korea) using the universal primers, M13/pUC Reverse (5'-CAGGAAACAGCTATGAC-3') and M13/pUC Forward (5'-GTAAAACGACGGCCAGT-3') and reported using the BioEdit sequence alignment program. In the resulting DNA sequences, only target mutations were detected (Figure 4.32 – 4.33). Sequencing revealed that the code for the amino acid tyrosine 65 was converted to the TTT and CTG codons, which code for the amino acids phenylalanine 65 and leucine 65.

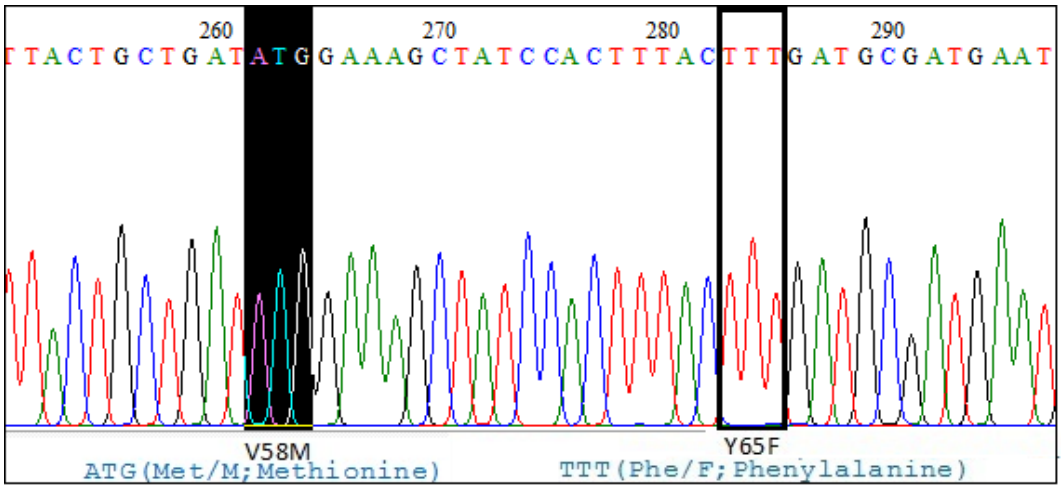

Figure 4.32. The target mutation of pCON1V58M-Y65F. Valine-58 (V) codon, GTA, was converted to Methionine (M) codon, ATG and Tyrosine-65 (Y) codon, TAC, was converted to Phenylelanine (F) codon, TTT, labelled with a frame.

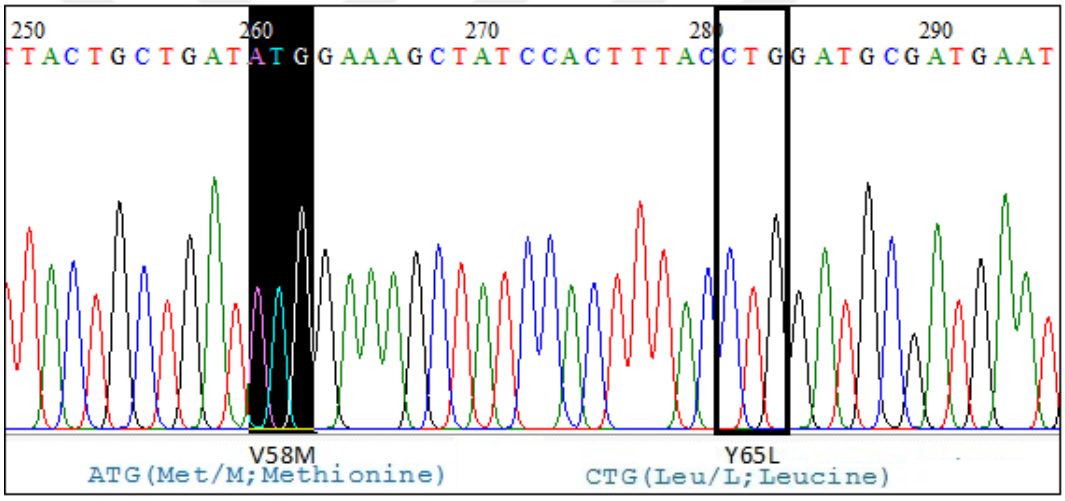

Figure 4.33. The target mutation of pCON1V58M-Y65L. Valine-58 (V) codon, GTA, was converted to Methionine (M) codon, ATG and Tyrosine-65 (Y) codon, TAC, was converted to Leucine (L) codon, CTG, labelled with a frame.

4.7 Making Mutant pZEKV58M-Y65F and pZEKV58M-Y65L Constructs

4.7.1 Digestion of Mutant pZEKV58M-Y65F and pZEKV58M-Y65L DNAs by *EcoR*I and *Not*I Restriction Enzymes

Following the restriction enzyme cuts of the pCON1V58M-Y65F and pCON1V58M-Y65L, plasmid DNAs with *Not*I and *Eco*RI, the resulting roughly 1 kbp mutant BSH fragments of DNA were extracted from gels with 1% agarose (Figure 4.34).

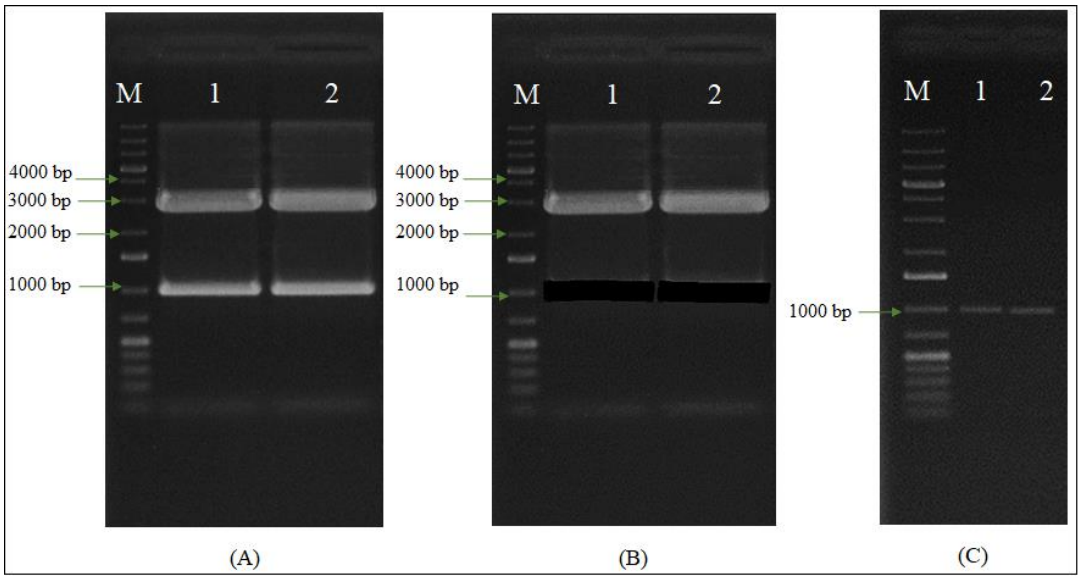

Figure 4.34. Digestion of pCON1V58M-Y65F and pCON1V58M-Y65L plasmid DNAs by *Not*I and *Eco*RI REs. M, 1 kb plus DNA ladder; A, 1: pCON1V58M-Y65F DNA cut with *Eco*RI and *Not*I REs; 2, pCON1V58M-Y65L DNA cut with *Eco*RI and *Not*I REs; B, 1, sliced V58M-Y65F *bsh* DNA fragment from pCON1V58M-Y65F DNA; 2, sliced V58M-Y65L *bsh* DNA fragment from pCON1V58M-Y65L DNA; C, 1, gel purified V58M-Y65F *bsh* DNA fragment from pCON1V58M-Y65F DNA; 2, gel purified V58M-Y65L *bsh* DNA fragment from pCON1V58M-Y65L DNA.

4.7.2 Accuracy of Mutant *bsh* Genes in pZEKV58M-Y65F and pZEKV58M-Y65L Constructs

The correct insertion of the mutant *bsh* genes, approximately 1.0 kbp in size, into the pET22b, 5.5 kbp, vector was confirmed by the restriction enzymes *Not*I and *EcoR*I (Figure 4.35). Correctly defined transformants were named pZEKV58M-Y65F and pZEKV58M-Y65L.

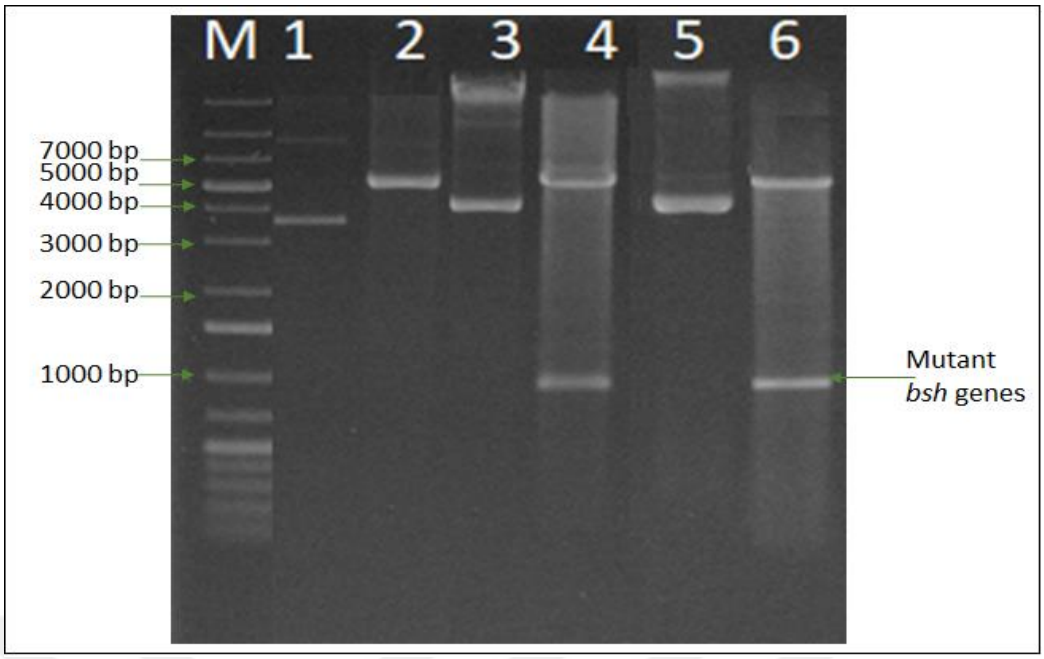

Figure 4.35. Accuracy of mutant *bsh* genes in pZEKV58M-Y65F and pZEKV58M-Y65L constructs. M, 1 kb plus DNA ladder; 1, circular DNAs of pET22b; 2, *Not*I and *Eco*RI REs digested DNAs of pET22b; 3 circular DNAs of in pZEKV58M-Y65F; 4, *Not*I and *Eco*RI REs digested DNAs of pZEKV58M-Y65F; 5 circular DNAs of in pZEKV58M-Y65L; 6, *Not*I and *Eco*RI REs digested DNAs of pZEKV58M-Y65L.

4.7.3 Substrate Specificity of V58M-Y65F and V58M-Y65L Mutants BSH Enzymes

pCON2 with wild type BSH enzyme, mutant pZEKV58M BSH, double mutants pZEKV58M-Y65F and pZEKV58M-Y65L BSHs exhibited varying levels of relative activity against six BAs, GCA, TCA, GDCA, TDCA, GCDCA, and TCDCA, as depicted in Figures 4.35. The double mutant pZEKV58M-Y65F BSH with values of 26.6%, 41.1%, 20%, 3.68%, 7.14% and 3.1% and also pZEKV58M-Y65L BSH with values of 15.1%, 26.03%, 14.3%, 3.5%, 6.34% and 3% are shown in the Figures 4.36 and Figures 4.37. The ninhydrine results indicated that the double mutations, V58M-Y65F and V58M-Y65L, exhibited a further reduction in BSH activity against conjugated BAs with taurine and glycine compared to the single mutations, V58M, Y65F and Y65L (Figures 4.36 and Figures 4.37). However, the V58M-Y65F and V58M-Y65L mutations did not result in any alterations to substrate selectivity.

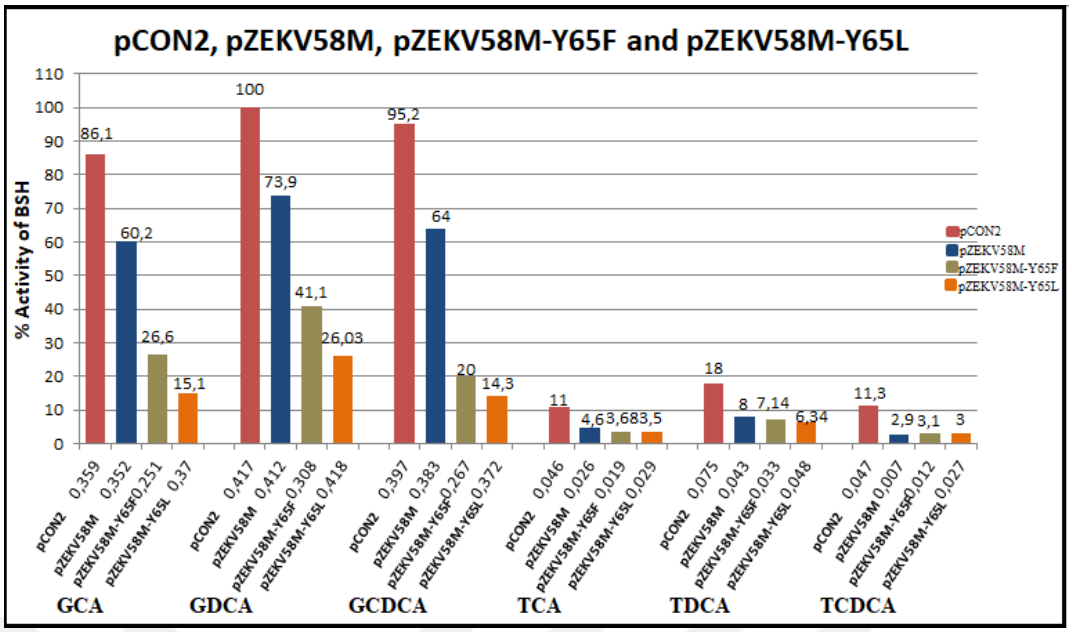

Figure 4.36. Comparison of substrate specificity between BSH enzymes of pZEKV58M-Y65F and pZEKV58M-Y65L and pCON2 using six bile salts. The deconjugation activity for each substrate was measured relative to the highest activity in the experiment, with 100% considered as GDCA.

BSHs	GCA	GDCA	GCDCA	TCA	TDCA	TCDCA
pCON2 wild type	86.1 %	100 %	95.2 %	11 %	18 %	11.3%
pZEKV58M	60.2%	73.9 %	64 %	4.6 %	8 %	2.9 %
pCON2Y65F	64 %	77 %	50.4 %	15.3 %	13.4 %	3.8 %
pCON2Y65L	21 %	38.6 %	23.3 %	4.3 %	6.5 %	10.3 %
pZEKV58M-Y65F	26.6 %	41.1 %	20 %	3.68 %	7.14 %	3.1 %
pZEKV58M-Y65L	15.1 %	26.03 %	14.3 %	3.5 %	6.34 %	3 %

Figure 4.37. The activity profiles of pCON2, pZEKV58M, pCON2Y65F, pCON2Y65L, pZEKV58M-Y65F and pZEKV58M-Y65L in relation to each other. The deconjugation activity for each substrate was measured relative to the highest activity in the experiment, with 100% considered as GDCA.

5. DISCUSSION

BSHs are special enzymes that play a major role in the deconjugation reaction. They present a promising approach to managing a wide range of illnesses, from inflammatory diseases, infectious and to metabolic disorders. Research focusing on the molecular characteristics of BSH enzymes, such as genetic regulation and protein structure, would be extremely relevant to properly discuss and assess the implications of BSHs as a therapeutic tool. The hydrophobic interactions between BAs and BSH were derived from crystal structures and in silico analyses The high hydrophobic complementarity between CGH members is a critical factor influencing catalytic activity and substrate specificity. CGH loops II and III also play a role in substrate binding, as with PVA (32, 54, 179). Upon substrate binding to subunits surrounding the tetramer, loop II can convey conformational changes to neighbouring tetramer subunits. Conformational changes within the active site could potentially affect substrate binding and catalysis (180).

Sequence alignment of BSHs shows low sequence identity and likely positions of residues contributing to substrate selectivity in various BSH isotypes. The crystal structure's homology modelling the and sequence alignment of BSHs revealed that Y65, which is closer to Cys2 and may be important for the catalytic activity of LpBSH, is more conserved around catalytic sites than V58 in BSHs.

It is probable that distinct BSH isotypes' substrate selectivity is influenced by residues at various locations. The substrate binding profile in LpBSH is determined by two essential residues in loop 2, which were found and experimentally investigated in this work. The contribution of Tyr65 and Val58 mutations in LpBSH to substrate selectivity was shown. The substitution of Val58 with methionine on LpBSH leads to a modified substrate specificity. Presumably, Val58 establishes an H-bond network with manifold pocket residues instead of having a direct interaction with BA. Consequently, the mutation of Val58 can change the hydrophilic features and structure of the pocket, which in turn potentially affects the binding mechanism of substrates that involve glycol and tauro conjugations. Similarly, Karlov et al. (181) performed site-directed mutagenesis to determine the function of A58 in the reaction catalysis and substrate

binding of *Lactobacillus salivarus* BSH and observed small differences in hydrolysis for some glyco- and tauro-conjugates.

However, it is noteworthy that in both EfBSH and LpBSH, Tyr65 is conserved indicating that this amino acid residue may play a crucial role in substrate specificity. The crystal structure of EfBSH, along with homology modelling and sequence alignment, revealed that in BSHs, the Y65 residue close to the catalytic sites is conserved to a greater extent than V58. Additionally, Y65 is in closer proximity to Cys2 and may play a crucial role in the catalytic activity of LpBSH. During the post-translational processing of CGHs, Chand et al's (34) research highlights the importance of two adjacent residues, Y65and Y20 in relation to the Cys nucleophile. Furthermore, Xu et al (182) carried out site-directed mutagenesis to ascertain the function of Y65 in the reaction catalysis and substrate binding of *Lactobacillus salivarus* BSH (LsBSH). To illustrate its role in stabilising the sterane ring of bile salts, the amino acid F65 was modified. F65's mutation reduced hydrolytic activity against GCDCA but eliminated it entirely against GDCA and GCA. In comparison to the wild-type LsBSH, the activity of the mutant LsBSH towards TDCA and TCA was diminished by 40 to 50%. However, no changes were observed in TCDCA. This is directly supported by our experimental data which show that BSH's catalytic activity for BAs is significantly decreased when Y65 is converted to C65, F65, and L65. Comparing the BSH activity of the V58M-Y65F and V58M-Y65L to that of the single mutations V58M, Y65F, and Y65L, they showed a further decrease against conjugated BAs taurine and glycine (Figures 4.36 and 4.37). Substrate selectivity was unaffected by the V58M-Y65F and V58M-Y65L mutations, though. All these results suggest that although amino acids in certain regions of BSH play a very important role in substrate activity, substrate selectivity may depend on multiple variables rather than a single criterion.

The BSH enzyme primarily recognizes possible substrates by their amino acid moieties, as opposed to the cholate steroid nucleus (166). Furthermore, in comparison to their taurine-conjugated equivalents, glycine-conjugated bile salts are more likely to be deconjugated by the majority of BSH enzymes (22, 183). Moreover, certain host species display an increased level of BAs conjugated with glycine in their stomachs in comparison to taurine-conjugated BAs, potentially acting as a selective pressure for this specific substrate preference (47). By contrast, our prior research (177) and current findings demonstrate considerable variance in

BSH catalytic activity towards different BA cholate groups, indicating that the cholate group instead of the amino acid moieties, may determine BSH substrate specificity.

In summary, BSH enzymes are crucial for maintaining intestinal microbiota balance, regulating cholesterol levels, and supporting metabolic health. They deconjugate bile acids, which affects intestinal bacterial composition, lowers serum cholesterol, and modulates lipid and glucose metabolism. BSH enzymes are important for selecting effective probiotics, developing pharmaceuticals for bile acid-related disorders, and creating nutritional supplements to improve digestive health and cholesterol management. Their role in metabolic regulation and potential applications in health and medicine make BSH enzymes an important area of research and innovation. Industrially, BSH enzymes can improve probiotic formulations, increase animal feed efficiency and support biotechnological applications. In the probiotic industry, BSH enzymes can support gut health and metabolic balance by helping to develop strains that function effectively in the gastrointestinal tract. In livestock farming, BSH free probiotics in feed can reduce the need for antibiotics and promote sustainable animal husbandry by improving nutrient absorption and growth performance. Furthermore, BSH enzymes have potential applications in synthesis of bioactive compounds, making them valuable for the environmental and pharmaceutical industries. These versatile benefits may position BSH enzymes as essential tools in a variety of industrial processes aimed at improving health, sustainability and efficiency.

6. CONCLUSIONS AND RECOMMENDATIONS

The study showed experimentally that the turnover of substrate binding and catalytic activity is altered by mutations of residues V58 and Y65 in LpBSH loop II. This suggests that these residues play a significant role in the specificity for substrate and the catalytic process. Furthermore, it appears that loop II's V58 and, in particular, the Y65 residues may play a significant role in establishing the structural site that controls substrate specificity. Prior studies (166) suggest that the cholate steroid nucleus is not the primary factor used by the BSH enzyme to identify potential substrates; however, our data show significant fluctuations in the catalytic activity of BSH toward various cholate groups in BA, suggesting that the cholate group may be the determining factor in BSH substrate specificity rather than amino acid moieties. These findings are new, but they need confirmation in BSHs of other related CGHs. Thus, to identify residues that the BSHs prefer as a substrate and to understand the substrate preferences of BSHs with particular substrates, additional structural analyses and mutagenesis with amino acid replacement of BSHs are necessary.

7. REFERENCES

"Vancouver citation system was used in this thesis."

1. Chand D, Avinash VS, Yadav Y, Pundle AV, Suresh CG, Ramasamy S. Molecular features of bile salt hydrolases and relevance in human health. Biochim Biophys Acta Gen Subj. 2017;1861(1 Pt A):2981-91.

2. Horackova S, Plockova M, Demnerova K. Importance of microbial defence systems to bile salts and mechanisms of serum cholesterol reduction. Biotechnol Adv. 2018;36(3):682-90.

3. Inagaki T, Moschetta A, Lee YK, Peng L, Zhao G, Downes M, et al. Regulation of antibacterial defense in the small intestine by the nuclear bile acid receptor. Proc Natl Acad Sci U S A. 2006;103(10):3920-5.

4. Geng W, Lin J. Bacterial bile salt hydrolase: an intestinal microbiome target for enhanced animal health. Anim Health Res Rev. 2016;17(2):148-58.

5. Foley MH, O'Flaherty S, Barrangou R, Theriot CM. Bile salt hydrolases: Gatekeepers of bile acid metabolism and host-microbiome crosstalk in the gastrointestinal tract. PLoS Pathog. 2019;15(3):e1007581.

6. Patel AK, Singhania RR, Pandey A, Chincholkar SB. Probiotic bile salt hydrolase: current developments and perspectives. Appl Biochem Biotechnol. 2010;162(1):166-80.

7. Tsai CC, Lin PP, Hsieh YM, Zhang ZY, Wu HC, Huang CC. Cholesterol-lowering potentials of lactic acid bacteria based on bile-salt hydrolase activity and effect of potent strains on cholesterol metabolism in vitro and in vivo. ScientificWorldJournal. 2014;2014:690752.

8. Tanaka H, Doesburg K, Iwasaki T, Mierau I. Screening of lactic acid bacteria for bile salt hydrolase activity. J Dairy Sci. 1999;82(12):2530-5.

9. Fiorucci S, Distrutti E. Bile Acid-Activated Receptors, Intestinal Microbiota, and the Treatment of Metabolic Disorders. Trends Mol Med. 2015;21(11):702-14.

10. Chiang JY. Bile acids: regulation of synthesis. J Lipid Res. 2009;50(10):1955-66.

11. Ridlon JM, Hylemon PB. Identification and characterization of two bile acid coenzyme A transferases from *Clostridium scindens*, a bile acid 7alpha-dehydroxylating intestinal bacterium. J Lipid Res. 2012;53(1):66-76.

12. Eggert T, Bakonyi D, Hummel W. Enzymatic routes for the synthesis of ursodeoxycholic acid. J Biotechnol. 2014;191:11-21.

13. Fukiya, S., Arata, M., Kawashima, H., Yoshida, D., Kaneko, M., Minamida, K., Watanabe, J., Ogura, Y., Uchida, K., Itoh, K., Wada, M., Ito, S., Yokota, A.,. Conversion of cholic acid and chenodeoxycholic acid into their 7-oxo derivatives by *Bacteroides intestinalis* AM-1 isolated from human feces. FEMS Microbiol. Lett. 2009; 293, 263–270.

14. Lepercq P, Gerard P, Beguet F, Raibaud P, Grill JP, Relano P, et al. Epimerization of chenodeoxycholic acid to ursodeoxycholic acid by *Clostridium baratii* isolated from human feces. FEMS Microbiol Lett. 2004;235(1):65-72.

15. Gerard C, Vidal H. Impact of Gut Microbiota on Host Glycemic Control. Front Endocrinol (Lausanne). 2019;10:29.

16. Takemura N, Hagio M, Ishizuka S, Ito H, Morita T, Sonoyama K. Inulin prolongs survival of intragastrically administered *Lactobacillus plantarum* No. 14 in the gut of mice fed a high-fat diet. J Nutr. 2010;140(11):1963-9.

17. Ridlon JM, Harris SC, Bhowmik S, Kang DJ, Hylemon PB. Consequences of bile salt biotransformations by intestinal bacteria. Gut Microbes. 2016;7(1):22-39.

18. Ridlon JM, Bajaj JS. The human gut sterolbiome: bile acid-microbiome endocrine aspects and therapeutics. Acta Pharm Sin B. 2015;5(2):99-105.

19. Li T, Chiang JY. Bile acid signaling in metabolic disease and drug therapy. Pharmacol Rev. 2014;66(4):948-83.

20. Jahan A, Chiang JY. Cytokine regulation of human sterol 12alpha-hydroxylase (CYP8B1) gene. Am J Physiol Gastrointest Liver Physiol. 2005;288(4):G685-95.

21. Pathak P, Chiang JYL. Sterol 12alpha-Hydroxylase Aggravates Dyslipidemia by Activating the Ceramide/mTORC1/SREBP-1C Pathway via FGF21 and FGF15. Gene Expr. 2019;19(3):161-73.

22. Dong Z, Lee BH. Bile salt hydrolases: Structure and function, substrate preference, and inhibitor development. Protein Sci. 2018;27(10):1742-54.

23. Abrigo J, Gonzalez F, Aguirre F, Tacchi F, Gonzalez A, Meza MP, et al. Cholic acid and deoxycholic acid induce skeletal muscle atrophy through a mechanism dependent on TGR5 receptor. J Cell Physiol. 2021;236(1):260-72.

24. Goldstein J, Levy C. Novel and emerging therapies for cholestatic liver diseases. Liver Int. 2018;38(9):1520-35.

25. Teodoro JS, Rolo AP, Palmeira CM. Hepatic FXR: key regulator of whole-body energy metabolism. Trends Endocrinol Metab. 2011;22(11):458-66.

26. Han CY. Update on FXR Biology: Promising Therapeutic Target? Int J Mol Sci. 2018;19(7).

27. Rodrigues RR, Greer RL, Dong X, KN DS, Gurung M, Wu JY, et al. Antibiotic-Induced Alterations in Gut Microbiota Are Associated with Changes in Glucose Metabolism in Healthy Mice. Front Microbiol. 2017;8:2306.

28. Chiang JYL, Ferrell JM. Bile Acid Metabolism in Liver Pathobiology. Gene Expr. 2018;18(2):71-87.

29. Begley M, Hill C, Gahan CG. Bile salt hydrolase activity in probiotics. Appl Environ Microbiol. 2006;72(3):1729-38.

30. Philem PD, Yadav Y, Vellore Sunder A, Ghosh D, Prabhune A, Ramasamy S. Structural and enzymatic analysis of a dimeric cholylglycine hydrolase like acylase active on N-acyl homoserine lactones. Biochimie. 2020;177:108-16.

31. Oinonen C, Rouvinen J. Structural comparison of Ntn-hydrolases. Protein Sci. 2000;9(12):2329-37.

32. Rossocha M, Schultz-Heienbrok R, von Moeller H, Coleman JP, Saenger W. Conjugated bile acid hydrolase is a tetrameric N-terminal thiol hydrolase with specific recognition of its cholyl but not of its tauryl product. Biochemistry. 2005;44(15):5739-48.

33. Kumar RS, Brannigan JA, Prabhune AA, Pundle AV, Dodson GG, Dodson EJ, Suresh CG. Structural and functional analysis of a conjugated bile salt hydrolase from *Bifidobacterium longum* reveals an evolutionary relationship with penicillin V acylase. J Biol Chem. 2006;281(43):32516-25.

34. Chand D, Panigrahi P, Varshney N, Ramasamy S, Suresh CG. Structure and function of a highly active Bile Salt Hydrolase (BSH) from *Enterococcus faecalis* and post-translational processing of BSH enzymes. Biochim Biophys Acta Proteins Proteom. 2018;1866(4):507-18.

35. Jones BV, Begley M, Hill C, Gahan CG, Marchesi JR. Functional and comparative metagenomic analysis of bile salt hydrolase activity in the human gut microbiome. Proc Natl Acad Sci U S A. 2008;105(36):13580-5.

36. Kim GB, Lee BH. Biochemical and molecular insights into bile salt hydrolase in the gastrointestinal microflora-a review. Asian-Austral J Anim Sci 2005; 18: 1505–1512.

37. Liang L, Yi Y, Lv Y, Qian J, Lei X, Zhang G. A Comprehensive Genome Survey Provides Novel Insights into Bile Salt Hydrolase (BSH) in Lactobacillaceae. Molecules. 2018;23(5).

38. Song Z, Cai Y, Lao X, Wang X, Lin X, Cui Y, et al. Taxonomic profiling and populational patterns of bacterial bile salt hydrolase (BSH) genes based on worldwide human gut microbiome. Microbiome. 2019;7(1):9.

39. Jia B, Park D, Hahn Y, Jeon CO. Metagenomic analysis of the human microbiome reveals the association between the abundance of gut bile salt hydrolases and host health. Gut Microbes. 2020;11(5):1300-13.

40. Nguyen TD, Kang JH, Lee MS. Characterization of *Lactobacillus plantarum* PH04, a potential probiotic bacterium with cholesterol-lowering effects. Int J Food Microbiol. 2007;113(3):358-61.

41. Ramasamy K, Abdullah N, Wong MC, Karuthan C, Ho YW. Bile salt deconjugation and cholesterol removal from media by Lactobacillus strains used as probiotics in chickens. J Sci Food Agric. 2010;90(1):65-9.

42. Xu F, Guo F, Hu XJ, Lin J. Crystal structure of bile salt hydrolase from *Lactobacillus salivarius*. Acta Crystallogr F Struct Biol Commun. 2016;72(Pt 5):376-81.

43. Adhikari AA, Seegar TCM, Ficarro SB, McCurry MD, Ramachandran D, Yao L, et al. Development of a covalent inhibitor of gut bacterial bile salt hydrolases. Nat Chem Biol. 2020;16(3):318-26.

44. Huijghebaert SM, Hofmann AF. Influence of the amino acid moiety on deconjugation of bile acid amidates by cholylglycine hydrolase or human fecal cultures. J Lipid Res. 1986;27(7):742-52.

45. Batta AK, Salen G, Shefer S. Substrate specificity of cholylglycine hydrolase for the hydrolysis of bile acid conjugates. J Biol Chem. 1984;259(24):15035-9.

46. Hu PL, Yuan YH, Yue TL, Guo CF. A new method for the in vitro determination of the bile tolerance of potentially probiotic lactobacilli. Appl Microbiol Biotechnol. 2018;102(4):1903-10.

47. Sjovall J. Dietary glycine and taurine on bile acid conjugation in man; bile acids and steroids 75. Proc Soc Exp Biol Med. 1959;100(4):676-8.

48. McAuliffe O, Cano RJ, Klaenhammer TR. Genetic analysis of two bile salt hydrolase activities in *Lactobacillus acidophilus* NCFM. Appl Environ Microbiol. 2005;71(8):4925-9.

49. Moser SA, Savage DC. Bile salt hydrolase activity and resistance to toxicity of conjugated bile salts are unrelated properties in lactobacilli. Appl Environ Microbiol. 2001;67(8):3476-80.

50. Oh HK, Lee JY, Lim SJ, Kim MJ, Kim GB, Kim JH, et al. Molecular cloning and characterization of a bile salt hydrolase from *Lactobacillus acidophilus* PF01. J Microbiol Biotechnol. 2008;18(3):449-56.

51. Haupt VJ, Daminelli S, Schroeder M. Drug Promiscuity in PDB: Protein Binding Site Similarity Is Key. PLoS One. 2013;8(6):e65894.

52. Ruiz L, Margolles A, Sanchez B. Bile resistance mechanisms in Lactobacillus and Bifidobacterium. Front Microbiol. 2013;4:396.

53. Lambert JM, Siezen RJ, de Vos WM, Kleerebezem M. Improved annotation of conjugated bile acid hydrolase superfamily members in Gram-positive bacteria. Microbiology (Reading). 2008;154(Pt 8):2492-500.

54. Panigrahi P, Sule M, Sharma R, Ramasamy S, Suresh CG. An improved method for specificity annotation shows a distinct evolutionary divergence among the microbial enzymes of the cholylglycine hydrolase family. Microbiology (Reading). 2014;160(Pt 6):1162-74.

55. Chien, Y.L., Wu, L.Y., Lee, T.C., Hwang, L.S.,. Cholesterol-lowering effect of phytosterol-containing lactic-fermented milk powder in hamsters. Food Chem 2010; 119, 1121–1126.

56. Jeun J, Kim S, Cho SY, Jun HJ, Park HJ, Seo JG, et al. Hypocholesterolemic effects of *Lactobacillus plantarum* KCTC3928 by increased bile acid excretion in C57BL/6 mice. Nutrition. 2010;26(3):321-30.

57. Gerard P. Metabolism of cholesterol and bile acids by the gut microbiota. Pathogens. 2013;3(1):14-24.

58. Y. Ahn, G. Kim, K. Lim, Y. Baek, H. Kim, Deconjugation of bile salts by *Lactobacillus acidophilus* isolates, Int. Dairy J. 13 (4) (2003) 303–311.

59. Lye HS, Rusul G, Liong MT. Removal of cholesterol by lactobacilli via incorporation and conversion to coprostanol. J Dairy Sci. 2010;93(4):1383-92.

60. Ma C, Zhang S, Lu J, Zhang C, Pang X, Lv J. Screening for Cholesterol-Lowering Probiotics from Lactic Acid Bacteria Isolated from Corn Silage Based on Three Hypothesized Pathways. Int J Mol Sci. 2019;20(9).

61. I. Smet, L. Hoorde, N. Saeyer, M. Woestyne, W. Verstraete, In vitro study of bile salt hydrolase (BSH) activity of BSH isogenic *Lactobacillus plantarum* 80 strains and estimation of cholesterol lowering through enhanced BSH activity, Microb. Ecol. Health Dis. 7 (6) (1994) 315–329.

62. Liong MT, Shah NP. Acid and bile tolerance and cholesterol removal ability of lactobacilli strains. J Dairy Sci. 2005;88(1):55-66.

63. E. Tok, B. Aslim, Cholesterol removal by some lactic acid bacteria that can be used as probiotic, Microbiol. Immunol. 54 (5) (2010) 257–264.

64. Jones ML, Chen H, Ouyang W, Metz T, Prakash S. Microencapsulated Genetically Engineered *Lactobacillus plantarum* 80 (pCBH1) for Bile Acid Deconjugation and Its Implication in Lowering Cholesterol. J Biomed Biotechnol. 2004;2004(1):61-9.

65. Lepercq P, Relano P, Cayuela C, Juste C. *Bifidobacterium animalis* strain DN-173 010 hydrolyses bile salts in the gastrointestinal tract of pigs. Scand J Gastroenterol. 2004;39(12):1266-71.

66. Lee DK, Jang S, Baek EH, Kim MJ, Lee KS, Shin HS, et al. Lactic acid bacteria affect serum cholesterol levels, harmful fecal enzyme activity, and fecal water content. Lipids Health Dis. 2009;8:21.

67. Y. Huang, X. Wang, J. Wang, F. Wu, Y. Sui, L. Yang, Z. Wang, *Lactobacillus plantarum* strains as potential probiotic cultures with cholesterol-lowering activity, J. Dairy Sci. 96 (5) (2013) 2746–2753.

68. Jones ML, Martoni CJ, Parent M, Prakash S. Cholesterol-lowering efficacy of a microencapsulated bile salt hydrolase-active *Lactobacillus reuteri* NCIMB 30242 yoghurt formulation in hypercholesterolaemic adults. Br J Nutr. 2012;107(10):1505-13.

69. Jones ML, Martoni CJ, Prakash S. Cholesterol lowering and inhibition of sterol absorption by *Lactobacillus reuteri* NCIMB 30242: a randomized controlled trial. Eur J Clin Nutr. 2012;66(11):1234-41.

70. A. Baars, A. Oosting, J. Knol, J. Garsse, J. van Bergenhenegouwen, The gut microbiota as a therapeutic target in IBD and metabolic disease: a role for the bile acid receptors FXR and TGR5, Microorganisms 3 (4) (2015) 641–666.

71. Costabile A, Buttarazzi I, Kolida S, Quercia S, Baldini J, Swann JR, et al. An in vivo assessment of the cholesterol-lowering efficacy of *Lactobacillus plantarum* ECGC 13110402 in normal to mildly hypercholesterolaemic adults. PLoS One. 2017;12(12):e0187964.

72. Oner O, Aslim B, Aydas SB. Mechanisms of cholesterol-lowering effects of lactobacilli and bifidobacteria strains as potential probiotics with their bsh gene analysis. J Mol Microbiol Biotechnol. 2014;24(1):12-8.

73. Lye HS, Kato T, Low WY, Taylor TD, Prakash T, Lew LC, et al. *Lactobacillus fermentum* FTDC 8312 combats hypercholesterolemia via alteration of gut microbiota. J Biotechnol. 2017;262:75-83.

74. Sridevi, N.; Vishwe, P.; Prabhune, A. Hypocholesteremic effect of bile salt hydrolase from *Lactobacillus buchneri* ATCC 4005. Food Res. Int. 2009, 42, 516–520.

75. Prakash, S.; Jones, M.L.; Martoni, C. Bacterial Compositions for Prophylaxis and Treatment of Degenerative Disease. U.S. Patent 10,660,857, 26 May 2020.

76. Castellana, J.C. *Lactobacillus plantarum* Strains as Hypocholesterolemic Agents. U.S. Patent 8,668,906, 11 March 2014.

77. Zhen-Mei, L.; Mei-Gi, H.; Wen-Hsin, L. *Lactobacillus plantarum* bb9 Capable of Adhering to Gastrointestinal Tract and Cholesterol Removal. U.S. Patent 12/622,428, 19 May 2011.

78. Rothschild, P.; Connolly, E.; Möllstam, B. Use of Selected Lactic Acid Bacteria for Reducing Atherosclerosis. U.S. Patent 11/786,356, 23 October 2008.

79. Liong, M.T.; Shah, N.P. Bile salt deconjugation ability, bile salt hydrolase activity and cholesterol co-precipitation ability of lactobacilli strains. Int. Dairy J. 2005, 15, 391–398.

80. Jones H, Alpini G, Francis H. Bile acid signaling and biliary functions. Acta Pharm Sin B. 2015;5(2):123-8.

81. Ryan KK, Tremaroli V, Clemmensen C, Kovatcheva-Datchary P, Myronovych A, Karns R, et al. FXR is a molecular target for the effects of vertical sleeve gastrectomy. Nature. 2014;509(7499):183-8.

82. Sheng L, Jena PK, Liu HX, Hu Y, Nagar N, Bronner DN, et al. Obesity treatment by epigallocatechin-3-gallate-regulated bile acid signaling and its enriched Akkermansia muciniphila. FASEB J. 2018;32(12):fj201800370R.

83. Joyce SA, Shanahan F, Hill C, Gahan CG. Bacterial bile salt hydrolase in host metabolism: Potential for influencing gastrointestinal microbe-host crosstalk. Gut Microbes. 2014;5(5):669-74.

84. Duboc H, Tache Y, Hofmann AF. The bile acid TGR5 membrane receptor: from basic research to clinical application. Dig Liver Dis. 2014;46(4):302-12.

85. Fiorucci S, Biagioli M, Zampella A, Distrutti E. Bile Acids Activated Receptors Regulate Innate Immunity. Front Immunol. 2018;9:1853.

86. Malhi H, Camilleri M. Modulating bile acid pathways and TGR5 receptors for treating liver and GI diseases. Curr Opin Pharmacol. 2017;37:80-6.

87. Chiang JYL, Ferrell JM. Bile Acid Biology, Pathophysiology, and Therapeutics. Clin Liver Dis (Hoboken). 2020;15(3):91-4.

88. Chiang JYL, Ferrell JM. Bile Acids as Metabolic Regulators and Nutrient Sensors. Annu Rev Nutr. 2019;39:175-200.

89. Watanabe M, Houten SM, Mataki C, Christoffolete MA, Kim BW, Sato H, et al. Bile acids induce energy expenditure by promoting intracellular thyroid hormone activation. Nature. 2006;439(7075):484-9.

90. Thompson RC, Monis PT. Variation in Giardia: implications for taxonomy and epidemiology. Adv Parasitol. 2004;58:69-137.

91. Thompson RC, Monis P. Giardia--from genome to proteome. Adv Parasitol. 2012;78:57-95.

92. Savioli L, Smith H, Thompson A. Giardia and Cryptosporidium join the 'Neglected Diseases Initiative'. Trends Parasitol. 2006;22(5):203-8.

93. Harris JC, Plummer S, Lloyd D. Antigiardial drugs. Appl Microbiol Biotechnol. 2001;57(5-6):614-9.

94. Upcroft P, Upcroft JA. Drug targets and mechanisms of resistance in the anaerobic protozoa. Clin Microbiol Rev. 2001;14(1):150-64.

95. Travers MA, Florent I, Kohl L, Grellier P. Probiotics for the control of parasites: an overview. J Parasitol Res. 2011;2011:610769.

96. Bengmark S. Gut microbiota, immune development and function. Pharmacol Res. 2013;69(1):87-113.

97. Sanders ME. Probiotics: definition, sources, selection, and uses. Clin Infect Dis. 2008;46 Suppl 2:S58-61; discussion S144-51.

98. Martin R, Miquel S, Ulmer J, Kechaou N, Langella P, Bermudez-Humaran LG. Role of commensal and probiotic bacteria in human health: a focus on inflammatory bowel disease. Microb Cell Fact. 2013;12:71.

99. Sokol H. Probiotics and antibiotics in IBD. Dig Dis. 2014;32 Suppl 1:10-7.

100. Singer SM, Nash TE. The role of normal flora in Giardia lamblia infections in mice. J Infect Dis. 2000;181(4):1510-2.

101. Barash NR, Maloney JG, Singer SM, Dawson SC. Giardia Alters Commensal Microbial Diversity throughout the Murine Gut. Infect Immun. 2017;85(6).

102. Bartelt LA, Bolick DT, Mayneris-Perxachs J, Kolling GL, Medlock GL, Zaenker EI, et al. Cross-modulation of pathogen-specific pathways enhances malnutrition during enteric co-infection with Giardia lamblia and enteroaggregative *Escherichia coli*. PLoS Pathog. 2017;13(7):e1006471.

103. Allain T, Amat CB, Motta JP, Manko A, Buret AG. Interactions of Giardia sp. with the intestinal barrier: Epithelium, mucus, and microbiota. Tissue Barriers. 2017;5(1):e1274354.

104. Vitetta L, Saltzman ET, Nikov T, Ibrahim I, Hall S. Modulating the Gut Micro-Environment in the Treatment of Intestinal Parasites. J Clin Med. 2016;5(11).

105. Bustos, A.Y.; de Valdez, G.F.; Fadda, S.; Taranto, M.P. New insights into bacterial bile resistance mechanisms: The role of bile salt hydrolase and its impact on human health. Food Res. Int. 2018, 112, 250–262.

106. Travers MA, Sow C, Zirah S, Deregnaucourt C, Chaouch S, Queiroz RM, et al. Deconjugated Bile Salts Produced by Extracellular Bile-Salt Hydrolase-Like Activities from the Probiotic *Lactobacillus johnsonii* La1 Inhibit Giardia duodenalis In vitro Growth. Front Microbiol. 2016;7:1453.

107. Allain T, Chaouch S, Thomas M, Vallee I, Buret AG, Langella P, et al. Bile-Salt-Hydrolases from the Probiotic Strain *Lactobacillus johnsonii* La1 Mediate Anti-giardial Activity in Vitro and in Vivo. Front Microbiol. 2017;8:2707.

108. Allain T, Chaouch S, Thomas M, Travers MA, Valle I, Langella P, et al. Bile Salt Hydrolase Activities: A Novel Target to Screen Anti-Giardia Lactobacilli? Front Microbiol. 2018;9:89.

109. Smith AB, Soto Ocana J, Zackular JP. From Nursery to Nursing Home: Emerging Concepts in *Clostridioides difficile* Pathogenesis. Infect Immun. 2020;88(7).

110. Rupnik M, Wilcox MH, Gerding DN. *Clostridium difficile* infection: new developments in epidemiology and pathogenesis. Nat Rev Microbiol. 2009;7(7):526-36.

111. Zhu D, Sorg JA, Sun X. *Clostridioides difficile* Biology: Sporulation, Germination, and Corresponding Therapies for C. difficile Infection. Front Cell Infect Microbiol. 2018;8:29.

112. Abt MC, McKenney PT, Pamer EG. *Clostridium difficile* colitis: pathogenesis and host defence. Nat Rev Microbiol. 2016;14(10):609-20.

113. Francis MB, Sorg JA. Dipicolinic Acid Release by Germinating *Clostridium difficile* Spores Occurs through a Mechanosensing Mechanism. mSphere. 2016;1(6).

114. Francis MB, Allen CA, Shrestha R, Sorg JA. Bile acid recognition by the *Clostridium difficile* germinant receptor, CspC, is important for establishing infection. PLoS Pathog. 2013;9(5):e1003356.

115. Francis MB, Allen CA, Sorg JA. Spore Cortex Hydrolysis Precedes Dipicolinic Acid Release during *Clostridium difficile* Spore Germination. J Bacteriol. 2015;197(14):2276-83.

116. Sorg, J.A.; Sonenshein, A.L. Bile salts and glycine as cogerminants for *Clostridium difficile* spores. J. Bacteriol. 2008, 190, 2505–2512.

117. Mullish BH, McDonald JAK, Pechlivanis A, Allegretti JR, Kao D, Barker GF, et al. Microbial bile salt hydrolases mediate the efficacy of faecal microbiota transplant in the treatment of recurrent *Clostridioides difficile* infection. Gut. 2019;68(10):1791-800.

118. Weingarden AR, Chen C, Bobr A, Yao D, Lu Y, Nelson VM, et al. Microbiota transplantation restores normal fecal bile acid composition in recurrent *Clostridium difficile* infection. Am J Physiol Gastrointest Liver Physiol. 2014;306(4):G310-9.

119. Hsiao A, Ahmed AM, Subramanian S, Griffin NW, Drewry LL, Petri WA, Jr., et al. Members of the human gut microbiota involved in recovery from *Vibrio cholerae* infection. Nature. 2014;515(7527):423-6.

120. Ovadia C, Perdones-Montero A, Fan HM, Mullish BH, McDonald JAK, Papacleovoulou G, et al. Ursodeoxycholic acid enriches intestinal bile salt hydrolase-expressing Bacteroidetes in cholestatic pregnancy. Sci Rep. 2020;10(1):3895.

121. Tabibian JH, O'Hara SP, Trussoni CE, Tietz PS, Splinter PL, Mounajjed T, et al. Absence of the intestinal microbiota exacerbates hepatobiliary disease in a murine model of primary sclerosing cholangitis. Hepatology. 2016;63(1):185-96.

122. Ma C, Han M, Heinrich B, Fu Q, Zhang Q, Sandhu M, et al. Gut microbiome-mediated bile acid metabolism regulates liver cancer via NKT cells. Science. 2018;360(6391).

123. De Smet I, Van Hoorde L, Vande Woestyne M, Christiaens H, Verstraete W. Significance of bile salt hydrolytic activities of lactobacilli. J Appl Bacteriol. 1995;79(3):292-301.

124. De Boever P, Wouters R, Verschaeve L, Berckmans P, Schoeters G, Verstraete W. Protective effect of the bile salt hydrolase-active *Lactobacillus reuteri* against bile salt cytotoxicity. Appl Microbiol Biotechnol. 2000;53(6):709-14.

125. Grill JP, Cayuela C, Antoine JM, Schneider F. Isolation and characterization of a *Lactobacillus amylovorus* mutant depleted in conjugated bile salt hydrolase activity: relation between activity and bile salt resistance. J Appl Microbiol. 2000;89(4):553-63.

126. Bernstein C, Holubec H, Bhattacharyya AK, Nguyen H, Payne CM, Zaitlin B, Bernstein H. Carcinogenicity of deoxycholate, a secondary bile acid. Arch Toxicol. 2011;85(8):863-71.

127. Payne CM, Holubec H, Crowley-Skillicorn C, Nguyen H, Bernstein H, Wilcox G, Bernstein C. Maspin is a deoxycholate-inducible, anti-apoptotic stress-response protein differentially expressed during colon carcinogenesis. Clin Exp Gastroenterol. 2011;4:239-53.

128. Yoshimoto, S., Loo, T.M., Atarashi, K., Kanda, H., Sato, S., Oyadomari, S., Iwakura, Y., Oshima, K., Morita, H., Hattori, M., Honda, K., Ishikawa, Y., Hara, E., Ohtani, N.,. Obesity-induced gut microbial metabolite promotes liver cancer through senescence secretome. 2013 Nature 499, 97–101.

129. Noriega, L., Cuevas, I., Margolles, A., de los Reyes-Gavilán, C.G.,. Deconjugation and bile salt hydrolase activity by Bifidobacterium strains with resistance to bile. Int. Dairy J. 2006.16, 850–855.

130. Park MY, Kim SJ, Ko EK, Ahn SH, Seo H, Sung MK. Gut microbiota-associated bile acid deconjugation accelerates hepatic steatosis in ob/ob mice. J Appl Microbiol. 2016;121(3):800-10.

131. A. Morgan, K. Mooney, S. Wilkinson, N. Pickles, M. Mc Auley, Cholesterol metabolism: a review of how ageing disrupts the biological mechanisms responsible for its regulation, Ageing Res. Rev. 27 (2016) 108–124.

132. Nagengast FM, van der Werf SD, Lamers HL, Hectors MP, Buys WC, van Tongeren JM. Influence of age, intestinal transit time, and dietary composition on fecal bile acid profiles in healthy subjects. Dig Dis Sci. 1988;33(6):673-8.

133. Salemans JM, Nagengast FM, Tangerman A, van Schaik A, Hopman WP, de Haan AF, Jansen JB. Effect of ageing on postprandial conjugated and unconjugated serum bile acid levels in healthy subjects. Eur J Clin Invest. 1993;23(3):192-8.

134. van der Werf SD, Huijbregts AW, Lamers HL, van Berge Henegouwen GP, van Tongeren JH. Age dependent differences in human bile acid metabolism and 7 alpha-dehydroxylation. Eur J Clin Invest. 1981;11(6):425-31.

135. Dibner JJ, Richards JD. Antibiotic growth promoters in agriculture: history and mode of action. Poult Sci. 2005;84(4):634-43.

136. Marshall BM, Levy SB. Food animals and antimicrobials: impacts on human health. Clin Microbiol Rev. 2011;24(4):718-33.

137. Wegener HC. Antibiotics in animal feed and their role in resistance development. Curr Opin Microbiol. 2003;6(5):439-45.

138. Gaskins HR, Collier CT, Anderson DB. Antibiotics as growth promotants: mode of action. Anim Biotechnol. 2002;13(1):29-42.

139. Smith K, Zeng X, Lin J. Discovery of bile salt hydrolase inhibitors using an efficient high-throughput screening system. PLoS One. 2014;9(1):e85344.

140. Knarreborg A, Lauridsen C, Engberg RM, Jensen SK. Dietary antibiotic growth promoters enhance the bioavailability of alpha-tocopheryl acetate in broilers by altering lipid absorption. J Nutr. 2004;134(6):1487-92.

141. Guban J, Korver DR, Allison GE, Tannock GW. Relationship of dietary antimicrobial drug administration with broiler performance, decreased population levels of *Lactobacillus salivarius,* and reduced bile salt deconjugation in the ileum of broiler chickens. Poult Sci. 2006;85(12):2186-94.

142. Dumonceaux TJ, Hill JE, Hemmingsen SM, Van Kessel AG. Characterization of intestinal microbiota and response to dietary virginiamycin supplementation in the broiler chicken. Appl Environ Microbiol. 2006;72(4):2815-23.

143. Jacela JY, Derouchey JM, Tokach MD, Goodband RD, Nelssen JL, Renter DG, Dritz SS. Feed additives for swine: fact sheets – high dietary levels of copper and zinc for young pigs, and phytase. Anim Sci Abroad 2011;18:87–89.

144. Korpela K, Salonen A, Virta LJ, Kekkonen RA, Forslund K, Bork P, Vos WMD. Intestinal microbiome is related to lifetime antibiotic use in Finnish pre-school children. Nat Commun 2016;7:10410.

145. Shelton NW, Tokach MD, Nelssen JL, Goodband RD, Dritz SS, DeRouchey JM, Hill GM. Effects of copper sulfate, tri-basic copper chloride, and zinc oxide on weanling pig performance. J Anim Sci. 2011;89(8):2440-51.

146. Arias VJ, Koutsos EA. Effects of copper source and level on intestinal physiology and growth of broiler chickens. Poult Sci. 2006;85(6):999-1007.

147. Liu ZH, Lu L, Li SF, Zhang LY, Xi L, Zhang KY, Luo XG. Effects of supplemental zinc source and level on growth performance, carcass traits, and meat quality of broilers. Poult Sci. 2011;90(8):1782-90.

148. Long, S.L.; Gahan, C.G.M.; Joyce, S.A. Interactions between gut bacteria and bile in health and disease. Mol. Asp. Med. 2017, 56, 54–65.

149. Kim GB, Yi SH, Lee BH. Purification and characterization of three different types of bile salt hydrolases from Bifidobacterium strains. J Dairy Sci. 2004;87(2):258-66.

150. Lambert JM, Bongers RS, de Vos WM, Kleerebezem M. Functional analysis of four bile salt hydrolase and penicillin acylase family members in *Lactobacillus plantarum* WCFS1. Appl Environ Microbiol. 2008;74(15):4719-26.

151. Ren J, Sun K, Wu Z, Yao J, Guo B. All 4 bile salt hydrolase proteins are responsible for the hydrolysis activity in *Lactobacillus plantarum* ST-III. J Food Sci. 2011;76(9):M622-8.

152. Wijaya A, Hermann A, Abriouel H, Specht I, Yousif NM, Holzapfel WH, Franz CM. Cloning of the bile salt hydrolase (bsh) gene from *Enterococcus faecium* FAIR-E 345 and chromosomal location of *bsh* genes in food enterococci. J Food Prot. 2004;67(12):2772-8.

153. Lim HJ, Kim SY, Lee WK. Isolation of cholesterol-lowering lactic acid bacteria from human intestine for probiotic use. J Vet Sci. 2004;5(4):391-5.

154. Kumar R, Grover S, Mohanty AK, Batish VK. Molecular cloning and sequence analysis of bile salt hydrolase gene (bsh) from *Lactobacillus plantarum* MBUL90 strain of human origin. Food Biotechnol. 2010;24:215–226.

155. Delpino MV, Marchesini MI, Estein SM, Comerci DJ, Cassataro J, Fossati CA, Baldi PC. A bile salt hydrolase of Brucella abortus contributes to the establishment of a successful infection through the oral route in mice. Infect Immun. 2007;75(1):299-305.

156. Dussurget O, Cabanes D, Dehoux P, Lecuit M, Buchrieser C, Glaser P, et al. *Listeria monocytogenes* bile salt hydrolase is a PrfA-regulated virulence factor involved in the intestinal and hepatic phases of listeriosis. Mol Microbiol. 2002;45(4):1095-106.

157. Coleman JP, Hudson LL. Cloning and characterization of a conjugated bile acid hydrolase gene from *Clostridium perfringens*. Appl Environ Microbiol. 1995;61(7):2514-20.

158. Dean M, Cervellati C, Casanova E, Squerzanti M, Lanzara V, Medici A, et al. Characterization of cholylglycine hydrolase from a bile-adapted strain of *Xanthomonas maltophilia* and its application for quantitative hydrolysis of conjugated bile salts. Appl Environ Microbiol. 2002;68(6):3126-8.

159. Pedrini P, Andreotti E, Guerrini A, Dean M, Fantin G, Giovannini PP. *Xanthomonas maltophilia* CBS 897.97 as a source of new 7beta- and 7alpha-hydroxysteroid dehydrogenases and cholylglycine hydrolase: improved biotransformations of bile acids. Steroids. 2006;71(3):189-98.

160. Kawamoto K, Horibe I, Uchida K. Purification and characterization of a new hydrolase for conjugated bile acids, chenodeoxycholyltaurine hydrolase, from *Bacteroides vulgatus*. J Biochem. 1989;106(6):1049-53.

161. Stellwag EJ, Hylemon PB. Purification and characterization of bile salt hydrolase from *Bacteroides fragilis subsp. fragilis*. Biochim Biophys Acta. 1976;452:165–176.

162. Sridevi N, Prabhune AA. Brevibacillus sp: a novel thermophilic source for the production of bile salt hydrolase. Appl Biochem Biotechnol. 2009;157(2):254-62.

163. Sridevi N, Srivastava S, Khan BM, Prabhune AA. Characterization of the smallest dimeric bile salt hydrolase from a thermophile Brevibacillus sp. Extremophiles. 2009;13(2):363-70.

164. Panigrahi P, Sule M, Sharma R, Ramasamy S, Suresh CG. An improved method for specificity annotation shows a distinct evolutionary divergence among the microbial enzymes of the cholylglycine hydrolase family. Microbiol-SGM 2014;160:1162–1174.

165. Jiang, J., Hang, X., Zhang, M., Liu, X., Li, D., Yang, H. Diversity of bile salt hydrolase activities in different lactobacilli toward human bile salts. Ann. Microbiol. 2010;60, 81–88.

166. Rani RP, Anandharaj M, Ravindran AD. Characterization of Bile Salt Hydrolase from *Lactobacillus gasseri* FR4 and Demonstration of Its Substrate Specificity and Inhibitory Mechanism Using Molecular Docking Analysis. Front Microbiol. 2017;8:1004.

167. Elkins CA, Moser SA, Savage DC. Genes encoding bile salt hydrolases and conjugated bile salt transporters in *Lactobacillus johnsonii* 100-100 and other Lactobacillus species. Microbiology (Reading). 2001;147(Pt 12):3403-12.

168. Chae JP, Valeriano VD, Kim GB, Kang DK. Molecular cloning, characterization and comparison of bile salt hydrolases from *Lactobacillus johnsonii* PF01. J Appl Microbiol. 2013;114(1):121-33.

169. Bi, J., Fang, F., Lu, S., Du, G., Chen, J. New insight into the catalytic properties of bile salt hydrolase. J. Mol. Catal. B Enzym. 2013;96, 46–51.

170. O'Flaherty S, Briner Crawley A, Theriot CM, Barrangou R. The Lactobacillus Bile Salt Hydrolase Repertoire Reveals Niche-Specific Adaptation. mSphere. 2018;3(3).

171. Tanaka H, Hashiba H, Kok J, Mierau I. Bile salt hydrolase of *Bifidobacterium longum*-biochemical and genetic characterization. Appl Environ Microbiol. 2000;66(6):2502-12.

172. Oelschlaeger TA. Mechanisms of probiotic actions - A review. Int J Med Microbiol. 2010;300(1):57-62.

173. Reyes-Nava, L.A., Rivera-Espinoza, Y. Isolation sources of bile salt hydrolase microorganisms. Herald J. Agric. Food Sci. Res.2014;3, 49–54.

174. Joyce SA, Gahan CG. Disease-Associated Changes in Bile Acid Profiles and Links to Altered Gut Microbiota. Dig Dis. 2017;35(3):169-77.

175. Ajouz H, Mukherji D, Shamseddine A. Secondary bile acids: an underrecognized cause of colon cancer. World J Surg Oncol. 2014;12:164.

176. Öztürk, M., K. Hacıbeyoğlu, Z. Kılıçsaymaz, and C. Önal. Construction of R16F and D19L mutations in the loop I of bile salt hydrolase (BSH) enzyme from *Lactobacillus plantarum* B14 and functional analysis of the mutant BSHs. *Food Biotechnol.* 2019;33 (2):125–141.

177. Öztürk, M., and C. Önal. Asparagine 79 is an important amino acid for catalytic activity and substrate specificity of bile salt hydrolase (BSH). *Mol. Biol. Rep*. 2019;46:4361–4368. doi:10. 1007/s11033-019-04889-2.

178. Lowry OH, Rosebrough NJ, Farr AL and Randal RJ. Protein measurement with the Folin phenol reagent. J. Biol. Chem.1951;193: 265-275.

179. Kim GB, Brochet M, Lee BH. Cloning and characterization of a bile salt hydrolase (bsh) from *Bifidobacterium adolescentis*. Biotechnol Lett. 2005;27(12):817-22.

180. Petit CM, Zhang J, Sapienza PJ, Fuentes EJ, Lee AL. Hidden dynamic allostery in a PDZ domain. Proc Natl Acad Sci U S A. 2009;106(43):18249-54.

181. Karlov DS, Long SL, Zeng X, Xu F, Lal K, Cao L, et al. Characterization of the mechanism of bile salt hydrolase substrate specificity by experimental and computational analyses. Structure. 2023;31(5):629-38 e5.

182. Xu F, Hu XJ, Singh W, Geng W, Tikhonova IG, Lin J. The complex structure of bile salt hydrolase from *Lactobacillus salivarius* reveals the structural basis of substrate specificity. Sci Rep. 2019;9(1):12438.

183. Hu PL, Yuan YH, Yue TL, Guo CF. A new method for the in vitro determination of the bile tolerance of potentially probiotic lactobacilli. Appl Microbiol Biotechnol. 2018;102(4):1903-1.

184. Laemmli UK.Cleavage of structural proteins during the assembly of the head of bacteriophage T4. Nature. 1970; 227(5259):680-5.

185. Bertani G. Studies on lysogenesis. I. The mode of phage liberation by lysogenic Escherichia coli. J Bacteriol 1951:62, 293–300.

186. Feher Joseph Pancreatic and Biliary Secretion, in Quantitative Human Physiology (Second Edition), 2017.

187. Christiaens H, Leer RJ, Pouwels PH and Verstraete W "Cloning and expression of a conjugated bile acid hydrolase gene from *Lactobacillus plantarum* by using a direct plate assay", Appl Environ Microbiol, 1992; 58(12):3792-8.